VNIVERSITAT DE VALÈNCIA

PhD program in Biomedicine and Biotechnology

Understanding the effect of Vitamin D treatment on human uterine leiomyoma growth using *in vitro* and *in vivo* models

Author:

Ana Corachán García

Supervised by:

Dr. Hortensia Ferrero

Prof. Antonio Pellicer

Valencia, June 2019

Dra. Hortensia Ferrero Cháfer, Doctora en Biomedicina y Biotecnología, Investigadora principal del área de Diagnóstico y Tratamiento de Enfermedades Uterinas en Fundación IVI.

CERTIFICA:

Que el trabajo de investigación titulado: "**Understanding the effect of Vitamin D treatment on human uterine leiomyoma growth using *in vitro* and *in vivo* models**" ha sido realizado íntegramente por Ana Corachán bajo mi dirección. Dicha memoria está concluida y reúne todos los requisitos para su presentación y defensa como TESIS DOCTORAL ante un tribunal.

Y para que así conste a los efectos oportunos, firmo la presente certificación en Valencia a 6 de junio de 2019.

Fdo. Dra. Hortensia Ferrero Cháfer

Prof. Antonio Pellicer Martínez, Catedrático en Ginecología, Doctor en Medicina y Cirugía, Profesor titular del Departamento de Pediatría, Obstetricia y Ginecología de la Facultad de Medicina de la Universidad de Valencia, fundador del Instituto Valenciano de Infertilidad y presidente de la Fundación IVI.

CERTIFICA:

Que el trabajo de investigación titulado: "**Understanding the effect of Vitamin D treatment on human uterine leiomyoma growth using *in vitro* and *in vivo* models**" ha sido realizado íntegramente por Ana Corachán bajo mi dirección. Dicha memoria está concluida y reúne todos los requisitos para su presentación y defensa como TESIS DOCTORAL ante un tribunal.

Y para que así conste a los efectos oportunos, firmo la presente certificación en Valencia a 6 de junio de 2019.

Fdo. Dr. Antonio Pellicer Martínez

AGRADECIMIENTOS

Nunca pensé que me costaría tanto escribir este apartado. Después de tanto tiempo deseando que llegara este momento, ahora que por fin estoy aquí me siento incapaz de hacerlo… Será que empiezo a ser consciente de que esto se acaba. Tras tanto tiempo y esfuerzo, quiero aprovechar estas líneas para dar las gracias a todas las personas que han formado parte de mi tesis de una u otra manera.

En primer lugar, quería dar las gracias a mis directores. Al Dr. Antonio Pellicer por darme la oportunidad de empezar mi carrera investigadora y realizar mi tesis en Fundación IVI. A la Dra. Hortensia Ferrero sin la que, sin lugar a duda, esta tesis no habría sido posible. Horten, gracias por contar conmigo desde el primer momento, por esforzarte tanto o más que yo en este largo camino en el que, aunque a veces lo hayamos pasado mal, hemos disfrutado y nos hemos reído muchísimo. Gracias por tu tiempo y tu paciencia (tienes mucha más de la que piensas). Gracias por ayudarme a crecer tanto profesional como personalmente y, sobre todo, por enseñarme a trabajar desde la humildad y la constancia. Tengo muy claro que no podría haber tenido una mejor directora de tesis y que eres de las mejores cosas que me llevo de esta etapa.

También me gustaría agradecer a mis compañeros de Fundación IVI por hacer que no haya habido ni un solo día en el trabajo en el que no me haya reído. Gracias a Paco por ayudarme siempre que lo he necesitado. A Irene por toda la ayuda, los consejos y el tiempo que has dedicado a esta tesis, y por todas las risas que hemos compartido. Gracias Ali, por ayudarme siempre con una sonrisa y por nuestros momentos en los almuerzos, comidas y “cigarros”. Amparo, gracias por enseñarme como voy a ser dentro de unos años. Creo que no podría haber encontrado a alguien tan parecido a mí, y a la vez tan diferente en ciertas cosas. Gracias por ayudarme siempre, aunque tú tal vez pienses que, en vez de ayudar, yo mando y tú trabajas. Pero, por encima de todo, gracias por escucharme y aconsejarme siempre que lo he necesitado. Tú eres otra de esas grandes cosas que me llevo de aquí.

A mis compañeros, en especial a aquéllos con lo que he pasado más tiempo, Hannes gracias por la ayuda sobre todo en esta última etapa, y Silvia gracias por enseñarme siempre el lado positivo de las cosas. Al resto de compañeros con los que comparto o he compartido el día a día, Anna, Luismi, Jessi, María, Sonia, Sara, Lucía, Majo, Patri Diaz, Patri Sebastián, Stefy, Andrea, Rober, María Cristina, Gaby… gracias por las risas y el compañerismo.

Al personal del servicio de Obstetricia y Ginecología del Hospital La Fe, en especial al Dr. Monleón, a Alejandra, Nuria y Julia por la ayuda en la recogida de muestras y sus aportaciones a lo largo de este proyecto. Al personal del animalario de la Facultad de Medicina de la Universidad de Valencia, especialmente a Ana Díaz y a Eva Blanch y Musta por las largas horas del PET.

A mis amigas, Nuri, Cris, Ester, Patri y Bárbara, gracias por estar siempre y seguir haciendo las mismas tonterías (o más) que cuando nos conocimos. Siempre aquí.

Por último, quería agradecer a mi familia, mi abuela (la artista responsable de la portada), mis tías Amparín, Lupe y Mª José, mis primas Belén, Amparo, y los peques, Vega, Mateo y Candela. Gracias por enseñarme lo que es el apoyo incondicional, por hacer que el tiempo vuele cuando estoy con vosotros y por enseñarme qué es lo que de verdad importa. Gracias a mi padre, por inculcarme el valor de la responsabilidad en el trabajo. A Migue, por ser el mejor padrastro posible, gracias por todo. A mis hermanas, que creo que saben perfectamente que son lo más importante de mi vida. A Ángela por estar siempre conmigo a pesar de la distancia. A Irene por aguantarme en el día a día, escucharme y aconsejarme siempre. Creo que somos conscientes de que no somos dos y una, siempre hemos sido y seremos tres.

Finalmente, quería dedicar esta tesis a mi madre. Mamá, gracias por creer y confiar en mí ciegamente, por tus consejos y, sobre todo, por enseñarme que soy fuerte.

El presente trabajo de tesis doctoral ha sido realizado en los laboratorios de la Fundación IVI, así como en el animalario de la Facultad de Medicina de la Universitat de València. Gracias a la ayuda para la contratación de personal investigador en formación de carácter predoctoral, Programa VALi+d de la Generalitat Valenciana y el Fondo Social Europeo (ACIF/2016/444) y a la ayuda Acción Estratégica de Salud del Instituto de Salud Carlos III (PI 15/00312).

RESUMEN

INTRODUCCIÓN

EL ÚTERO: ANATOMÍA Y ENDOCRINOLOGÍA

El aparato reproductor femenino está formado por los genitales externos (vulva y perineo) y los genitales internos que pueden dividirse a su vez en dos partes: el ovario, glándula en la cual se forman los ovocitos, y un sistema de conductos que incluye las trompas de Falopio, el útero y la vagina, cuya función es el transporte de los ovocitos desde la superficie ovárica hasta la cavidad uterina.

El **útero** es un órgano hueco con forma de pera invertida que consta de tres partes: fondo, cuerpo y cérvix. Su función es alojar y alimentar al ovocito fecundado durante el embarazo, proceso durante el cual aumenta su tamaño entre 4 y 5 veces. La pared uterina está formada por tres capas: endometrio, miometrio y perimetrio. El endometrio, es la capa mucosa que recubre el interior de la cavidad uterina la cual a su vez consta de: la capa funcional, que se desprenden durante la menstruación, y la capa basal que permanece y se encarga de regenerar la capa funcional. El miometrio, la capa más gruesa (12-15mm) y más vascularizada del útero, se encuentra por debajo del endometrio y está formada por células musculares lisas embebidas en una abundante matriz extracelular rica principalmente en colágeno. Durante el embarazo, las células musculares se dividen (hiperplasia) y crecen (hipertrofia), de modo que el útero gestante aumenta su tamaño mientras el endometrio nutre al embrión. Finalmente, el perimetrio, la capa más externa que se conoce como serosa y cubre el cuerpo y fondo uterinos.

La **matriz extracelular (MEC) del miometrio** juega un importante papel en los procesos de crecimiento y remodelación del útero, característicos del embarazo, parto y posparto, debido a sus funciones relacionadas con la adhesión, comunicación célula-célula y diferenciación. La MEC es una red tridimensional de macromoléculas extracelulares que proporciona soporte estructural y bioquímico a las células adyacentes. Uno de los principales componentes de la MEC son las fibras de colágeno, entre las cuales se distribuyen las células musculares lisas. El colágeno no es una proteína única, si no que forma parte de una familia

de proteínas que engloba 29 tipos de colágenos los cuales presentan tres cadenas polipeptídicas ensambladas en una estructura de triple hélice. Los principales tipos de colágeno del miometrio son el Tipo I, Tipo III y Tipo IV, responsables de la fuerza mecánica del tejido uterino. Además del colágeno, la MEC del miometrio está formada por otros componentes tales como proteoglicanos, implicados en el control del crecimiento celular y la diferenciación; elastina, que proporciona elasticidad al útero; integrinas, implicadas en procesos de adhesión, señalización y supervivencia celular, y fibronectina, que participa en la organización de los diferentes componentes de la MEC, así como en procesos de migración, adhesión, crecimiento y diferenciación celular y fibrosis.

Los cambios que experimenta la MEC del útero están controlados por el sistema de metaloproteinasas de matriz extracelular (MMPs por sus siglas en inglés; *matrix metalloproteinases*). Las MMPs son enzimas con actividad proteolítica reguladas por los inhibidores de tejido de MMPs (TIMPs por sus siglas en inglés; *tissue inhibitors of metalloproteinases*). A su vez, la expresión de MMPs y TIMPs está influenciada por citoquinas proinflamatorias, hormonas o factores de crecimiento tales como *Transforming Growth Factor β* (TGFβ). El equilibrio entre la expresión de MMPs y TIMPs es esencial en el control de la actividad del sistema de MMPs, fundamental en los cambios estructurales asociados con el ciclo menstrual, así como en el embarazo. Consecuentemente, el control inapropiado de dicho sistema daría lugar a condiciones patológicas tales como ovario poliquístico, endometriosis y miomas uterinos.

En lo referente a la **endocrinología del útero**, la edad reproductiva de la mujer se caracteriza por el ciclo menstrual, el cual es el resultado de cambios mensuales cíclicos en las tasas de secreción de las hormonas sexuales, controlados por el eje hipotálamo-hipófisis-ovario. Este control comienza en el hipotálamo donde la hormona liberadora de la gonadotropina (GnRH por sus siglas en inglés; *gonadotropin-releasing hormone*) es liberada en pulsos y desde donde viaja hasta la hipófisis. La liberación pulsátil de la GnRH es crucial para la función reproductiva, lo cual implica que un aumento o una disminución de GnRH apaga todo el sistema. En la hipófisis, la GnRH estimula la síntesis de dos gonadotropinas encargadas del control del ovario: la hormona luteinizante (LH por sus siglas en inglés; *luteinizing hormone*) y la hormona folículo estimulante (FSH por sus siglas en inglés; *follicle stimulating hormone*).

El ciclo menstrual incluye el ciclo ovárico y el ciclo endometrial, los cuales ocurren al mismo tiempo y están altamente coordinados a través de interacciones mutuas.

El ciclo ovárico presenta dos fases separadas por la ovulación: la fase folicular y la fase lútea. Durante la fase folicular, la FSH es la gonadotropina predominante, la cual estimula el crecimiento del folículo ovárico y controla la producción de estrógenos en el ovario. Por el contrario, la LH predomina durante la segunda fase del ciclo, empezando a ser liberada tras la ovulación, momento tras el cual estimula y mantiene la producción de progesterona. A su vez ambas hormonas esteroides, estrógenos y progesterona, proporcionan un feedback negativo sobre el hipotálamo y la hipófisis resultando en la represión de las hormonas estimulantes.

El ciclo endometrial consta de dos fases: la fase proliferativa y la fase secretora, que corresponden, respectivamente, a las fases folicular y lútea del ciclo ovárico. La fase proliferativa comprende el periodo de tiempo entre la menstruación y la ovulación. Durante esta fase el tejido endometrial prolifera y crece debido a la acción de los estrógenos. Por otra parte, la fase secretora va desde la ovulación hasta la menstruación. En dicho periodo, la progesterona producida por el cuerpo lúteo tras la ovulación hace que en endometrio secrete glicógeno y moco durante la fase secretora temprana. Posteriormente, en la fase secretora media, el endometrio comienza a decidualizarse y convertirse en receptivo para el ovocito fertilizado. Finalmente, en la fase secretora tardía, si no se produce embarazo, los niveles de estrógenos y progesterona decaen, resultando en una reducción el flujo sanguíneo del endometrio lo que causa su involución.

MIOMAS UTERINOS

Los miomas uterinos, también llamados leiomiomas, son tumores benignos estrógeno-dependientes que se desarrollan en la capa de tejido de miometrio. Están formados por células musculares lisas y fibroblastos intercalados en una abundante MEC compuesta por colágeno, fibronectina y proteoglicanos. La formación de dicha MEC juega un papel importante en la expansión tumoral, sin embargo, es importante destacar que los miomas uterinos tienen tasas de proliferación *in vivo* bajas, por lo que son tumores benignos.

La **clasificación de los miomas uterinos** está basada en su localización en las capas del útero. En base a ella, los miomas submucosos son aquellos que deforman el endometrio o protruyen

la cavidad uterina. Los miomas subserosos, protruyen desde la capa más externa del útero (la serosa), dando lugar a úteros con forma irregular. Finalmente, los miomas que crecen entre la pared uterina se denominan miomas intramurales. La mayoría de los miomas son en realidad una combinación de varios de estos tipos.

Aunque la mayoría de los miomas son asintomáticos, en el 25% de los casos están asociados a **síntomas graves** los cuales pueden dividirse en tres grupos principales: sangrado uterino anormal, dolor y/o presión pélvica y disfunción reproductiva. Tanto la localización como el tamaño de los miomas uterinos son determinantes en sus manifestaciones clínicas o síntomas. Mientras que los miomas subserosos están más relacionados con el dolor y la presión pélvica, los miomas submucosos afectan a la integridad endometrial, implantación y la capacidad de contracción del miometrio. Como resultado, este tipo de miomas suelen asociarse con sangrado uterino anormal, infertilidad y aborto de repetición.

Aunque la **patogénesis de los miomas uterinos** es desconocida, tradicionalmente éstos han sido definidos como tumores monoclonales, lo que significa que cada mioma surge de la expansión clonal de una única célula muscular del miometrio transformada por una mutación. Esta definición ha sido apoyada por diferentes evidencias científicas que demuestran la presencia de células madre en el miometrio y su implicación en la formación de los miomas uterinos. El miometrio humano, como otros tejidos y órganos, contiene una población de células madre somáticas que representa el 2% de su población celular total. Las células madre de los tejidos adultos, mediante división asimétrica, mantienen su habilidad de auto-renovación mientras dan lugar a células hijas parcialmente diferenciadas, las cuales se diferencian y participan en los procesos de regeneración y reparación. Una de las hipótesis más apoyadas acerca de la patogénesis de los miomas propone que las células madre del miometrio están implicadas en el desarrollo de los miomas. De acuerdo con esta hipótesis, las células madre de los miomas surgirían de una célula madre miometrial la cual sufre una transformación tumorigénica debido a una mutación o cambio. Dicha transformación resulta en una célula madre con una aumentada capacidad de auto-renovación y proliferación que da lugar a un mioma.

De acuerdo con esta teoría, se han descrito cuatro tipos de miomas en función de sus **alteraciones genéticas**. Los miomas con mutación en el gen *mediator complex subunit 12*

(*MED12*), los cuales son los más abundantes con una frecuencia entre 48-92% en función del grupo étnico. Dada la relación entre *MED12* y la ruta de señalización Wingless-type (Wnt)/β-catenina, se ha demostrado que los miomas con esta mutación presentan esta ruta sobreexpresada, resultando en un aumento de la proliferación. Así mismo, la deficiencia de *MED12* resulta en la activación de la ruta de señalización de TGFβ, lo cual daría lugar a un aumento en la producción de MEC. El resto de las alteraciones genéticas descritas en los miomas son los reordenamientos del gen *high mobility AT-hook 2* (*HMAG2*), la inactivación del gen *fumarate hidratase* (*FH*) y las deleciones del gen *collagen type IV α5* (*COL4A5*) y *α6* (*COL4A6*).

Dentro de la patogénesis de los miomas se ha descrito la relación paracrina entre las diferentes poblaciones celulares del mioma implicada en el desarrollo de los mismos. En este sentido, se conoce que las células madre del miometrio y del mioma expresan menos receptores de estrógenos y progesterona en comparación con las células diferenciadas. Del mismo modo, se ha descrito que los estrógenos y la progesterona actúan al nivel de las células maduras, enviando a través de ellas factores paracrinos a las células madre e induciendo su proliferación. En esta interacción paracrina la ruta de señalización Wnt/β-catenina desempeña un papel importante. Más en detalle, se ha propuesto que los estrógenos y la progesterona inducen la expresión de ligandos Wnt en las células maduras de mioma y miometrio, los cuales a su vez inducen la entrada nuclear de la β-catenina en las células madre del mioma, la cual se une a los factores TCF/LEF (por sus siglas en inglés *T-cell factor/lymphoid enhancer factor*) estimulando la expresión de sus genes diana implicados en la regulación de procesos celulares importantes como la proliferación. Además, la ruta Wnt/β-catenina puede estimular la expresión del *TGFβ3,* resultando en un aumento en la producción de MEC y proliferación celular. El resultado biológico de esta interacción paracrina es un aumento en el crecimiento del tumor como consecuencia del aumento en la proliferación celular y la formación de MEC, así como una disminución en la apoptosis.

Los miomas uterinos, al ser dependientes de las hormonas ováricas, representan el tumor benigno más común del tracto reproductivo en mujeres con una **incidencia** del 70% en mujeres en edad reproductiva. Además de las hormonas esteroideas otros factores han sido relacionados con el riesgo de presentar miomas uterinos: edad, raza, estado reproductivo, historia familiar, obesidad y dieta. Así mismo, es importante destacar que se ha demostrado

una relación entre el riesgo de miomas uterinos y el déficit de Vitamina D. Diferentes estudios han reportado niveles de Vitamina D insuficientes en mujeres con miomas, así como una relación inversamente proporcional entre el tamaño del mioma y el nivel de Vitamina D en suero.

Las opciones actuales para el **tratamiento de los miomas uterinos** pueden dividirse en tres grandes grupos: opciones quirúrgicas, no quirúrgicas y médicas. Las opciones quirúrgicas, histerectomía o miomectomía, son las más agresivas. Entre las opciones no quirúrgicas se encuentran la embolización de la arteria uterina o la miolisis, las cuales presentan la ventaja de ser menos agresivas pero sus efectos sobre la fertilidad todavía no han sido aclarados.

En cuanto a los tratamientos médicos existen opciones que alivian los síntomas de los miomas, pero no reducen su tamaño. Dentro de éstos encontramos, los tratamientos no hormonales, como los antiinflamatorios no esteroides, los anticonceptivos orales o el dispositivo intrauterino que libera progesterona. Por otro lado, los análogos de la GnRH han sido ampliamente utilizados para reducir el tamaño de los miomas, aunque en la actualidad están en desuso debido a que generan una "pseudomenopausia" que causa sofocos y pérdida de densidad mineral ósea además de impedir la gestación durante el periodo de tratamiento. Otra de las opciones son los moduladores selectivos de los receptores de progesterona como el Tamoxifeno y el Raloxifeno, los cuales a pesar de ser efectivos en el tratamiento de los miomas presentan efectos secundarios como cambios endometriales, desarrollo de quistes ováricos, sofocos, aumento del apetito y de peso. En cuanto a los inhibidores de la aromatasa, como el Letrozol y el Anastrozol, aunque se ha demostrado que son eficaces disminuyendo el tamaño de los miomas, no existen evidencias suficientes para recomendar su uso para el tratamiento de miomas sintomáticos. Por último, el uso de moduladores selectivos de los receptores de progesterona para el tratamiento de los miomas ha ido creciendo en los últimos años. Dentro de este grupo de compuestos cabe destacar el Acetato de Ulipristal, el más utilizado en la actualidad por reducir el tamaño de los miomas uterinos, así como el sangrado y el dolor asociados a los mismos. Sin embargo, dicho tratamiento causa cambios endometriales conocidos como PAEC (del inglés *Progesterone receptor modulator Associated Endometrial Changes)* que impiden administrarlo durante periodos largos. Así mismo, en febrero de 2018 la Agencia Española del Medicamento y Productos Sanitarios (AEMPS) notificó casos graves de daño hepático en mujeres tratadas con Acetato de Ulipristal,

recomendado no iniciar nuevos tratamientos. Finalmente, en julio del mismo año, tras una reevaluación del riesgo, la AEMPS restringió el uso de Acetato de Ulipristal como tratamiento preoperatorio de los miomas uterinos con una duración máxima de 3 meses.

Por lo tanto, pese a la gran incidencia de los miomas uterinos y la gran variedad de opciones terapéuticas, en la actualidad no existe ningún tratamiento que reduzca el tamaño de los miomas de manera eficiente, mínimamente invasiva y sin efectos secundarios.

POTENCIALES TRATAMIENTOS DE LOS MIOMAS UTERINOS: VITAMINA D

En la búsqueda de nuevos tratamientos para los miomas uterinos, la correlación negativa entre el déficit de Vitamina D y el riesgo de miomas uterinos, junto con el potencial terapéutico de dicha vitamina descrito en cáncer, centraron la atención en la Vitamina D como posible tratamiento.

Aunque históricamente se ha considerado a la homeostasis del calcio como la función principal de la Vitamina D, más en concreto su metabolito activo 1,25-dihydroxyvitamina D_3 ($1,25(OH)_2D_3$) ésta es una hormona multifuncional que también regula múltiples procesos celulares como la proliferación y diferenciación celular. En este sentido, diversos estudios han demostrado los efectos anticancerígenos de $1,25(OH)_2D_3$ en diferentes tipos de cáncer y se ha propuesto que dichos efectos son mediados a través de tres mecanismos principales que se detallan a continuación. Por un lado, se ha demostrado que la Vitamina D en células de **cáncer** induce un arresto del ciclo celular, impidiendo la progresión del mismo y, por tanto, disminuyendo la proliferación. Por otra parte, la Vitamina D inhibe la ruta de señalización Wnt/β-catenina resultando en una disminución de sus genes diana, los cuales participan en procesos celulares tales como proliferación celular, migración y diferenciación. Finalmente, se ha demostrado que la acción antitumoral de la Vitamina D no es debida solamente a su efecto antiproliferativo si no que también es capaz de inducir apoptosis en las células del cáncer.

Teniendo en cuenta los efectos anticancerígenos de la Vitamina D descritos en cáncer, los cuales proponen a esta vitamina como un posible tratamiento para inhibir el crecimiento tumoral, y la correlación entre déficit de Vitamina D y el riesgo de miomas, diversos estudios han centrado su interés en elucidar si dicha vitamina tiene efectos antiproliferativos sobre los miomas. En este sentido diversos estudios *in vitro* han demostrado que la Vitamina D es capaz

de inhibir la proliferación y la producción de proteínas de la MEC, así como aumentar la apoptosis en una línea celular de miomas humanos. De manera similar, estudios *in vivo* han analizado el efecto del tratamiento con Vitamina D en los miomas de ratas Eker y miomas formados en ratones a partir de una línea celular derivada de miomas de ratas Eker, corroborando que dicho tratamiento disminuye el tamaño de los mismos. Finalmente, un estudio llevado a cabo en pacientes con miomas uterinos y déficit de Vitamina D demostró que la suplementación con dicha vitamina mantuvo el tamaño de los miomas tras un año de tratamiento.

Sin embargo, hasta la fecha no existe ningún estudio que evalúe en profundidad el efecto de la Vitamina D sobre los mecanismos moleculares implicados en el desarrollo de los miomas uterinos en células humanas de mioma, ni en modelos animales que utilicen tejido humano, los cuales mantienen las características fisiológicas de los miomas.

HIPÓTESIS

La Vitamina D, concretamente su metabolito activo 1,25-dihydroxyvitamina D_3, podría jugar un papel importante en la patogénesis de los miomas uterinos a través de la regulación de sus rutas de señalización: ciclo celular, proliferación celular, ruta de señalización Wnt/β-catenina y apoptosis, disminuyendo el crecimiento de los miomas uterinos.

OBJETIVOS

El principal objetivo de esta tesis es analizar el efecto del tratamiento con Vitamina D en el crecimiento de los miomas uterinos con el fin de evaluar su potencial como agente terapéutico para reducir su tamaño.

Objetivos específicos:

1. Determinar *in vitro* el efecto del tratamiento con Vitamina D en células de miomas uterinos humanos a través de la regulación del ciclo celular, la proliferación celular, la ruta de señalización Wnt/β-catenina y la apoptosis.
2. Determinar *in vivo* en un modelo animal heterólogo el efecto del tratamiento con Vitamina D a través de la regulación de la proliferación celular, la formación de matriz extracelular y la apoptosis.

METODOLOGÍA

Las muestras humanas de miomas uterinos, así como miometrio adyacente utilizados en este estudio, ensayos *in vitro* e *in vivo,* fueron recogidas de pacientes con edades comprendidas entre 35-54 años las cuales se sometieron a miomectomía o histerectomía debido a miomas uterinos sintomáticos. Ninguna de las pacientes recibió tratamiento en los meses previos a la cirugía. Este estudio fue aprobado por el Comité Ético del Hospital Universitario y Politécnico La Fe (España) (2014/0691) y todas las pacientes entregaron el consentimiento informado.

ENSAYO *IN VITRO*

Evaluación de los tejidos de mioma uterino y miometrio adyacente

Con el fin de determinar la implicación de la proliferación, la ruta Wnt/β-catenina y la apoptosis en el desarrollo de los miomas uterinos, la expresión de las proteínas PCNA (por sus siglas en inglés*; proliferating cell nuclear antigen*), WISP1 (por sus siglas en inglés; *Wnt1-inducible-signaling pathway protein 1*), BCL2 (por sus siglas en inglés, *B-cell lymphoma-2*), y BAX (por su siglas en inglés, *BCL2 Associated-X*) fue medida mediante western blot en los tejidos de mioma y miometrio adyacente (n=22).

Tratamiento con Vitamina D en células primarias de miomas uterinos humanos y ensayos funcionales

Para testar el efecto de la Vitamina D sobre los miomas uterinos *in vitro*, los miomas recogidos fueron procesados mediante medios mecánicos y enzimáticos para obtener células primarias de miomas.

Dichas células primarias de miomas humanos fueron cultivadas a 37°C y 5% CO_2 en medio de cultivo y tratadas con/sin 100nM de Vitamina D ($1,25(OH)_2D_3$) para evaluar su efecto sobre las vías de acción de dicha vitamina, las cuales han sido previamente descritas en cáncer, mediante diferentes ensayos funcionales:

- Arresto del ciclo celular: Las células derivadas de miomas humanos (n=22) fueron tratadas en ausencia o presencia de 100nM de $1,25(OH)_2D_3$ durante 144 horas, y el análisis del ciclo

celular y del contenido de ADN se llevó a cabo mediante citometría de flujo por tinción con ioduro de propidio (IP).

- Proliferación: Las células primarias de miomas humanos (n=15) fueron tratadas en ausencia o presencia de 100nM de $1,25(OH)_2D_3$ durante 48 horas y la expresión de PCNA fue medida mediante western blot con el fin de evaluar la proliferación celular.
- Ruta de señalización Wnt/β-catenina: Las células primarias de miomas humanos (n=11) fueron tratadas en ausencia o presencia de 100nM de $1,25(OH)_2D_3$ durante 48 horas y el efecto de dicho tratamiento sobre la ruta Wnt/β-catenina a nivel genético fue evaluado mediante RT^2-Profiler PCR Arrays (Qiagen, Alemania) y a nivel proteico mediante Quantibody Human Cytokine array (RayBiotech, EE. UU.).
- Apoptosis: Las células de miomas humanos (n=11) fueron tratadas en ausencia o presencia de 100nM de $1,25(OH)_2D_3$ durante 48 horas y el efecto de dicho tratamiento sobre la apoptosis a nivel genético fue evaluado mediante RT^2-Profiler PCR Arrays (Qiagen, Alemania). Además, el porcentaje de células apoptóticas se midió mediante ensayo TUNEL.

ENSAYO *IN VIVO*

Con el objetivo de evaluar *in vivo* el efecto del tratamiento con Vitamina D en miomas uterinos humanos, generamos un modelo animal heterólogo y, seguidamente evaluamos el efecto del tratamiento con Vitamina D a corto y largo plazo en dicho modelo. Los procedimientos realizados con animales fueron aprobados por el Comité Ético de Bienestar Animal de la Universitat de València (2017/VSC/PEA/00017).

Establecimiento de un modelo animal heterólogo de miomas uterinos

Para la generación de un modelo animal heterólogo de miomas, se recogieron miomas intramurales de pacientes las cuales se sometieron a miomectomía o histerectomía, los cuales se cortaron en fragmentos de aproximadamente 3-4 mm^3. Posteriormente, dos fragmentos de miomas humanos se implantaron intraperitonealmente en ratonas NOD-SCID (código de cepa 394; NOD.CB17-Prkdcscid/N) (Charles River Laboratories, Francia) previamente ovariectomizadas y suplementadas con estrógenos y progesterona.

Tratamiento con Vitamina D en un modelo animal heterólogo de miomas uterinos humanos y ensayos funcionales

Una semana después del implante de los miomas uterinos, los animales fueron divididos en tres grupos de estudio:

1) Control (tratados con Etanol, vehículo de la Vitamina D)

2) $1,25(OH)_2D_3$ 0.5 µg/kg/día

3) $1,25(OH)_2D_3$ 1 µg/kg/día

En el ensayo *in vivo* los tratamientos se administraron mediante bombas osmóticas (Alzet, EE. UU.) durante 21 días en el tratamiento a corto plazo (10 animales /grupo) y durante 60 días en el tratamiento a largo plazo (6 animales /grupo).

Durante el tratamiento, se llevó a cabo la **monitorización no invasiva** de los miomas uterinos mediante la realización de estudios PET/TAC usando el radiofármaco ^{18}F-FDG, un análogo de la glucosa, que permite la detección de células con una alta captación de glucosa como son las células cancerígenas. Además de detectar los miomas generados, los estudios PET/TAC permiten medir la actividad metabólica de los mismos ayudando a evaluar el efecto del tratamiento sobre su tamaño.

Tras finalizar ambos estudios, a corto y largo plazo, los animales fueron sacrificados y se recogieron los miomas.

Para evaluar el efecto del tratamiento sobre el **tamaño de los miomas**, los fragmentos fueron medidos con un calibrador digital antes del implante y tras finalizar el tratamiento.

Posteriormente se llevaron a cabo diferentes ensayos funcionales para evaluar el efecto del tratamiento con Vitamina D a través de diferentes vías:

- Proliferación: el efecto del tratamiento se evaluó en los miomas generados, mediante el análisis de dos marcadores de proliferación: Ki67 mediante inmunohistoquímica y PCNA mediante qRT-PCR.
- Densidad celular: para determinar el porcentaje de células por área de tejido se realizó la tinción con hematoxilina y eosina en los fragmentos de mioma.

- Matriz extracelular: la expresión de las proteínas de matriz extracelular COLAGENO I, FIBRONECTINA y Plasminogen Activator Inhibitor-1 (PAI-1) en los miomas generados fue evaluada mediante western blot.
- Ruta de señalización TGFβ: la expresión del gen *TGFβ3* en los miomas generados fue evaluada mediante qRT-PCR.
- Apoptosis: para evaluar el efecto del tratamiento sobre la apoptosis, la expresión de las proteínas PRO-CASPASA 3 y CASPASA-3 en los miomas generados fue evaluada mediante western blot. Así mismo, el % de células apoptóticas se midió mediante ensayo TUNEL.

RESULTADOS

ENSAYO *IN VITRO*

Evaluación de los tejidos de mioma uterino y miometrio adyacente

La evaluación de la proliferación, la ruta Wnt/β-catenina y la apoptosis en los tejidos de mioma y miometrio reveló que el 95% de los miomas presentaba mayor proliferación que su miometrio adyacente. Del mismo modo, en el 77% de los miomas la expresión de la ruta Wnt/β-catenina fue mayor que en su miometrio adyacente. Por el contrario, la evaluación de las proteínas implicadas en la apoptosis no mostró diferencias en la expresión entre los tejidos.

Tratamiento con Vitamina D en células primarias de miomas uterinos humanos y ensayos funcionales

El análisis del **ciclo celular** por citometría de flujo en las células primarias de miomas humanos mostró que en el 50% de los casos el tratamiento con Vitamina D indujo arresto celular en las mismas, disminuyendo el porcentaje de células en fase S-G_2/M. Del mismo modo, la expresión protéica del marcador de **proliferación celular** PCNA fue disminuida significativamente en las células de mioma tratadas con Vitamina D, indicando una disminución de la proliferación con el tratamiento con Vitamina D.

En cuanto al efecto del tratamiento sobre la ruta **Wnt/β-catenina**, los resultados obtenidos mediante el Array de expresión génica de genes implicados en dicha ruta, demostraron que la

Vitamina D inhibe significativamente la ruta Wnt/β-catenina a nivel genético en las células primarias de miomas humanas. Así mismo, la expresión de las proteínas de dicha ruta fue disminuida en las células tratadas con Vitamina D en comparación con el grupo control. Estos resultados indicaron que la Vitamina D inhibe la ruta Wnt/β-catenina tanto a nivel transcripcional como a nivel postranscripcional.

Por el contrario, ni el análisis de la **apoptosis** a nivel genético mediante el array de expresión de genes implicados en dicha ruta, ni el porcentaje de células apoptóticas determinado mediante el ensayo TUNEL, mostraron cambios significativos en la apoptosis en las células primarias de miomas humanos tratadas con Vitamina D.

ENSAYO *IN VIVO*

La evaluación de la **actividad metabólica** de los miomas generados en nuestro modelo animal heterólogo mediante monitorización no invasiva mostró que tras 21 días de tratamiento (ensayo a corto plazo) la actividad metabólica de los diferentes grupos de estudio fue similar. En cambio, en el ensayo a largo plazo, la actividad metabólica al final del tratamiento (60 días) de los miomas fue significativamente menor en los dos grupos tratados con Vitamina D al compararlos con el grupo control.

Del mismo modo, en el ensayo a corto plazo la evaluación del **tamaño de los miomas** generados a día 0 y día 21 no mostró diferencias en ninguno de los grupos de estudio a pesar de que, en el grupo control se observó una tendencia al aumento mientras que, en los grupos tratados con Vitamina D el tamaño se mantenía. Por el contrario, en el ensayo a largo plazo el tamaño de los miomas del grupo tratado con Vitamina D 1 µg/kg/día fue significativamente menor a día 60 comparado con su tamaño a día 0.

La evaluación de la **proliferación** en los miomas procedentes de los diferentes grupos de estudio al final del tratamiento con Vitamina D mostró resultados similares. Mientras que en el ensayo a corto plazo no se observaron diferencias en la expresión de los marcadores de proliferación Ki67 y PCNA en ninguno de los grupos, a largo plazo el tratamiento con Vitamina D 1 µg/kg/día disminuyó la expresión de Ki67 y PCNA, siendo dicha disminución significativa en el caso del Ki67, indicando que la Vitamina D disminuye la proliferación de las células de mioma.

El análisis de la expresión de proteínas de la **matriz extracelular (MEC)** mostró que, la expresión de COLAGENO I fue disminuida tanto a corto como a largo plazo, siendo esta disminución estadísticamente significativa con la dosis alta de Vitamina D (1 µg/kg/día) a largo plazo. En cuanto a la FIBRONECTINA, no se observaron cambios significativos en su expresión, aunque en el grupo tratado con Vitamina D 1 µg/kg/día durante 60 días se observó una disminución. Finalmente, la expresión de la proteína PAI-1 fue similar entre grupos en el ensayo a corto plazo, mientras que en el ensayo a largo plazo la expresión disminuyó con ambas dosis de Vitamina D, siendo dicha disminución significativa solo en el grupo tratado con la dosis alta (1 µg/kg/día). Posteriormente, con el fin de evaluar si la Vitamina D inhibe la expresión de proteínas de la matriz extracelular en los miomas uterinos a través de la **vía de señalización TGFβ**, la expresión del gen ***TGFβ3*** en los miomas generados en nuestro modelo animal fue evaluada. Los resultados mostraron una disminución de la expresión de dicho gen a corto plazo en ambos grupos tratados con Vitamina D. Además, en el ensayo a largo plazo, el grupo tratado con Vitamina D 1 µg/kg/día mostró una expresión significativamente menor de *TGFβ3* comparado con el grupo control.

Posteriormente, con el fin de confirmar que el tratamiento con Vitamina D disminuye la formación de MEC, se evaluó la **densidad celular** en los miomas generados. Tal y como esperábamos, el grupo tratado con la dosis alta de Vitamina D (1 µg/kg/día) durante 60 días mostró un aumento significativo del porcentaje de núcleos por área de tejido comparado con el grupo control, corroborando la disminución de la formación de MEC en los miomas tratados con Vitamina D.

Finalmente, la evaluación de la apoptosis mostró una disminución significativa de la expresión de la PRO-CASPASA 3 en ambos grupos tratados con Vitamina D en el ensayo a corto plazo. Del mismo modo, la expresión de ésta fue disminuida en el grupo tratado con Vitamina D 1 µg/kg/día durante 60 días. En cuanto a la CASPASA 3, no se observaron cambios entre grupos a corto plazo mientras que a largo plazo la expresión de dicha proteína aumento de manera dependiente de la dosis. Además, el porcentaje de células apoptóticas aumentó en ambos ensayos en el grupo tratado con Vitamina D 1 µg/kg/día comparado con su respectivo control. Estos resultados muestran un efecto anti-apoptótico de la Vitamina D sobre los miomas uterinos.

DISCUSIÓN

Los miomas uterinos son el tumor benigno más frecuente del tracto reproductivo femenino, afectando al 70% de las mujeres en edad reproductiva. A pesar de su alta prevalencia y de la gran variedad de tratamientos disponibles, en la actualidad no existe ningún tratamiento que reduzca el tamaño de los miomas uterinos de forma mínimamente invasiva y sin efectos secundarios. Aunque se desconoce la patogénesis exacta de los miomas, la relación descrita entre déficit de Vitamina D en suero y el riesgo de miomas uterinos, junto con los efectos antiproliferativos de dicha vitamina descritos en cáncer, señalaron a la Vitamina D como una posible opción terapéutica en el tratamiento de estos tumores. En este sentido, la acción de la Vitamina D en cáncer ha sido ampliamente estudiada, demostrando que sus efectos antitumorales implican mecanismos asociados con arresto del ciclo celular, inhibición de la ruta Wnt/β-catenina e inducción de la apoptosis.

En los miomas uterinos, aunque la acción de la Vitamina D ha sido evaluada en ensayos *in vitro* e *in vivo*, éstos utilizan líneas celulares de mioma, el modelo de la rata Eker o células derivadas del mismo, y centran su atención en una única ruta de señalización o mecanismo. Por lo tanto, los mecanismos moleculares a través de los cuales la Vitamina D podría actuar en las células primarias y tejidos de miomas humanos no han sido investigados de manera precisa.

Considerando lo anterior, el principal objetivo de esta tesis fue analizar el efecto del **tratamiento con Vitamina D** tanto ***in vitro,*** en células primarias de miomas humanos, como ***in vivo***, en un modelo animal generado a partir de miomas humanos, a través de los mecanismos descritos en cáncer, manteniendo las condiciones fisiológicas propias de los miomas uterinos y, por tanto, considerando la gran variabilidad inter-paciente, con el fin de evaluar su potencial terapéutico.

La evaluación de los tejidos previa al estudio *in vitro* reveló que la aumentada proliferación celular junto con la desregulación de la ruta de señalización Wnt/β-catenina en los miomas uterinos podrían ser una pieza clave en el desarrollo y crecimiento de los mismos, mientras que la apoptosis parece no estar implicada. Así mismo, los resultados ***in vitro*** demostraron que la Vitamina D ejerce una acción antiproliferativa en las células primarias de miomas humanos a través del arresto del ciclo celular y la inhibición de la ruta Wnt/β-catenina a nivel transcriptómico y post-transcriptómico, pero no a través de la regulación de la apoptosis. De

acuerdo con nuestros datos, sugerimos que la Vitamina D podría ser un tratamiento efectivo para prevenir el crecimiento de los miomas y estabilizar su tamaño.

El siguiente objetivo de la presente tesis fue corroborar ***in vivo*** el efecto antiproliferativo de la Vitamina D observado *in vitro,* en un modelo animal heterólogo generado por la implantación de fragmentos de mioma uterinos humanos en ratón, así como evaluar la apoptosis y la formación de MEC (lo cual es posible en el modelo animal gracias al mantenimiento de la estructura tridimensional de dicha MEC). Para ello, fragmentos de miomas uterinos humanos fueron implantados en ratonas las cuales fueron posteriormente tratadas sin Vitamina D o con Vitamina D (0.5 µg/kg/día y 1 µg/kg/día) a corto y largo plazo.

El estudio *in vivo* reveló que mientras el tratamiento con Vitamina D a corto plazo solo fue capaz de mantener el tamaño de los miomas, a largo plazo el tratamiento redujo significativamente su tamaño a través de la disminución de la proliferación celular, inhibición de la formación de MEC y aumento de la apoptosis en las células que lo forman, sin efectos secundarios. Nuestros datos sugieren que un tratamiento prolongado con Vitamina D podría ser considerado como un tratamiento efectivo para reducir el tamaño de los miomas uterinos en mujeres con déficit de dicha vitamina.

CONCLUSIONES

- Una aumentada proliferación celular junto con la desregulación de la ruta de señalización Wnt/β-catenina en los tejidos de miomas uterinos humanos podrían ser una pieza clave en el desarrollo y crecimiento de los mismos, mientras que la apoptosis parece no estar implicada en este tumor benigno.
- El tratamiento con Vitamina D inhibe el crecimiento de las células primarias de miomas humanos cultivadas *in vitro* a través de la inducción del arresto del ciclo celular en fase G_0/G_1 (disminuyendo el porcentaje de células en división) y la inhibición de la proliferación celular.
- La Vitamina D disminuye la expresión de genes y proteínas de la ruta Wnt/β-catenina implicados en mecanismos moleculares tales como migración, crecimiento y proliferación celular en las células primarias de miomas humanas *in vitro*, inhibiendo significativamente dicha ruta, sin embargo, la apoptosis no se vio aumentada por el tratamiento con Vitamina D en las células primarias de miomas humanos cultivadas *in vitro*.

- Aunque el tratamiento *in vivo* a corto plazo con la dosis alta de Vitamina D (1 µg/kg/día) disminuyó la proliferación celular y la producción de colágeno y aumentó la apoptosis, dichos efectos no fueron estadísticamente significativos, lo cual se ve reflejado en el mantenimiento del tamaño y actividad metabólica de los miomas generados en nuestro modelo animal.
- La dosis alta de Vitamina D (1 µg/kg/día) a largo plazo disminuyó significativamente la proliferación celular, la producción de proteínas de la matriz extracelular a través de inhibición de la vía de señalización TGFβ, así como aumentó la apoptosis, lo cual se vio reflejado en la disminución significativa del tamaño y actividad metabólica de los miomas generados en nuestro modelo animal.
- El tratamiento con Vitamina D a corto plazo podría ser una terapia efectiva para prevenir el crecimiento de los miomas y mantener su tamaño, mientras que un tratamiento con Vitamina D durante un periodo prolongado podría disminuir el tamaño de los miomas uterinos de manera efectiva, sin efectos secundarios asociados.

INDEX

ABBREVIATIONS

^{18}F-FDG	2-deoxy-2-[fluorine-18] fluoro-D-glucose
AEMPS	Spanish Agency of Medicine and Health Products
AMIDE	Amide's a Medical Image Data Examiner
ATS-DL	Alport syndrome with diffuse leiomyomatosis
Bb	Bilirubin
BCL-XL	B-cell lymphoma extra-large
BCL2	B-cell lymphoma 2
BMI	Body mass index
BSA	Bovine serum albumin
CCND1	Cyclin D1
CDKs	Cyclin-dependent kinase
cDNA	Complementary DNA
CKIs	CDK inhibitors
COL4A5	Collagen type IV α5
COL4A6	Collagen type IV α6
CT	Computed tomography
DKK	Dickkopf
DMEM	Dulbecco's Modified Eagle Medium
DNase I	Deoxyribonuclease I
ECM	Extracellular matriX

EDTA	Ethylenediaminetetraacetic acid
ELT-3	Eker rat-derived uterine leiomyoma cell line
ER	Estrogen receptor
EtOH	Ethanol
FBS	Fetal bovine serum
FH	Fumarate hydratase
FIGO	Federation of Gynecology and Obstetrics
FSH	Follicle-stimulating hormone
GDC	Genomic DNA Control well
GLU	Glucose
GnRH	Gonadotropin-releasing hormone
H&E	Hematoxylin and eosin
HLRCC	Hereditary leiomyomatosis and renal-cancer
HMGA2	High mobility AT-hook 2
HuLM	Human uterine leiomyoma
HULP	Human Uterine Leiomyoma Primary
IGF-1	Insulin-like growth factor 1
IHC	Inmunohistochemistry
IRS4	Insulin receptor substrate 4
KEGG	Kyoto Encyclopedia of Genes and Genomes
L	Leiomyoma
LH	Luteinizing hormone
LNG-IUS	Levonorgestrel-releasing intrauterine device

M	Myometrium
MED12	Mediator complex subunit 12
memVDR	Membrane Vitamin D receptor
MMP	Matrix Metalloproteinase
MRgFUS	Magnetic resonance-guided focused ultrasound surgery
NRF2	Nuclear factor erythroid 2-related factor 2
NSAIDs	Nonsteroidal anti-inflammatory drugs
PAEC	Progesterone receptor modulator associated endometrial changes
PAI-1	Plasminogen activator inhibitor-1
PBS	Phosphate Buffered Saline
PCNA	Proliferating cell nuclear antigen
PET	Positron emission tomography
PI	Propidium Iodine
PLAG1	Pleomorphic adenoma gene 1
PPC	Positive PCR Control
PR	Progesterone receptor
pRB	Retinoblastoma protein
PVDF	Polyvinylidene difluoride
qRT-PCR	Quantitative-real time polymerase chain reaction
RIN	RNA integrity number
RIN	Secreted Frizzled-related proteins
RIPA	Radioimmunoprecipitation assay
RNA	Ribonucleic acid
RNase A	Ribonuclease A

RTC Reverse Transcription Control

RXR Retinoid X receptor

SD Standard Deviation

SDS Sodium dodecyl sulfate

SDS-PAGE Sodium dodecyl sulphate-polyacrylamide

SERMs S elective Estrogen Receptor Modulators

SPF Specified pathogen free

SPRMs Selective Progesterone Receptor Modulators

SSC Somatic stem cells

TCF T-cell factor

TERT Telomerase reverse transcriptase

TGF- β Transforming growth factor β

TIMPs Tissue inhibitors of MMPs

Tsc2 Tuberous sclerosis 2

TUNEL Transferase-mediated dUTP nick end-labeling

UAE Uterine artery embolization

UF Uterine fibroids

UPA Ulipristal Acetate

UVB Ultraviolet B

VDR Vitamin D receptor

VDREs Vitamin D response elements

Vit D Vitamin D

WIF-1 Wnt inhibitory factor-1

WISP1 WNT1 Inducible Signaling Pathway Protein 1

Wnt Wingless-type

LIST OF FIGURES

LIST OF TABLES

I. INTRODUCTION

I. INTRODUCTION

1. UTERUS: ANATOMY AND ENDOCRINOLOGY

1.1. Female reproductive system

The female genital system consists of external genitalia—perineum and vulva—and internal organs—ovaries, fallopian tubes, uterus and vagina (Figure 1). These internal genitalia, located deep within the pelvic cavity, comprise two parts: the ovary, a glandular body where oocytes are formed; and a duct system of fallopian or uterine tubes, uterus and vagina. The fallopian tubes transport oocytes from the ovarian surface to uterine cavity. The uterus is a hollow organ shaped like an inverted pear that is responsible for housing and nurturing the fertilized oocyte during pregnancy. An adult uterus measures about 7 cm long, 5 cm wide and 3 cm thick, but during pregnancy it is enlarged four to five times (Ramírez-González *et al.*, 2016; Rogers, 2011).

The uterus itself comprises three parts: fundus, body and cervix. The uterine fundus is the superior part of the uterus and, in conjunction with the body, forms the superior two-thirds of the organ. The uterotubal union, where fallopian tubes enter the uterus, is located between the fundus and the body. The cervix, separated from the body by the uterine isthmus, connects the uterus with the vagina, the lowest portion of the female genital tract (Ramírez-González *et al.*, 2016).

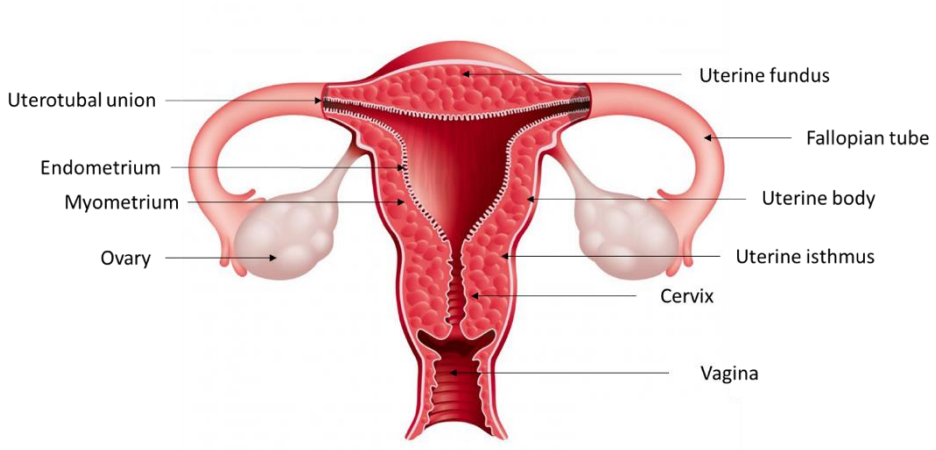

Figure 1. Female internal reproductive organs. *The uterus is divided in three parts: fundus, body and cervix. The vagina is the inferior portion of the female reproductive tract and connects with the cervix. Fallopian tubes, located between the uterine fundus and body, connect the uterus with the ovaries. Image adapted from www.biologianet.com*

The uterine wall is composed of three layers: endometrium, myometrium and perimetrium (Figure 2). The endometrium is a mucosal layer that covers the uterine cavity, which is divided in two parts: *stratum functionalis,* which is shed during menstruation, and *stratum basale*, adjacent to the myometrium, which is retained and serves to regenerate the functional layer. The myometrium is the thickest (12-15 mm) and most vascularized layer of the uterus, and is composed of smooth muscle cells embedded in a collagen-rich extracellular matrix (ECM). The smooth muscle is distributed in three distinct anatomical layers in which the muscle presents different orientations: the innermost layer, arranged in a circular orientation; the middle and thickest layer with fibers in all directions and lacking any orderly arrangement; and the outermost layer, which has longitudinal fibers. During pregnancy the muscle cells both divide (hyperplasia) and enlarge (hypertrophy), so that the uterus can grow while the endometrium nourishes the pregnancy. The perimetrium is a serosal layer that covers the uterine body and fundus (Coad and Dunstall, 2011; Ramírez-González *et al.*, 2016; Rogers, 2011).

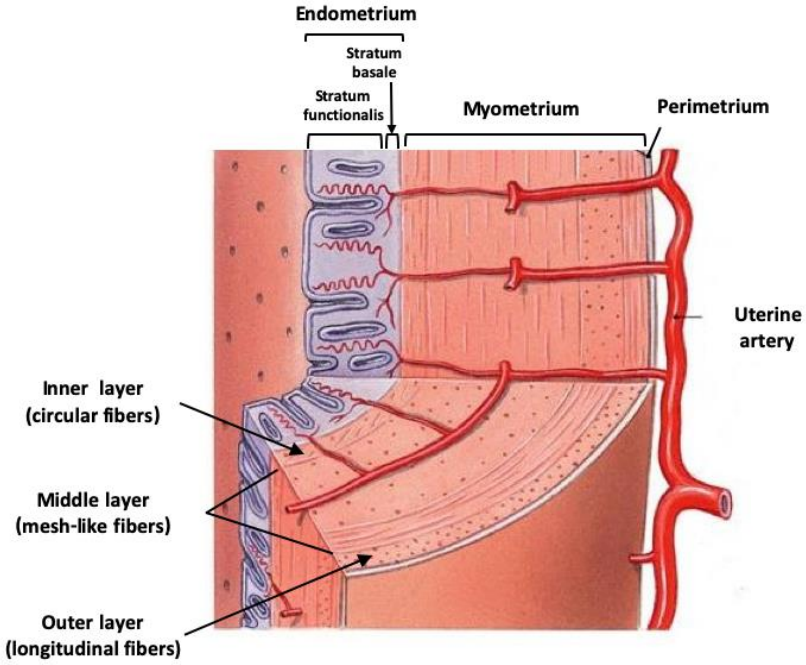

Figure 2. The uterine wall. *The uterine wall consists of three layers: endometrium, myometrium and perimetrium. The myometrium is the most vascularized layer and consists of three different layers in which muscle fibers present different orientations: circular orientation in the inner layer, multi-directional fibers in the middle layer, and longitudinal orientation in the outer layer. Image adapted from www.austincc.edu*

1.2. Extracellular matrix of the uterus

The extracellular matrix (ECM) is an important part of the uterine myometrium. The ECM plays a crucial role in the growth and remodeling of the uterus during pregnancy, parturition and the postpartum period, due to the its principal functions in adhesion, cell-to-cell communication and differentiation. This ECM is a three-dimensional network of extracellular macromolecules that provides structural and biochemical support to surrounding cells. Components of ECM are produced intracellularly by resident cells and secreted into the ECM via exocytosis. Once secreted, they are aggregated in the existing matrix. ECM is composed of an interlocking mesh of fibrous proteins and glycosaminoglycans (Basu, 2016).

One of the major components of uterine ECM are collagen fibrils, among which smooth muscle cells are interspersed. The collagen superfamily proteins include twenty-nine types of collagens that have three polypeptide chains assembled into triple-helical structures. The main collagens found in myometrium are Type I, Type III and Type V, which are responsible for the mechanical strength of uterine tissue (Leppert *et al.*, 2014).

Another important component of ECM are proteoglycans, which are glycoproteins consisting on a protein core with glycosaminoglycans attached covalently. These molecules attract cations and bind water, allowing the tissue to adapt to pressure changes. Some of the proteoglycans present in the uterine ECM are decorin, hyaluron or versican, which are involved important processes, such as the control of cell growth and differentiation.

Elastin, a hydrophobic protein, is another essential component of this matrix that provides elasticity to tissues, allowing them to stretch and recoil back to their original state (Basu, 2016). In the uterus, elastin is found in fibrils and thin sheets that, during pregnancy, allow the uterus to increase in size, stretch and eventually recoil (Leppert *et al.*, 2014).

Moreover, integrins are transmembrane receptors formed by two subunits (α and β) that contain three portions: cytoplasmic, transmembrane and extracellular. These receptors mediate signals between cells and ECM and vice versa and act as mechanosensors participating in important processes, such us adhesion, ECM organization, signaling or cell survival (Leppert *et al.*, 2014; Vinatier, 1995).

Finally, fibronectin is a multifunctional ECM molecule that acts as an organizer of matrix assembly binding collagen, integrins and other ECM molecules (Leppert *et al.*, 2014). In addition, fibronectin participates in processes involving ECM remodeling or assembly such as cell migration, adhesion, growth, differentiation or fibrosis (Islam *et al.*, 2018).

The degradation and changes that uterine ECM undergoes are controlled by the matrix metalloproteinase (MMP) system. MMPs are enzymes with proteolytic activity and are partly regulated by tissue inhibitors of MMPs (TIMPs). The expression of MMPs and TIMPs is influenced by pro-inflammatory cytokines, hormones and growth factors such as transforming growth factor β (TGFβ). In particular, TGFβ1 increases the expression of TIMPs and decreases the expression MMPs in human uterine myometrial cells, highlighting the role of TGFβ in the myometrium ECM turnover (Ma and Chegini, 1999). The balance between the expression of both MMPs and TIMPs is essential to the control of MMP activity, and therefore fundamental in the dynamic structural changes associated with the menstrual cycle as well as pregnancy-related ECM remodeling processes. Consequently, an improper control of the MMP system can promote pathological conditions such as ovarian cysts, endometriosis or uterine fibroids (Curry and Osteen, 2003; Ma and Chegini, 1999).

1.3. Endocrinology of the uterus

The reproductive years in women are characterized by the menstrual cycle, which is the result of monthly rhythmic changes in the rates of secretion of sex hormones controlled by the hypothalamus-pituitary-ovarian axis. This control starts in the hypothalamus, where gonadotropin-releasing hormone (GnRH) is released in a pulsatile way and travels to the pituitary. The pulsatile release of GnRH is critical to reproductive function. This means that an increase or decrease in GnRH inhibits the entire system. At the pituitary level, GnRH stimulates the biosynthesis and release of two gonadotropins that control the ovaries: luteinizing hormone (LH) and follicle-stimulating hormone (FSH) (Coad and Dunstall, 2011). The menstrual cycle includes the ovarian cycle and the endometrial cycle, both of which occur at the same time and are highly coordinated through mutual interaction.

The **ovarian cycle** presents two phases, the follicular and luteal phases, separated by ovulation. FSH is the predominant gonadotropin during the follicular phase, and stimulates the growth of the ovarian follicle while controlling the production of estrogen in the ovary (Coad and Dunstall, 2011) (Figure 3). LH plays the dominant role during the second half of the ovarian cycle, starting with an initial surge that leads to ovulation. After oocyte release, the corpus luteum is formed, and LH stimulates and maintains the production of progesterone (Figure 3). Both steroids hormones, estrogen and progesterone, provide negative feedback to the hypothalamus and pituitary, resulting in a repression of the stimulating hormones. In addition, these hormones also affect many body tissues such us breast, bone, hair follicles, muscle and, of course, uterus (Coad and Dunstall, 2011; Stewart, 2007).

The **endometrial cycle** comprises two parts: the proliferative phase, corresponding to the follicular phase in the ovary; and the secretory phase, corresponding to the luteal phase. The proliferative phase is the time from menstruation to ovulation. During this phase, the endometrial lining thickens, transforming it into a proliferative pattern due to the action of estrogen (Figure 3). The secretory phase includes the time from ovulation until menstruation. In this phase, progesterone is produced after ovulation by the corpus luteum causes the endometrium to secrete glycogen and mucus during the early secretory phase. In the mid-secretory phase, the endometrium becomes decidualized and receptive to a fertilized oocyte. Finally, in the late secretory phase, if pregnancy does not take place, estrogen and progesterone levels fall, leading to a reduced blood flow of the endometrium that causes its involution (Hawkins and Matzuk, 2008). Apart from its effect on the endometrium, progesterone decreases the frequency and intensity of uterine contractions, helping to prevent the expulsion of the implanted embryo (Hall and Guyton, 2011).

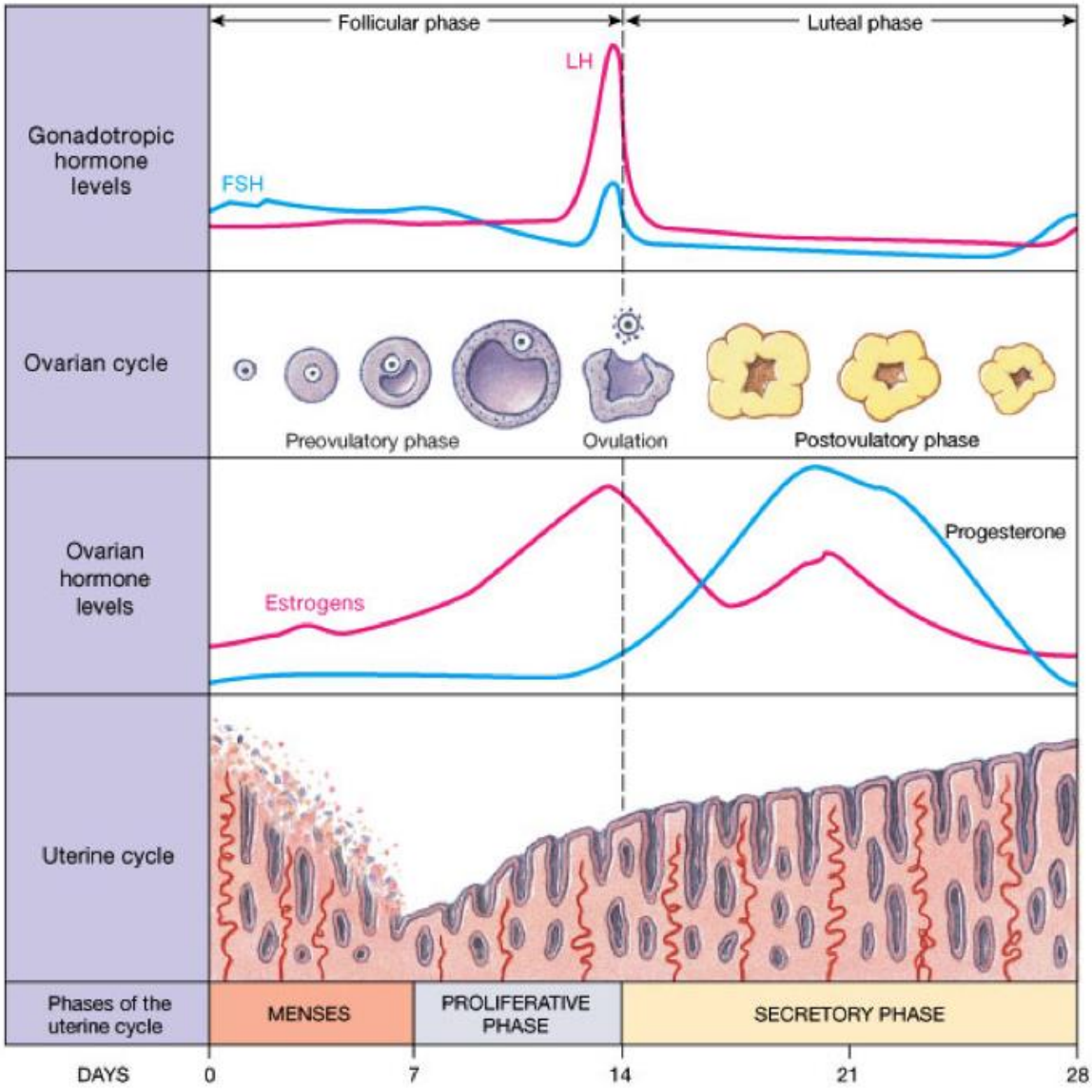

Figure 3. Ovarian and endometrial cycle. *Luteinizing hormone (LH) and follicle-stimulating hormone (FSH) control the ovarian cycle, which consists of two phases, follicular and luteal, separated by ovulation. The steroids hormones produced by the ovaries control the uterine or endometrial cycle, which has two parts: proliferative and secretory phases, corresponding with follicular and luteal phases, respectively. Image from http://physiologyplus.com*

2. UTERINE LEIOMYOMAS

2.1. Description

Uterine leiomyomas, also known as uterine fibroids, are benign estrogen-dependent tumors that arise from myometrium. They are composed of disordered smooth muscle cells and fibroblasts interspersed in an abundant ECM containing collagen, fibronectin and proteoglycans. Collagen fibers in uterine leiomyomas have a distorted spatial structure differing from their structure in normal myometrium. Uterine leiomyoma cells proliferate at a modest rate *in vivo* and ECM formation plays an important role in tumor expansion (Bulun, 2013; Parker, 2007).

2.2. Classification

Based on its localization in the uterine layers, leiomyomas can be divided in three groups: submucosal, subserosal and intramural. **Submucosal leiomyomas** are those that distort the endometrium or protrude into the endometrial cavity. **Subserosal leiomyomas** protrude from the outer layer of the uterus (serosa), resulting in an irregularly-shaped uterus. Finally, when fibroids grow within the uterine wall, they are named **intramural leiomyomas**. Most fibroids are combinations of these various types. The International Federation of Gynecology and Obstetrics (FIGO) established a classification system of the causes of abnormal uterine bleeding in women of reproductive age, which enables discrimination between the different leiomyoma types (Figure 4). This system uses an 8-point numerical scale to describe the location of uterine leiomyomas (Munro *et al.*, 2011). Type 0 includes intracavitary lesions that are attached to the endometrium by a narrow stalk, also called pedunculated. Type 1 and 2 are submucosal leiomyomas with a portion of intramural lesion with type 1 being <50% and type 2 at least 50%. Type 3 comprises leiomyomas with an intramural location but in contact with endometrium, while type 4 lesions are intramural leiomyomas that are entirely within the myometrium, with no extension to the endometrial surface or to the serosa. Types 5-7 are subserosal leiomyomas with type 5 being at least 50% intramural, type 6 being <50% intramural, and type 7 being attached to the serosa by a stalk. Lastly, type 8 is reserved for leiomyomas that do not involve the myometrium, such us cervical lesions or lesions in the round (Munro *et al.*, 2011; Stewart *et al.*, 2016).

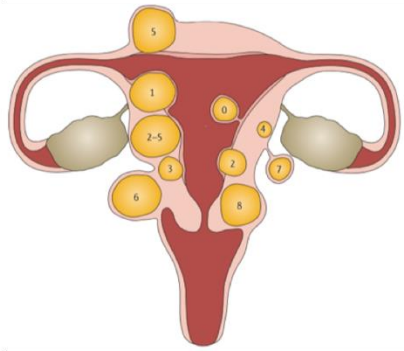

SUBMUCOSAL	**0**	Pedunculated intracavity
	1	< 50% intramural
	2	> 50% intramural
OTHER	**3**	contacts endometrium; 100% intramural
	4	Intramural
	5	Subserosal ≥ 50% intramural
	6	Subserosal < 50% intramural
	7	Subserosal pedunculated
	8	Other
	2-5	Hybrid leiomyomas

Figure 4. FIGO leiomyoma classification system. *The International Federation of Gynecology and Obstetrics (FIGO) established an 8-point numerical score to describe the location of uterine leiomyomas. Image adapted from (Munro et al. 2011) with the permission of John Wiley and Sons, and from (Stewart et al. 2016) with the permission of Springer Nature.*

2.3. Symptoms

Although most uterine leiomyomas are asymptomatic, severe symptoms occur in 25% of cases (Bulun, 2013; Stewart, 2001). These myoma-related symptoms can be divided in three main groups: abnormal uterine bleeding, mainly menorrhagia or hypermenorrhea; pelvic pressure and pain, and reproductive dysfunction (Stewart, 2001).

The location and size of uterine leiomyomas are determinants of their clinical manifestations or symptoms. While subserosal leiomyomas are more related with pelvic pressure and pain, submucosal leiomyomas affect endometrial integrity, implantation and myometrium capacity to contract and, therefore, stop endometrial bleeding. As a result, such fibroids are associated with abnormal uterine bleeding, infertility and recurrent pregnancy loss. Intramural leiomyomas are considered an intermediary group (Bulun, 2013; Stewart, 2001).

2.3.1. Abnormal uterine bleeding

The pathophysiology of heavy menstrual bleeding associated with uterine leiomyomas is unclear. However, several mechanisms have been proposed as possible causes. These potential mechanisms include increased endometrial surface area, increased uterine

vascularity, impaired uterine contractility, endometrial ulceration by submucosal fibroids or compression of the venus plexus within the myometrium (Sinai Talaulikar, 2018).

2.3.2. Pelvic pressure and pain

Women diagnosed with uterine leiomyoma more often experience significant pelvic pain, pressure on the bladder or inside the abdomen as well as painful sexual intercourse (Zimmermann *et al.*, 2012). Uterine leiomyomas can induce changes in uterus size and cause the organ to exert greater pressure on adjacent organs, resulting in pelvic pressure. Pelvic pain is proposed to result from two situations: when leiomyomas grow faster but with insufficient blood supply, or when a pedunculated leiomyoma twists (Stewart, 2007).

2.3.3. Reproductive dysfunction

Leiomyomas can have adverse effects on fertility. Importantly, these impacts are not only due to anatomic or functional changes of the uterine cavity or myometrium, but also to molecular changes.

Regardless of their localization, uterine fibroids can generate paracrine molecular changes that alter the adjacent endometrium and can cause excessive uterine bleeding or impair blastocyst implantation (Galliano *et al.*, 2015). Specifically, TGFβ produced by leiomyomas affects endometrial receptivity, as well as the production of anticoagulants in endometrium. Therefore, leiomyomas producing sufficient TGFβ levels and being localized near the endometrial cavity will affect fertility (Galliano *et al.*, 2015; Sinclair *et al.*, 2011). Similarly, the expression of HOX genes is decreased by uterine leiomyomas affecting endometrial receptivity and embryo implantation (Matsuzaki *et al.*, 2009; Purohit and Vigneswaran, 2016; Rackow and Taylor, 2010).

Moreover, obstetric outcomes can be affected by uterine leiomyomas. Women with uterine leiomyomas present higher risk of short cervix during pregnancy, as well as preterm delivery, primary cesarean section, breech presentation and lower-birthweight infants (Donnez and Dolmans, 2016).

2.4. Pathogenesis

The pathogenesis of uterine leiomyomas remains unclear, but they have been traditionally described as monoclonal tumors, meaning that each leiomyoma arises from the clonal expansion of a single myometrial smooth muscle cell transformed by a mutation (Bulun, 2013). This etiology has been confirmed by several studies.

2.4.1. Stem cells from myometrium and uterine leiomyoma formation.

Human myometrium, as with other tissues and organs, contains a population of somatic stem cells (SSC) that represent the 2% of its total cell population (Ono *et al.*, 2007). The SSC population of adult tissues, by asymmetric cell division, maintains their ability to self-renew while producing partially differentiated daughter cells known as transit amplifying cells. These cells are able to differentiate, resulting in terminally differentiated cell types that play a role in tissue regeneration and repair (Mas *et al.*, 2014; Ono *et al.*, 2012). During pregnancy, mechanical stretching of myometrium results in hypoxia. Taking into account that a hypoxic environment stimulates SSCs growth, hypoxia may promote the proliferation of myometrium SSCs and, consequently, uterine growth (Maruyama *et al.*, 2013).

One of the most supported hypotheses about uterine leiomyoma pathogenesis is that which proposes that myometrium SSCs are involved in leiomyoma development. According to this hypothesis, uterine leiomyoma stem cells arise from myometrium SSCs that have undergone tumorigenic transformation following a mutation. This transformation results in a stem cell with increased capacity for self-renewal and proliferation, giving rise to a leiomyoma. Among the factors proposed as possible causes of this transformation are uterine hypoxia, aberrant methylation or abnormal estrogen signaling (Ono *et al.*, 2012).

Finally, mutated myometrial SSC give rise to a population of leiomyoma stem cells, also called tumor-initiating cells, responsible for the formation and growth of the uterine leiomyoma, which comprises a small fraction of the smooth muscles that are part of the leiomyoma (1% of the total cell population) (Mas *et al.*, 2012; Ono *et al.*, 2012). As happens in SSCs, leiomyoma tumor-initiating cells undergo self-renewal, proliferate and clonally expand by giving rise to intermediately differentiated daughter cells. These daughter cells can then differentiate into a leiomyoma differentiated cell (Bulun *et al.*, 2015), leading to uterine leiomyoma formation.

2.4.2. Genetic alterations.

Recent studies based on high-throughput sequencing and hierarchical clustering have identified mutations or chromosomal alterations in key genes, demonstrating the existence of molecularly distinct subtypes of leiomyomas. Accordingly, four leiomyoma subtypes can be distinguished depending on the genetic alterations: mediator complex subunit 12 (*MED12*) mutation, high mobility AT-hook 2 (*HMGA2*) rearrangements, fumarate hydratase (*FH*) inactivation and collagen type IV α5 (*COL4A5*) and α6 (*COL4A6*) deletions (Mehine *et al.*, 2013, 2014, 2016).

→ ***MED12* mutations:** This mutation is detected at a frequency between 48 and 92% in leiomyomas from several studies with different ethnic groups (Mehine *et al.*, 2014). *MED12* encodes a subunit of the mediator complex, which regulates transcription by linking information between regulatory elements in gene promoters and the RNA polymerase II initiation complex (Bulun, 2013) and regulating signaling pathways involved in cell growth, cell differentiation and cell migration. β-catenin binds MED12 and activate Wingless-type (Wnt)/β-catenin signaling transcription (Kim *et al.*, 2006). Therefore, leiomyomas with *MED12* mutations express higher levels of *WNT4* and *β-catenin* compared to those lacking the mutation (Markowski *et al.*, 2012). Additionally, MED12 deficiency results in an activation of TGFβ signaling pathway (Huang *et al.*, 2012). It has been proposed that *MED12* mutations along with the activation of Wnt/β-catenin and TGFβ signaling pathways are part of a mechanism involved in leiomyoma stem-cell renewal, cell proliferation and fibrosis (Bulun, 2013).

→ ***HMGA2* rearrangements:** Cytogenetic rearrangements are present in 40 to 50% of leiomyomas. Among these, 20% exhibit a rearrangement of 12q14–q15, resulting in upregulation of the gene *HMGA2*. This gene encodes a transcription factor that induces conformational changes in chromatin structure affecting growth, differentiation, apoptosis and cellular transformation (Galindo *et al.*, 2018). Leiomyomas with rearrangements in *HMGA2* show an upregulation of the proto-oncogene pleomorphic adenoma gene 1 (*PLAG1*), whose ectopic expression is related to several benign tumors (Mehine *et al.*, 2016).

MED12 mutations and *HMGA2* rearrangements may account for 80%–90% of all leiomyomas. Although several studies support the idea that these alterations are mutually exclusive in leiomyomas (Bertsch *et al.*, 2014; Mehine *et al.*, 2014, 2016), a recent study showed that overexpression of *HMGA2* and *MED12* mutations frequently co-occur, suggesting their cooperation in leiomyoma development (Galindo *et al.*, 2018).

→ ***FH* inactivation:** The inactivation of *FH* results in the accumulation of intracellular fumarate and causes hereditary leiomyomatosis and renal-cancer (HLRCC) syndrome. Women with this mutation have a high risk of develop leiomyomas, which can have a distinct histology presenting increased cellularity as well as atypia with multinucleated cells (Mehine *et al.*, 2013; Stewart *et al.*, 2016). Although the mechanism of tumorigenesis of *FH* mutations remains unclear, leiomyomas with this mutation present deregulation of the nuclear factor erythroid 2-related factor 2 (NRF2) signaling pathway. This aberration suggests that the accumulation of fumarate results in the activation of the oncogenic transcription factor NRF2 (Mehine *et al.*, 2016), whose overexpression increases cell survival, cell growth and metastases (Arenas Valencia *et al.*, 2018).

→ ***COL4A5* and *COL4A6* deletions:** These deletions are found in a minority of leiomyomas. *COL4A5* and *COL4A6* deletions in the germline cause Alport syndrome with diffuse leiomyomatosis (ATS-DL), which displays leiomyomatosis of the esophageal, tracheobronchial and genitourinary tract. In uterine leiomyomas with deletions in *COL4A5-COL4A6,* insulin receptor substrate 4 (*IRS4*), a gene located downstream to *COL4A5*, is overexpressed. *IRS4* induces cell proliferation through the increase of insulin-like growth factor 1 (*IGF-1)* (Mehine *et al.*, 2014, 2016).

2.4.3. Paracrine interaction between leiomyoma cell populations.

In both myometrium and leiomyoma stem cell populations, the expression of estrogen and progesterone receptors is remarkably lower than in their differentiated cells (Mas *et al.*, 2012; Ono *et al.*, 2007). Estrogen and progesterone act on the tissue's mature cells and, through them, send paracrine factors to the stem cell population inducing its proliferation (Ono *et al.*, 2012). Thus, myometrium and leiomyoma growth are dependent on these steroid hormones. The presence of mature myometrial or leiomyoma cells along with this paracrine mechanism

are therefore essential for the proliferation of leiomyoma stem cells and consequent uterine leiomyoma formation.

Wnt/β-catenin signaling plays an important role in this paracrine pathway. In the presence of Wnt family signaling, β-catenin is activated and consequently translocated to the nucleus. There, β-catenin binds to the T-cell factor/lymphocyte enhancer factor (TCF/LEF) family of transcription factors, stimulating the expression of their target genes. Wnt/β-catenin target genes such as *C-MYC*, WNT1 Inducible Signaling Pathway Protein 1 (*WISP1*) or Cyclin D1 (*CCND1*) are important regulators of cell proliferation and, for that reason, this pathway plays a crucial role in neoplasia. A more detailed explanation of Wnt/β-catenin signaling pathway can be found in section 4.2.2. In leiomyomas, estrogen/progesterone treatment induces the expression of Wnt ligands in mature myometrial cells. This, in turn, induces nuclear translocation of β-catenin in leiomyoma stem cells, inducing TCF transcriptional activity and leading to the stem cell proliferation (Figure 5) (Ono *et al.*, 2013). The Wnt pathway can also stimulate the expression of transforming growth factor-β3 (*TGFβ3*), resulting in excessive ECM production and increased cell proliferation (Ciebiera *et al.*, 2017; Tanwar *et al.*, 2009) (Figure 5). Ultimately, paracrine stimulation results in enhanced tumor growth as a consequence of an increased cell proliferation and ECM formation, as well as a decreased apoptosis (Bulun, 2013).

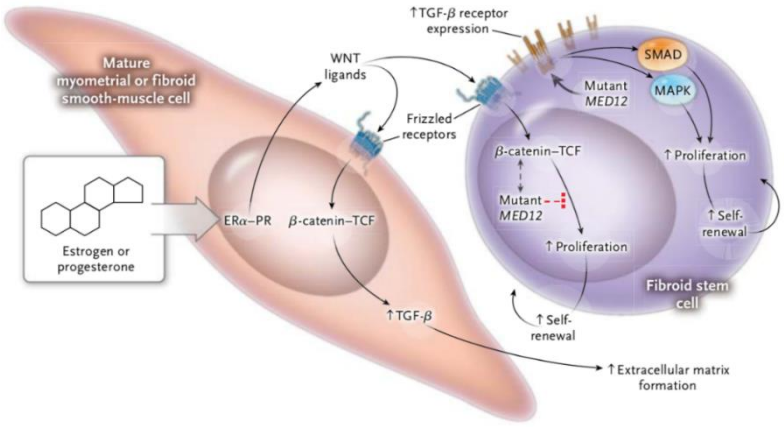

Figure 5. Paracrine interaction between leiomyoma cell populations. *In response to estrogen and progesterone, mature myometrial or leiomyoma cells secrete Wnt ligands, which stimulates the expression of Wnt/β-catenin signaling pathway target genes in leiomyoma stem cells, leading to increased proliferation. In addition, transforming growth factor β3 (TGFβ3) is also stimulated, resulting in increased extracellular matrix formation. Reproduced with permission from (Bulun SE. 2013), Copyright Massachusetts Medical Society.*

2.5. Incidence and epidemiology

Uterine fibroids are estrogen- and progesterone-dependent and represent the most common benign neoplasm of the reproductive tract, with a cumulative incidence of 70% in women of reproductive age. In addition to steroid hormones, other factors have been described as risk factor in uterine leiomyoma development and growth, such as age, ethnic group, reproductive status, family history, obesity, diet and Vitamin D deficiency.

2.5.1. Age

Because gonadal steroid production changes across the lifespan, age is a risk factor in leiomyoma development. Leiomyomas have not been described in pre-pubertal girls, but can begin to develop during adolescence. From adolescence, leiomyoma incidence increases, being most likely to be diagnosed in women aged between 30 and 40 years, when leiomyoma symptoms appear. Likewise, in many cases symptoms are relieved at the time of menopause (Bulun, 2013; Parker, 2007; Stewart *et al.*, 2016).

2.5.2. Ethnic group

The prevalence and incidence of uterine leiomyoma are higher in black women than in white women. In particular, the incidence of uterine fibroids in African-American women is 60% by age 35, increasing to >80% by age 50, while women of European descent show a rate of 40% and 70%, respectively (Baird *et al.*, 2003). In addition, black women develop uterine fibroids at an earlier age and are more likely to present severe symptoms than white women (Huyck *et al.*, 2008; Marshall *et al.*, 1997). Leiomyoma growth rates also decline with age in white women but not in black women, which could explain the greater presence of symptoms in the latter (Peddada *et al.*, 2008).

2.5.3. Reproductive status

Reproductive status is also involved in leiomyoma development and growth. Several studies have reported that the risk of fibroids decreases with an increasing number of pregnancies (Parazzini *et al.*, 1996; Ross *et al.*, 1986). It has been proposed that the remodeling process that the uterus undergoes during the postpartum period may have a protective effect (Day Baird and Dunson, 2003). Similarly, both time since last birth (Stewart *et al.*, 2017) and early

age at menarche (Marshall *et al.*, 1997) increase the risk of developing uterine leiomyomas. On the other hand, oral contraceptive use does not affect the development or growth of leiomyomas (Marshall *et al.*, 1998; Parazzini *et al.*, 1992; Qin *et al.*, 2013).

2.5.4. Family history

Family history of uterine leiomyomas is also related to an increased risk. This is likely due to the genetic factors involved in their development (Stewart *et al.*, 2017), specifically the *FH* inactivation involved in HLRCC syndrome (Stewart *et al.*, 2008).

2.5.5. Obesity

High body mass index (BMI) is correlated with the presence of uterine leiomyomas (Ross *et al.*, 1986), making obesity another risk factor in uterine leiomyoma development. This risk may be explained because obesity increases conversion of adrenal androgens to estrone, decreasing sex hormone-binding globulin and, therefore, increasing biologically available estrogen (Parker, 2007).

2.5.6. Diet

Diet is also involved in the risk of developing leiomyomas. Few studies have described that leiomyoma is associated with a diet heavy in red meat as well as alcohol consumption, whereas high intake of green vegetables seems to have a protective effect (Chiaffarino *et al.*, 1999; Wise *et al.*, 2004).

2.5.7. Vitamin D deficiency

Vitamin D deficiency has been strongly associated with an increased risk of uterine leiomyomas in both black and white women. Baird et al. found that 90% of black women and 50% of white women with uterine leiomyomas have levels of Vitamin D regarded as insufficient (≤20 ng/mL), suggesting that sufficient Vitamin D is associated with a reduced risk of uterine fibroids (Baird *et al.*, 2013). Moreover, several studies comparing Vitamin D serum levels in women with uterine leiomyomas versus control demonstrated that serum concentration of 25-hydroxyvitamin D_3 is significantly lower in affected women compared with controls (Paffoni *et al.*, 2013; Sabry *et al.*, 2013). In addition, an inverse correlation is observed between serum Vitamin D levels and total leiomyoma volume (Sabry *et al.*, 2013).

Considering that Vitamin D deficiency is more common in black women than in white women (Nesby-O'Dell *et al.*, 2002), this could explain why black women present higher risk of uterine leiomyoma than white women. All these data suggest that Vitamin D may play an important role in leiomyoma development.

3. CURRENT MANAGEMENT OF UTERINE LEIOMYOMAS

Uterine fibroid management options fall in three main groups: surgical, non-surgical and medical options. The choice among these management strategies depends on different factors such as the kind and size of leiomyoma, the symptoms and the age of the patient and her desire to preserve fertility. An example of an algorithm developed for the management of uterine fibroids according to the patient's profile can be found in Figure 6.

3.1. Surgical management.

Surgery is the main strategy for leiomyoma management; the most widely used surgical treatments are hysterectomy, laparoscopic myomectomy or hysteroscopic myomectomy. **Hysterectomy** is a surgery to remove the entire uterus and is the most radical option, but presents the advantage of the elimination of the risk of new fibroids. This option is usually selected in women not wishing to conceive or in their premenopausal age (40-50 years). On the other hand, **myomectomy** is a less invasive option that removes the leiomyoma while maintaining the uterus. For that reason, it is normally chosen in women seeking to reproduce. Myomectomy includes two options, laparoscopic or hysteroscopic, and the selection relies on the number, size and location of the leiomyomas (Donnez and Dolmans, 2016; Mas *et al.*, 2017). The main drawback of myomectomy is that it does not stop the process of leiomyoma formation and new ones may develop in the future (Stewart, 2007).

3.2. Non-surgical management.

Uterine artery embolization (UAE) is a minimally invasive treatment for uterine leiomyoma that temporarily blocks the blood supply to the uterus. This technique induces ischemic necrosis of the leiomyomas, while the myometrium revascularizes, allowing the treatment of multiple fibroids at the same time (Donnez and Dolmans, 2016; Stewart, 2007). In comparison with surgical options, UAE achieves similar results in terms of pain or discomfort. However,

the probability of reoperation is higher for UAE (Donnez and Dolmans, 2016; Mas *et al.*, 2017). Further, several reviews have founded poorer fertility outcomes after UAE than after myomectomy, although the authors noted the low-quality evidence around this association (Gupta *et al.*, 2014; Karlsen *et al.*, 2018).

Another non-surgical option is fibroid ablation, also known as **myolisis**, which consists in the destruction of the tissue using concentrated energy. High-frequency magnetic resonance-guided focused ultrasound surgery (MRgFUS) is used to induce necrosis in uterine leiomyomas. Even though it is an effective and minimally invasive alternative, its effect on future fertility is unclear (Donnez and Dolmans, 2016; Mas *et al.*, 2017).

3.3. Current medical management.

The medical treatment for leiomyomas aims to relieve symptoms, to shrink leiomyoma size and, if desired, to preserve fertility. The current medical options include several options.

3.3.1. Non-hormonal treatments

Nonsteroidal anti-inflammatory drugs (NSAIDs) along with tranexamic acid, an antifibrinolytic agent, are the non-hormonal treatments most commonly used to treat bleeding and pain associated with uterine fibroids.

NSAIDs are used to reduce prostaglandin levels due to the involvement of these molecules in the pathogenesis of heavy menstrual bleeding. Levels of prostaglandins E2 and F2α are higher in the endometrium of women with heavy menstrual bleeding compared to women with normal menses (Willman *et al.*, 1976). A systemic review about the effectiveness of NSAIDs for uterine fibroids concluded that this treatment reduces heavy menstrual bleeding when compared with placebo, but it is less effective than tranexamic acid or a levonorgestrel-releasing intrauterine device (Lethaby *et al.*, 2013).

Women with heavy menstrual bleeding present an increased activity of the fibrinolytic system in their endometrium during menstruation, which leads to accelerated degradation of the fibrin clot and increased menstrual blood loss (Chwalisz and Taylor, 2017). Tranexamic acid is a synthetic antifibrinolytic agent often used for the management of menorrhagia. Eder et al. demonstrated that treatment with tranexamic acid significantly reduce menstrual blood loss

in women with uterine leiomyomas. However, side effects such as menstrual discomfort, headache, backpain, nausea or anemia were reported (Eder *et al.*, 2013).

3.3.2. Combined oral contraceptives

Historically, the use of contraceptives containing synthetic analogues of steroid hormones has been considered as a risk factor for leiomyoma growth, due to the tumors' dependency on steroid hormones. However, the use of contraceptives does not influence the risk of leiomyoma development (Qin *et al.*, 2013). In the treatment of leiomyoma-related symptoms, combination oral contraceptives reduce menstrual bleeding, but they do not reduce leiomyoma size. Despite the latter, oral contraceptives are a good alternative in the treatment of heavy menstrual bleeding because they are easy accessible, administered orally and low cost (Sohn *et al.*, 2018).

3.3.3. Progesterone intrauterine device

The **levonorgestrel-releasing intrauterine system (LNG-IUS)** was originally developed for long-term (5 years) contraception, but is also used for the treatment of heavy menstrual bleeding. A T-shaped intrauterine device is sheathed with a reservoir of levonorgestrel that is released in the uterus. This local release has an antiproliferative action on the endometrium, which results in endometrial atrophy and, consequently, reduces both duration of bleeding and the amount of menstrual blood loss (Chwalisz and Taylor, 2017; Sinai Talaulikar, 2018). In uterine leiomyoma management, LNG-IUS decreases menstrual blood loss and increases blood hemoglobin, ferritin and hematocrit levels in women with symptomatic fibroids (Wrona *et al.*, 2017). The non-systemic administration of levonorgestrel reduces side effects. The main drawbacks of this device are that it can only be used in women in whom fibroids do not distort the endometrial cavity, and there is a higher risk of expulsion of the intrauterine device among patients with uterine leiomyomas (Sohn *et al.*, 2018; Stewart *et al.*, 2016).

3.3.4. GnRH analogs

One strategy for leiomyoma medical management focuses on the manipulation of the hypothalamus-pituitary-ovary axis. **GnRH agonists** have been widely used to shrink uterine leiomyomas, particularly before surgery. These compounds are structurally similar to natural

GnRH and therefore induce an increase in FSH and LH, known as the flare effect. Consequently, the expression of GnRH receptor is downregulated, resulting 1-3 weeks later in a hypoestrogenic state that causes a "pseudomenopause" and thereby, the impossibility of pregnancy during the treatment. The lack of estrogen leads to a decrease in leiomyoma size up to 47%. Derivative symptoms, however, such as hot flashes or decrease in bone mineral density, limit GnRH agonist to short-term therapy (Sohn *et al.*, 2018), 3-6 months at most. Furthermore, after discontinuation of the medication, leiomyomas rapidly increase in size, returning to pretreatment volume within 6 months (Stewart, 2001). With **GnRH antagonist** the result is the same, but these drugs present the advantage of the rapid onset of clinical effects. This is due to their mechanism of action; binding to the GnRH receptor inhibits its induced signaling and secretion. Despite this improvement, side effects associated with GnRH antagonists are the same as with agonists (Stewart *et al.*, 2016).

3.3.5. Selective estrogen receptor modulators

The expression of estrogen receptor (ER) in leiomyoma cells suggests that this hormone plays a role in its growth stimulation. **Selective Estrogen Receptor Modulators (SERMs)** are nonsteroidal, tissue-specific ER agonist/antagonist. Tamoxifen and Raloxifene are the SERMs studied in uterine leiomyomas.

Tamoxifen has been used in one prospective, randomized, blinded study comparing tamoxifen treatment with placebo in uterine leiomyoma patients (Sadan *et al.*, 2001). The results showed that tamoxifen significantly decreased blood loss as well as pain intensity. However, patients treated with tamoxifen present many side effects, including hot flashes, dizziness, endometrial changes and development of ovarian cysts. Therefore, the use of tamoxifen in leiomyoma treatment is not recommended (Sadan *et al.*, 2001; Sohn *et al.*, 2018).

On the other hand, the use of **Raloxifene** in the treatment of symptomatic uterine leiomyomas has been more studied. A Cochrane review includes three studies, with a total of 215 patients. Two of these trials reported a significant decrease in leiomyoma size from raloxifene therapy, and the third study found no significant differences in leiomyoma size in the group treated with Raloxifene, but a significant increase within control group. No serious adverse events

were reported, but some mild side effects, such as increased appetite, weight gain, gastralgia or hot flashes, were reported in two studies (Deng *et al.*, 2012).

3.3.6. Aromatase inhibitors

Aromatase inhibitors, specifically **Letrozole** and **Anastrozole**, have been studied as uterine leiomyoma therapy because they block the extragonadal conversion of androgens into estrogens. Although several studies reported the efficiency of these treatments in reducing leiomyoma size (Brito *et al.*, 2012; Duhan *et al.*, 2013; Parsanezhad *et al.*, 2010), a systemic review remarked that the current evidence is insufficient to recommend the use of aromatase inhibitors for treatment of symptomatic uterine leiomyomas (Song *et al.*, 2013).

3.3.7. Selective progesterone receptor modulators

Selective Progesterone Receptor Modulators (SPRMs) have recently emerged as a promising therapy in the medical management of fibroids. SPRMs are synthetic compounds that exert agonistic or antagonistic effect on progesterone receptor (PR), with its action contingent on tissue type (Donnez *et al.*, 2018). Four SPRMs have been investigated in phase II clinical trials: Mifepristone, Asoprisnil, Ulipristal Acetate (UPA), and Telapristone Acetate. All promoted a decrease leiomyoma size and reduced uterine bleeding (Donnez and Dolmans, 2016).

Mifepristone, also known as RU-86, was the first SPRM to be developed and commonly used. Primarily used as an abortifacient, in uterine leiomyoma patients this drug reduces bleeding and improves quality of life. However, it does not reduce leiomyoma size significantly. In addition, women treated with Mifepristone present abnormal endometrial histology and endometrial hyperplasia (Tristan *et al.*, 2012) .

The synthetic steroid **UPA**, CD-2914, is a selective PR modulator that binds progesterone receptors A and B (PR-A and PR-B) with high affinity. The use of UPA in the management of uterine leiomyomas has been studied in four large randomized trials, which were blinded phase III clinical studies (*PGL4001: Efficacy Assessment in Reduction of Symptoms Due to Uterine Leiomyomata, PEARL*) (Donnez *et al.*, 2014, 2015; Donnez, Tatarchuk, *et al.*, 2012; Donnez, Tomaszewski, *et al.*, 2012). These trials demonstrate the effectiveness of UPA in the reduction of the size of fibroids as well as the reduction of associated bleeding or pain.

However, UPA induced morphological changes in endometrial tissue known as progesterone receptor modulator associated endometrial changes (PAEC), such as large cystic glands and changes within the stromal compartment including the fibroblasts and vasculature, which are recognized as a distinct histological entity (Whitaker *et al.*, 2017). These endometrial changes induced by UPA do not allow long-term treatments. For that reason, it is recommended that UPA be prescribed in an intermittent mode (3-month therapy course followed by an interval of around 8 weeks, allowing two menstrual bleeds) (Donnez *et al.*, 2018). In 2012 the Spanish Agency of Medicine and Health Products (known by the Spanish acronym AEMPS) approved the use of UPA (Esmya®) for the treatment of uterine leiomyomas (AEMPS, 2011). However, in February 2018, after the notification of severe cases of liver damage in women treated with Esmya®, the AEMPS recommended not to start new treatments (AEMPS, 2018a). Finally, in July 2018, after a risk-benefit assessment, the use of Esmya® was restricted. In the case of the intermittent treatment the use of UPA is limited to women in whom surgery is not an option and, in preoperative treatment, the time is limited as a maximum of three months (AEMPS, 2018b).

In sum, although there are different management strategies for uterine leiomyomas, selected depending on different patient factors (Figure 6), none of them is sufficiently effective without minimal long-term side effects. For this reason, there is a need to define an efficient, non-surgical treatment for reducing uterine leiomyomas with lasting impact and minimal side effects.

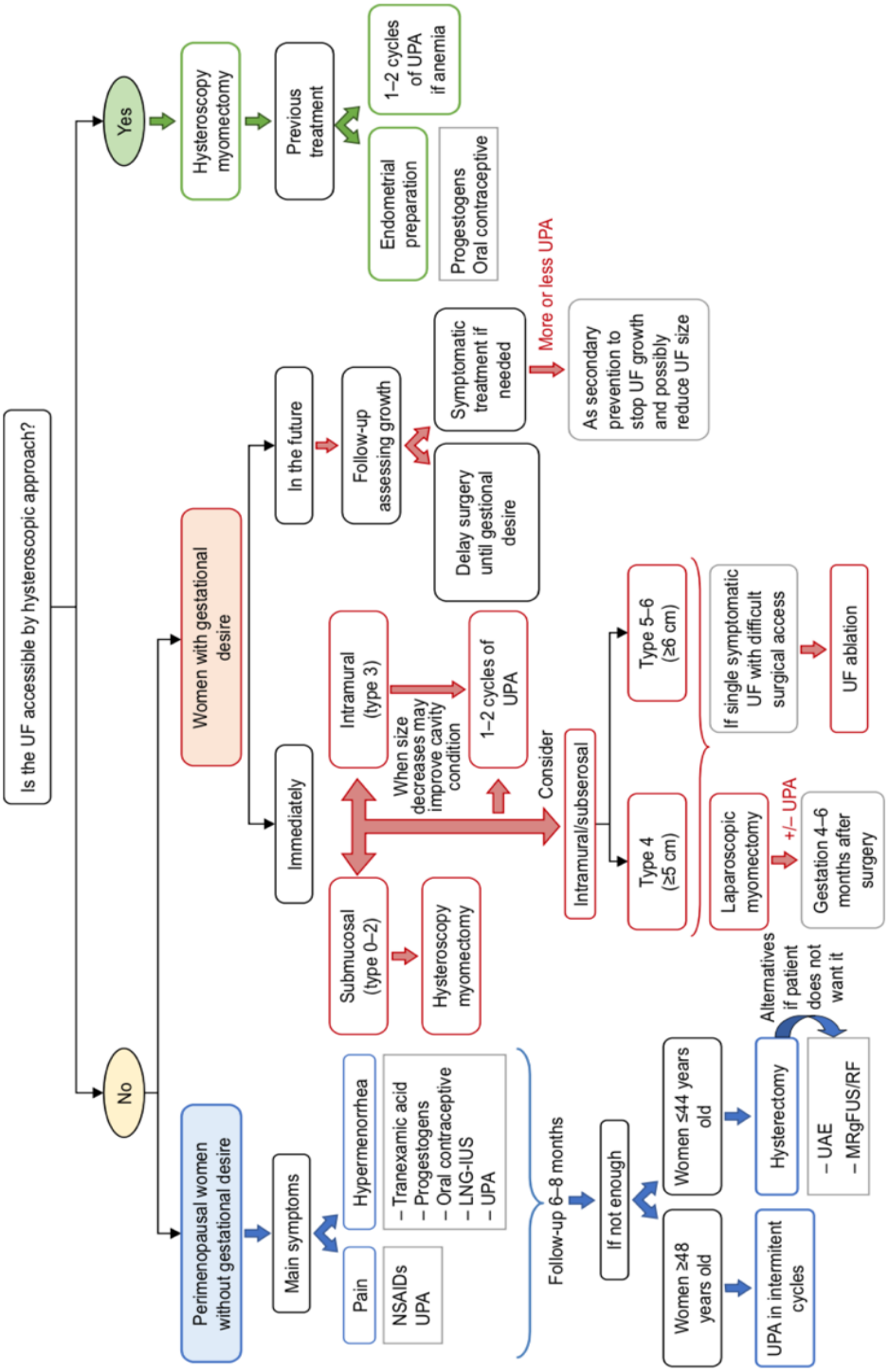

Figure 6. Algorithm for the management of uterine leiomyoma. *Example of an algorithm developed for the management of uterine fibroids (UF) according to patient profile. Abbreviations: LNG-IUS, levonorgestrel intrauterine system; MRgFUS, magnetic resonance-guided focused ultrasound surgery; NSAID, nonsteroidal anti-inflammatory drug; RF, radiofrequency ablation; UAE, uterine artery embolization; UPA, ulipristal acetate. Image reproduced from (Mas A et al. 2017) with the permission of Dove medical press.*

4. POTENTIAL NEW TREATMENTS FOR UTERINE LEIOMYOMAS: VITAMIN D

Despite the high prevalence of uterine leiomyomas, efficient non-surgical treatment options for reducing uterine leiomyomas with lasting impact and minimal side effects remain elusive. In the search for new treatments, the correlation between Vitamin D deficiency and uterine leiomyoma risk, along with the potential of Vitamin D as a therapeutic agent for cancer, focused the attention on this vitamin as a possible treatment for uterine leiomyoma.

4.1. Vitamin D metabolism

Vitamin D is a group of steroid compounds whose main activity concerns the control of calcium-phosphate balance as well as the correct structure and function of the skeleton. Vitamin D_3, also known as cholecalciferol, is a prohormone obtained from the diet or mainly formed in the skin as a result of ultraviolet irradiation of 7-dehydrocholesterol. Cholecalciferol is biologically inactive, and its activation requires two hydroxylation steps. First, it is converted to 25-hidroxyvitamin D_3 [25(OH)D] in the liver, catalyzed by the hepatic enzyme CYP2R1. Subsequently, 25(OH)D is hydroxylated in the kidney by the enzyme CYP27B1, leading to the final active product, 1,25-dihydroxyvitamin D_3 [$1,25(OH)_2D_3$] also known as calcitriol (Figure 7). CYP24A1 degrades both $1,25(OH)_2D_3$ and 25(OH)D and is expressed in several tissues along with the Vitamin D receptor (VDR) (Ciebiera *et al.*, 2018; Hall and Guyton, 2011; Iruzubieta *et al.*, 2014; Lorenzen *et al.*, 2017; Zangemeister-Wittke and Simon, 2001).

Although historically the maintenance of calcium and phosphate homeostasis has been considered the main action of $1,25(OH)_2D_3$, it is a pleiotropic hormone that, apart from that function, regulates multiple cellular processes with effects on normal and malignant cell growth and differentiation. The biological actions of $1,25(OH)_2D_3$ are mediated by VDR, a member of the steroid hormone receptor superfamily that regulates gene expression in a ligand-dependent manner. Generally, $1,25(OH)_2D_3$ enters the cell by diffusion and binds the VDR in the cytoplasm, resulting in its activation. Subsequently, the activated VDR enters the nucleus and forms a heterodimer complex with the retinoid X receptor (RXR) (Figure 7). This heterodimer specifically binds to Vitamin D response elements (VDREs) present in the promoter regions of target genes, regulating its transcription. In addition, $1,25(OH)_2D_3$ regulates nongenomic actions that are rapid and not dependent on transcription. This

mechanism is proposed to be mediated by non-classical membrane Vitamin D receptor (memVDR) (Christakos *et al.*, 2016; Deeb *et al.*, 2007; Lorenzen *et al.*, 2017).

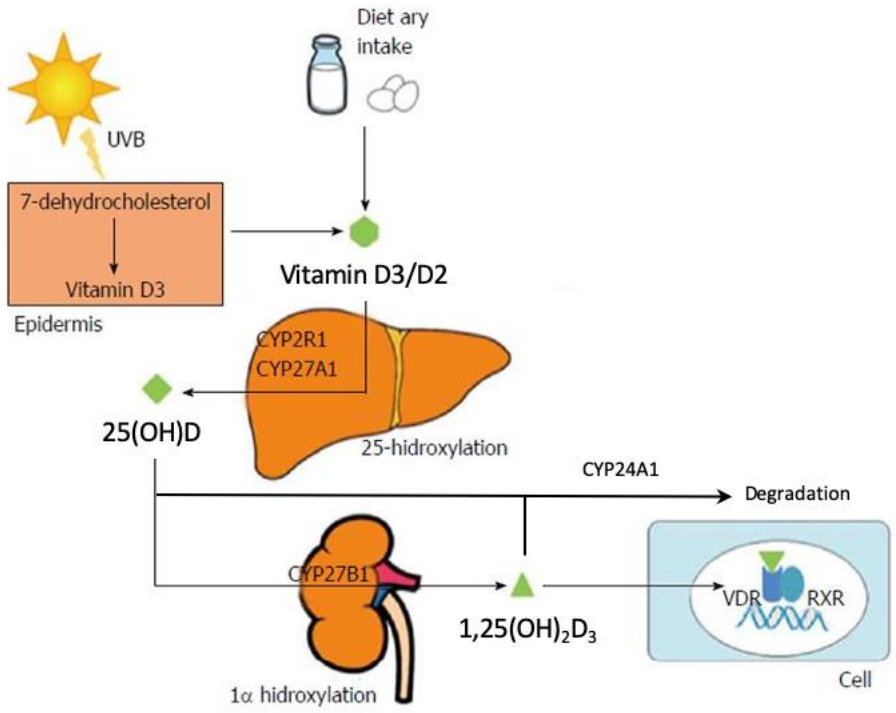

Figure 7. Vitamin D synthesis. *Vitamin D_3 is obtained from the diet or mainly formed in the epidermis as a result of ultraviolet B (UVB) irradiation of 7-dehydrocholesterol. Vitamin D is activated by two hydroxylation steps: first, it is converted to 25-hidroxyvitamin D_3 (25(OH)D) in the liver by the hepatic enzyme CYP2R1 and, subsequently, 25(OH)D is hydroxylated in the kidney by the enzyme CYP27B1, leading to the final active product, 1,25-dihydroxyvitamin D_3 ($1,25(OH)_2D_3$) also known as calcitriol. The biological actions of $1,25(OH)_2D_3$ are mediated by Vitamin D receptor (VDR) that enters the cell nucleus and forms heterodimers with the retinoid X receptor (RXR), which bind to specific gene promoters regulating their transcription. CYP24A1 degrades both $1,25(OH)_2D_3$ and 25(OH)D. Image adapted from (Iruzubieta et al., 2014).*

4.2. Vitamin D and cancer

The biological actions of Vitamin D are not only limited to normal cells. Several studies have demonstrated the anticancer effects of $1,25(OH)_2D_3$ in cancers of the ovary (Zhang *et al.*, 2005), lung (Nakagawa *et al.*, 2004), breast (Colston *et al.*, 1992) and colon (Ordóñez-Morán *et al.*, 2008). These antitumor effects are mediated through VDR and affect important cellular processes such as proliferation, cell cycle progression, differentiation and apoptosis (Deeb *et al.*, 2007).

4.2.1. Regulation of cell cycle

The cell cycle is the series of events through which cellular components are doubled and accurately separated into daughter cells. The cell cycle consists of four consecutive steps: G_1, S, G_2, M. DNA replication occurs in the Synthesis or S-phase; chromosome segregation takes place in the Mitosis or M-phase; and G_1 and G_2 are Gap phases in which cells increase in mass and prepare for chromosome segregation (Barnum and O'Connell, 2014). Cells that are not dividing enter a quiescent stage, G_0 phase. Progression through cell cycle is regulated by cyclins and their interaction with cyclin-dependent kinase (CDKs) and CDK inhibitors (CKIs). Cyclin/CDK complexes are formed during the different phases of the cell cycle and participate in the phosphorylation of target proteins. In the G_1/S phase transition, the retinoblastoma protein (pRB) should be phosphorylated by Cyclin E/CDK2 and Cyclin D1/CDK4,6. Vitamin D antiproliferative action is mediated mainly through a G_1/S phase block of the cell-cycle (Figure 8). In cancer, $1,25(OH)_2D_3$ acts by downregulating the expression of cyclins and CDKs, and increasing the expression of CKIs, such as p21 and p27. In this scenario, RB is not phosphorylated and, subsequently the G_1/S phase does not take place, leading to an accumulation of cells in the G_0/G_1 phase of the cycle (Christakos *et al.*, 2016; Ylikomi *et al.*, 2002).

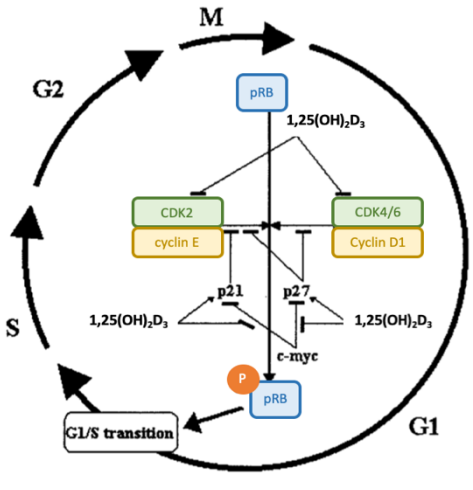

Figure 8. Cell cycle regulation by Vitamin D in cancer cells. *$1,25(OH)_2D_3$ inhibits the phosphorylation of the retinoblastoma protein (pRB) through the downregulation of cyclins and CDKs, and the upregulation of CDK inhibitors, such as p21 and p27. Consequently, G_1/S phase transition is blocked. Image adapted from Ylikomi et al. 2002.*

4.2.2. Regulation of Wnt/β-catenin pathway

Human Wnts are a family of 19 secreted proteins that control important developmental and homeostatic processes such as proliferation, survival, migration and differentiation. Secreted Wnt proteins bind to specific membrane receptors and activate several signaling pathways including the Wnt/β-catenin or canonical pathway and other β-catenin-independent non-canonical pathways (Larriba *et al.*, 2013; Pendás-Franco *et al.*, 2008).

The Wnt/β-catenin pathway controls intracellular β-catenin levels. In the absence of Wnt signals, β-catenin is phosphorylated, ubiquitinated and degraded by the proteasome. This process is promoted by the β-catenin destruction complex, whose components are the tumor suppressors AXIN and APC, and the protein kinases CK2 and GSK3β. In the presence of Wnt, it binds to Frizzled and LRP5/6 co-receptors, inhibiting the β-catenin destruction complex. Accordingly, unphosphorylated β-catenin is accumulated in the cytoplasm. Part of this β-catenin enters the nucleus where it associates TCF/LEF transcription factors and activates the transcription of target genes whose encode proteins involved in proliferation, cell cycle regulation, survival, migration, lineage commitment and differentiation (Figure 9). These target genes included *C-MYC, CCND1, WISP1* or *MMP7*, among others. Moreover, Wnt/β-catenin signaling is regulated by secreted extracellular Wnt antagonists. There are two kinds of Wnt inhibitors, those that act by binding directly to Wnts altering their ability to bind receptors [secreted Frizzled-related proteins (SFRPs)], such as Wnt inhibitory factor-1 (WIF-1) and Xenopus Cerberus; and those that bind LRP5/6, preventing Wnt-Frizzled-LRP interaction [Dickkopf (DKK) proteins and Wise] (Larriba *et al.*, 2013; Pendás-Franco *et al.*, 2008).

Due to the importance of Wnt/β-catenin target processes, its deregulation is associated with many disorders. Specifically, mutations that activate this pathway are involved in the initiation and progression of several types of cancer (Larriba et al., 2013; Pendás-Franco et al., 2008). In uterine leiomyomas, *MED12* mutation is associated with an activation of Wnt/ β-catenin signaling pathway. In colon cancer, the action of $1,25(OH)_2D_3$ on Wnt/β-catenin has been widely studied and three mechanisms through which Vitamin D antagonizes the Wnt/β-catenin pathway have been described (Figure 9). First, $1,25(OH)_2D_3$ induces VDR/β-catenin interaction, reducing the β-catenin available to bind TCF, and thereby reducing the expression

of β-catenin/TCF target genes. Second, Vitamin D induces the expression of E-cadherin, which leads to β-catenin nuclear exportation, and relocation to the plasma membrane adherent junction, resulting, as in the first mechanism, in a reduced expression of β-catenin/TCF target genes. Third, $1,25(OH)_2D_3$ induces the expression of the Wnt inhibitor Dickkopf (DKK)-1 (Pendás-Franco *et al.*, 2008). The consequence of the different mechanisms is a decreased expression of Wnt/β-catenin target genes, which affects proliferation, cell cycle regulation, survival, migration and differentiation, among other processes.

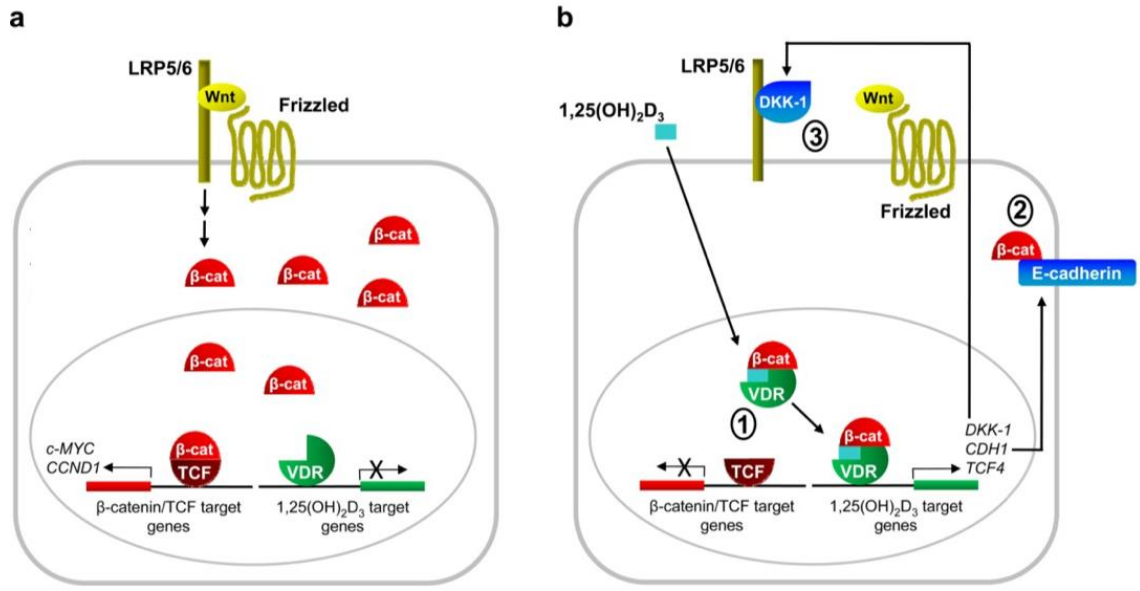

Figure 9. Vitamin D effect on Wnt/β-catenin pathway in cancer cells. *(a) In the absence of Vitamin D, Wnt ligands bind to Frizzled and LRP5/6 receptors, inhibiting the degradation of β-catenin, which is accumulated in the nucleus. Part of this β-catenin and associated TCF/LEF transcription factors activate the transcription of targets genes. (b) Vitamin D inhibits Wnt/β-catenin signaling pathway through three mechanism: 1) inducing VDR/β-catenin interaction, reducing β-catenin available to bind TCF, 2) inducing the expression of E-cadherin, which leads to β-catenin nuclear exportation, or 3) inducing the expression of* Wnt inhibitor Dickkopf (DKK)-1. *Image adapted from (Larriba et al. 2013) with permission of Cancers.*

4.2.3. Regulation of apoptosis

Apoptosis, or programed cell death, is a highly controlled process crucial in the development and homeostasis of tissues as well as in cancer prevention. Apoptosis is initiated by extracellular or intracellular signals that activate a complex cascade of events, which culminate in the activation of cysteine-aspartic proteases (caspases) and leads to the

degradation of nuclear DNA and dismantling of the cell. The process can be mediated via the intrinsic pathway (mitochondria mediated), and via the extrinsic pathway (death-receptor mediated). The BCL-2 family of proteins, which contain pro-apoptotic and anti-apoptotic (pro-survival) members, regulates the execution of intrinsic apoptosis. The dysregulation of apoptosis may play an important role in different pathologies, including cancer and neoplasia (Singh *et al.*, 2019; Zangemeister-Wittke and Simon, 2001).

The anti-tumor effect of $1,25(OH)_2D_3$ is not only due to its antiproliferative action, but also to its pro-apoptotic effect. The mechanisms through which $1,25(OH)_2D_3$ induces apoptosis in cancer cells include: the suppression of the anti-apoptotic proteins B-cell lymphoma 2 (BCL2) and B-cell lymphoma extra-large (BCL-XL), and the activation of the pro-apoptotic protein BAX, leading to the activation of downstream caspases. Other proposed mechanisms are the direct activation of caspase effector molecules, and the destabilization of telomerase reverse transcriptase (*TERT*) mRNA that downregulates telomerase activity, inducing apoptosis through telomere attrition (Deeb *et al.*, 2007) (Figure 10).

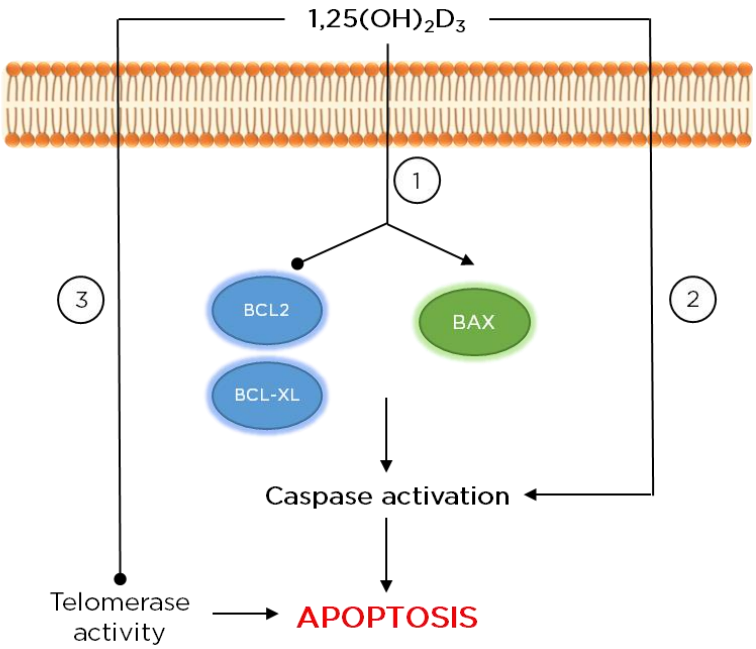

Figure 10. Vitamin D effect on apoptosis in cancer cells. *Vitamin D ($1,25(OH)_2D_3$) induces apoptosis through different mechanisms: 1) induction of the pro-apoptotic protein BAX expression and suppression of the anti-apoptotic proteins BCL2 and BCL-XL expression, which leads to the activation of downstream caspases; 2) direct activation of caspase effector molecules; and 3) downregulation of telomerase reverse transcriptase (TERT) mRNA, which results in a decreased telomerase activity.*

4.3. Vitamin D and uterine leiomyomas

In cancer, Vitamin D has the potential to inhibit tumor growth. Given the correlation between Vitamin D deficiency and uterine leiomyoma risk, several studies have investigated whether this vitamin could exert its antiproliferative action on leiomyoma cells.

4.3.1. *In vitro* studies

The first study aiming to test the effect of Vitamin D in leiomyoma cells was carried out by Bläuer et al. in 2009. In this work, both leiomyoma and myometrial primary cells from 6 patients were treated with Vitamin D. Their results showed, for the first time, that myometrial and leiomyoma cells are undoubtedly target cells of $1,25(OH)_2D_3$. The treatment decreased proliferation of both cell populations, suggesting a likely role of $1,25(OH)_2D_3$ deficiency in leiomyoma growth and development (Bläuer *et al.*, 2009).

Subsequently, several *in vitro* studies that assessed the effect of $1,25(OH)_2D_3$ on uterine leiomyomas were performed using immortalized human uterine leiomyoma (HuLM) cells instead of primary culture. Sharan et al. showed that Vitamin D inhibited HuLM cells proliferation through the downregulation of proliferating cell nuclear antigen (PCNA) and CDK1. In addition, the study suggested that $1,25(OH)_2D_3$ induces apoptosis in leiomyomas cells; however, only pro-apoptotic proteins (BCL2 and BCL-W) were evaluated (Sharan *et al.*, 2011).

Other studies investigated the effects of Vitamin D on ECM proteins. Halder et al. demonstrated that TGFβ3 induces the expression of collagen I, fibronectin and plasminogen activator inhibitor-1 (PAI-1) in HuLM cells. Treatment with $1,25(OH)_2D_3$ significantly decreases these TGFβ3-induced effects (Halder *et al.*, 2011). In addition, further studies from the same group showed that $1,25(OH)_2D_3$ treatment inhibits the expression of MMP-2 and MMP-9, as well as increasing the expression of TIMP-2 in HuLM and primary leiomyoma cells (Halder *et al.*, 2013a). These findings suggest Vitamin D as a key regulator of ECM formation. Further, Vitamin D treatment reduces the expression of the ECM leiomyoma proteins, such as collagen I, fibronectin and PAI-1, and the proteoglycans fibromodulin, versican and biglycan in HuLM cells (Halder *et al.*, 2013b). The main drawback of these studies is the use of HuLM cells, which provide uniform results without considering patient heterogeneity. In addition, these studies

used 2D culture instead of 3D culture systems that mimic the actual leiomyoma environment and are more suitable to evaluate ECM-related processes.

Finally, Al-Hendy et al. studied the effect of $1,25(OH)_2D_3$ on Wnt/β-catenin signaling pathway. Vitamin D treatment decreases the expression of Wnt4 and β-catenin in HuLM cells, suggesting an inhibitory effect of Vitamin D on Wnt/β-catenin pathway in this leiomyoma cell line. However, the inhibitory effect of Vitamin D was only demonstrated on Wnt4 expression in leiomyoma primary cells that came from a single patient (Al-Hendy *et al.*, 2016). In this regard, Vitamin D's effect in a heterogenic leiomyoma primary cell population has not yet been described.

4.3.2. *In vivo* studies

Halder et al. assessed the effect of Vitamin D *in vivo* in two different studies, using different leiomyoma animal models and different drugs. First, they tested the effect of $1,25(OH)_2D_3$ on leiomyomas using the Eker rat model. Eker rats develop leiomyomas in their uteri with a frequency of 65% due to a germ line mutation in the tuberous sclerosis 2 (*Tsc2*) tumor suppressor gene (Everitt *et al.*, 1995; Walker *et al.*, 2003). Their results showed that the treatment with $1,25(OH)_2D_3$ (0.5 μg/kg/day) for 3 weeks significantly reduces leiomyoma size, decreases the expression of genes involved in proliferation (*Pcna, Ccnd1, c-Myc, Cdk1, Cdk2* and *Cdk4*) and apoptosis (*Bcl2* and *Bcl-x*). At the protein level, the treatment reduces the expression of both proliferation markers PCNA and MKI67 and increases expression of Caspase 3 (Halder *et al.*, 2012).

Subsequently, the same group assessed the effect of $1,25(OH)_2D_3$ and its analog paricalcitol on a heterologous leiomyoma animal model, using the Eker rat-derived uterine leiomyoma cell line (ELT-3). They generated subcutaneous leiomyomas by injecting the ELT-3 cells in athymic nude mice supplemented with estrogen pellets. Then, mice were treated with paricalcitol (300 ng/kg/d) or 1,25-dihydroxyvitamin D3 (0.5 μg/kg/d) for 4 weeks. Both treatments reduce leiomyoma size, with shrinkage slightly higher in the paricalcitol group. Both treatments also decrease proliferation and collagen IV expression as well as increasing apoptosis (Halder *et al.*, 2014).

Both *in vivo* animal models concluded that $1,25(OH)_2D_3$ or its analogs could be a potential candidate for effective, safe and noninvasive medical treatments for uterine leiomyomas. However, both studies test the Vitamin D effect on leiomyoma size in Eker rats or its derived cells, which do not mimic the actual human leiomyoma physiology. So far, there is no *in vivo* study that assesses the effect of Vitamin D treatment on a leiomyoma animal model generated using human tissues or human uterine leiomyoma cells.

4.3.3. Vitamin D supplementation in women with uterine leiomyoma

The effect of Vitamin D on women with uterine leiomyomas is only reported in one trial. Ciavattini et al. studied the effect of Vitamin D supplementation in women with uterine leiomyomas and concomitant hypovitaminosis D [$25(OH)D_3$ serum level < 30 ng/mL]. Patients who met both criteria were offered Vitamin D supplementation therapy with 50,000 IU of cholecalciferol (oral solution) once per week for 8 weeks, followed by maintenance therapy of 2000 IU daily for 12 months. After that period, patients who properly performed Vitamin D supplementation therapy, formed the study group (n=43), while those that who did not performed it properly or refused it, constituted the control group (n=34). While in the control Vitamin D levels were maintained after 12 months, in the study group, Vitamin D serum levels increased significantly. A significant increase in leiomyoma size was found in the control group, while no significant difference was found in the study group, suggesting that Vitamin D would be an efficient treatment to maintain uterine leiomyoma size instead of to decrease its size. However, considering that this study only included peri and menopausal women with “small burden” leiomyomas, excluding premenopausal women with leiomyomas > 50 mm diameter, with more than 4 fibroids or with severe symptoms, and the control group comprised women who did not comply with the therapy (Ciavattini *et al.*, 2016), the obtained results could be biased.

It is important to highlight that Vitamin D effects have been demonstrated *in vitro* and *in vivo* in a human leiomyoma cell line, in Eker rats, or in rat-derived cells. None of these studies used leiomyoma primary cells or human tissue samples, and therefore they do not reflect either the heterogeneity of human general population or the actual human leiomyoma physiology. Considering this, an in-depth study of the molecular mechanisms through which Vitamin D

could act, as has been described in cancer cells, is still pending for human leiomyoma primary cells and human leiomyoma tissue.

II. HYPOTHESIS

II. HYPOTHESIS

Vitamin D, specifically its active metabolite 1,25-dihydroxyvitamin D_3, could play an important role in the pathogenesis of uterine leiomyomas through the regulation of Vitamin D signaling pathways: cell growth arrest induction, cell proliferation reduction, Wnt/β-catenin signaling pathway inhibition and apoptosis induction, and consequently, decreasing uterine leiomyoma growth.

III. OBJECTIVES

III. OBJECTIVES

The main objective of this study is to evaluate the effect of Vitamin D treatment on uterine leiomyomas growth in order to test its potential as a therapeutic agent to reduce its size.

Specific objectives:

1. Determine *in vitro* the effect of Vitamin D treatment in human uterine leiomyoma primary cells through the regulation of cell cycle, cell proliferation, Wnt/β-catenin signaling pathway and apoptosis.
2. Determine *in vivo* in a xenograft mouse model the effect of Vitamin D treatment in human uterine leiomyomas through the regulation of cell proliferation, extracellular matrix formation and apoptosis.

IV. MATERIALS AND METHODS

IV. MATERIALS AND METHODS

1. *IN VITRO* STUDY

1.1. HUMAN UTERINE LEIOMYOMA SAMPLE COLLECTION

This study was approved by the Clinical Ethics Committee at Hospital Univeristario y Politécnico La Fe (Spain) (2014/0691), and all participants provided informed consent.

Human uterine intramural leiomyomas and adjacent myometrium were collected from premenopausal women ages 35-54 years undergoing either myomectomy or hysterectomy due to symptomatic uterine leiomyoma pathologies without any previous hormonal treatment (Table I).

Table I. Patients characteristics.

Patient	Number of Intramural Leiomyomas	Average Size of Leiomyomas (cm)	AGE	BMI
1	1	4	44	33.71
2	1	10	45	28
3	>15	4.5	42	27.5
4	1	10	49	25.97
5	1	8	52	43
6	1	10	50	32
7	1	19	38	22
8	1	7	52	24.4
9	1	11	43	24
10	1	23	50	22.8
11	3	16	39	34
12	4	6	41	23.4
13	1	8	39	26.5
14	3	4	42	22.7
15	1	10	41	24.14
16	4	5	47	27.28
17	3	2	43	38.16
18	1	6	36	33.91
19	1	7	52	21.8
20	1	7.5	42	24.9
21	1	5	41	28
22	1	4	48	29.38
Mean ± SD	**2.2 ± 3**	**8.5 ± 5.1**	**44.4 ± 4.9**	**29.7 ± 14.6**

BMI= body mass index; SD= standard deviation;

After the collection, samples were placed in a maintenance medium containing Medium 199 Earle's salts, 10% fetal bovine serum (FBS), 0.5% penicillin-streptomycin, 0.5% fungizone

antimycotic solution and 1% of 1 M HEPES (all acquired from Gibco, Fisher Scientific, USA) and stored overnight at 4° C to be processed the next day.

Subsequently, uterine leiomyoma and myometrium were divided in two different fractions: 1) One fragment was used for protein extraction to evaluate the involvement of proliferation, Wnt/β-catenin pathway and apoptosis in uterine leiomyoma development by western blot and 2) another fragment was used for leiomyoma cell isolation and culture to determine Vitamin D's effect on the cells through cell cycle, Wnt/β-catenin signaling and apoptosis pathways.

1.2. EVALUATION OF HUMAN UTERINE LEIOMYOMA AND ADJACENT MYOMETRIAL TISSUES

To determine the involvement of proliferation, Wnt/β-catenin pathway and apoptosis in uterine leiomyoma development, the expression for proliferating cell nuclear antigen (PCNA), Wnt1-inducible-signaling pathway protein 1 (WISP1), B-cell lymphoma-2 (BCL2), and BCL2 Associated-X (BAX) was assessed by western blot in leiomyoma and adjacent myometrium tissues.

1.2.1. Protein extraction

Protein was extracted from uterine leiomyoma and myometrial tissue fragments (n=22) using radioimmunoprecipitation assay (RIPA) Buffer, containing 50 mM Tris(hydroxymethyl)amino-methane-HCl pH 7.5, 150 mM NaCl, 1% Triton-X 100, 1% sodium deoxycholate, 1% IGEPAL CA-630 (Sigma-Aldrich, USA), EDTA-free protease inhibitor cocktail (Roche, Switzerland) and 0.1% of sodium dodecyl sulfate (SDS) (Bio-Rad, USA). Samples were maintained on ice to avoid protein degradation. Briefly, a small fragment of each tissue sample (5 x 5 mm) was mechanically dissected with scalpels to obtain fragments smaller than 1 mm^3. Subsequently, RIPA buffer was added and samples were incubated for 30 minutes. After incubation, samples were centrifuged for 15 minutes, at 160000 g at 4° C. Supernatant containing the proteins was collected and placed in a new tube. Protein concentrations were quantified by a colorimetric assay based on the Bradford method with Bio-Rad Protein Assay Dye Reagent Concentrate (Bio-Rad, USA) following the manufacturer's instructions and using SpectraMax 190 Microplate Reader (Molecular Devices, USA).

1.2.2. Western blot

The same amount of each tissue lysate sample (30 μg) was denatured at 95°C for 5 minutes and separated by **electrophoresis** in 10% sodium dodecyl sulphate-polyacrylamide (SDS-PAGE) gel. Molecular weight markers (Bio-Rad, USA) were used for determining fragment size. Electrophoresis was performed with Tris/glycine/SDS Buffer (Bio-Rad, USA) for 1 hour at 180 V and the gel percentage was selected depending on the size of the protein of interest. Separated proteins were **transferred** from the gel to a polyvinylidene difluoride (PVDF) membrane (Bio-Rad, USA) for 2 hours at 220 mA using Tris/glycine Buffer (Bio-Rad, USA). Membrane was incubated 1 hour at room temperature on a shaker with **blocking** solution [phosphate-buffered saline (PBS), 0.05% Tween and 5% nonfat milk] and incubated with the **primary antibody** overnight at 4° C on an orbital shaker. Primary antibodies were prepared in blocking solution (PBS, 0.05% Tween and 3% nonfat milk) at the following dilutions: PCNA (sc-56, 1:200), WISP1 (sc-133126, 1:200), BCL2 (sc-7382, 1:200) and BAX (sc-20067, 1:200) from Santa Cruz Biotechnology (USA). After the incubation, the membrane was rinsed 3 times for 5 minutes with PBS-Tween 0.05% and incubated with the HRP-conjugated **secondary antibody** (sc-516102; 1:2000; Santa Cruz biotechnology, USA) for 1 hour at room temperature on a shaker. Membrane was rinsed as previously mentioned and **antigen-antibody complex detection** was performed with an enhanced chemiluminescence detection system (Super Signal West Femto Maximum Sensitivity Substrate, ThermoFisher, USA). Specific protein bands were visualized by chemiluminescence imaging using the LAS-3000 Imaging-System (Fujifilm, Japan) and the intensity of each protein band was quantified with Image J software (National Institutes of Health, USA). Expression of each protein was normalized in relation to housekeeping protein β-actin (1:2000; sc-516102, Santa Cruz Biotechnology, USA). For that, membrane was incubated with Restore Western Blot Stripping Buffer (ThermoFisher, USA) for 15 minutes at room temperature on a shaker and followed rinsed with PBS-Tween 0.05%. Then, membrane was blocked again with blocking solution, incubated with the primary and secondary antibodies, detected and quantified as previously described.

1.3. VITAMIN D TREATMENT OF HUMAN UTERINE PRIMARY LEIOMYOMA CELLS

To assess the effect of Vitamin D treatment on uterine leiomyoma *in vitro*, Human Uterine Primary Leiomyoma (HUPL) cells were isolated and treated with $1,25(OH)_2D_3$. Subsequently, functional analysis was carried out to analyze cell cycle, proliferation, Wnt/β-catenin pathway and apoptosis in treated and control cells.

1.3.1. Human uterine leiomyoma primary cell isolation

Leiomyoma samples were disaggregated in sterile conditions by mechanical and enzymatic procedures to obtain cell suspensions. Briefly, leiomyoma samples were dissected and minced manually into small pieces (1 mm^3) and enzymatically digested at 37° C on a shaker with disaggregation medium (2 mg/mL type II collagenase [Labclinics, Spain] and 1 mg/mL deoxyribonuclease I [DNase I] [Sigma-Aldrich, USA] in PBS) for 1 hour. Subsequently, the medium was filtered through 40-µm cell strainers (pluriSelect, Germany) to remove undigested tissue and centrifuged 5 minutes at 600 g to obtain the cellular fraction. Remaining tissue was incubated again with disaggregation medium for 30 minutes 2 times, with filtration and centrifugation at the end of each disaggregation step. Finally, harvested cells were treated with erythrocyte lysis buffer (1.5 M NH_4Cl, 100 mM $NaHCO_3$ and ethylenediaminetetraacetic acid [EDTA] 1 mM) at pH 7.4 to eliminate blood cells by hypotonic shock.

Human uterine leiomyoma primary (HULP) cells were resuspended in cell culture medium containing Dulbecco's Modified Eagle Medium (DMEM)/F-12 with 10% FBS, 0.1% penicillin-streptomycin, 0.1% fungizone antimycotic solution (Gibco, Fisher Scientific, USA) and counted with Neubauer chamber in a solution with trypan blue to denote dead cells (Labclinics, Spain).

1.3.2. Preliminary studies

1.3.2.1. Vitamin D treatment: Dose-time response assay

A preliminary study with HULP cell samples (n=6) was conducted to establish cell culture and Vitamin D treatment conditions. HULP cells were incubated at 37 °C and 5% CO_2 in cell culture medium. Once HULP cells achieved 70-80% confluence, they were divided into five experimental groups to select the dose of Vitamin D, and treatments were administered in cell culture medium for 24 and 48 hours. To prepare the treatments, 10 µg of 1,25-

dihydroxyvitamin D_3 (Sigma-Aldrich, USA; molecular weight = 416.64 g/mol), were dissolved in 1.2 mL of ethanol (EtOH) to achieve a final concentration of 20 µM.

Treatment groups:

1) Cell culture medium (Control) (n=6)

2) 0.5% EtOH (vehicle of Vitamin D) (n=6)

3) $1,25(OH)_2D_3$ 10 nM (n=6)

4) $1,25(OH)_2D_3$ 100 nM (n=6)

5) $1,25(OH)_2D_3$ 1000 nM (n=6)

Cultured HULP cells collection

After treatment, culture medium was removed, and attached cells were treated with trypsin-EDTA (0.25%) (Fisher Scientific, USA) for 5 minutes at 37° C to induce cell dissociation. Subsequently, cell culture medium was added to stop trypsin reaction, and the total volume was collected and centrifuged (5 minutes, 600 g). Supernatant was discarded and the pellet containing the cells was stored at -80° C until ribonucleic acid (RNA) extraction procedure.

***CYP24A1* expression by quantitative-real time polymerase chain reaction (qRT-PCR)**

To assess cell response to Vitamin D in HULP cells, we measured gene expression of *CYP24A1*, which is strongly induced by $1,25(OH)_2D_3$. Total RNA was extracted from HULP cells treated with and without Vitamin D using *Quick*-RNA Microprep (Zymo Research, USA) following manufacturer's instructions. RNA concentration was measured by Qubit Fluorometric Quantification using Qubit RNA HS assay kit (ThermoFisher, USA). Subsequently, complementary cDNA was synthesized from 1 µg of RNA with PrimeScript RT reagent Kit (Takara, Japan), and cDNA concentration was measured by Qubit Fluorometric Quantification using Qubit dsDNA HS assay kit (ThermoFisher, USA). qRT-PCR was performed with StepOnePlus™ Real-Time PCR System (Applied Biosystems, USA) using PowerUp SYBR Green (ThermoFisher, USA). Expression of the housekeeping gene *β-ACTIN* was used to normalize the expression of *CYP24A1*. The sequence of primers used is detailed in Annex I. The amount

of sample used in each reaction was 4 ng, and the fold changes were calculated with the method ΔΔCt using Qiagen Data Analysis Software.

1.3.2.2. Cell viability assay

To assess if Vitamin D vehicle has a detrimental effect on HULP cells, cell viability was calculated by flow cytometry.

Briefly, once HULP cells achieved 70-80% of confluence, they were divided into three groups: 1) Cell culture medium (control); 2) 0.5 % EtOH (vehicle); and 3) $1,25(OH)_2D_3$ 100 nM groups (n=6) for 48 and 144 hours. Subsequently, cells were collected as described in section 1.3.2.1. and fixed with ice-cold 70% EtOH. Fixed cells were suspended in 100 µg/mL ribonuclease A (RNase A) and 50 µg/mL propidium iodide (PI) in PBS (Sigma-Aldrich, USA) to stain DNA. Then, HULP cells were incubated in darkness at 4 °C overnight and analyzed in a Cytomics-FC500 (Beckman-Coulter, USA) flow cytometer. PI fluorescence was detected in a 620-nm fluorescence channel; analysis was performed using FlowJo software for flow cytometry data to identify the percentage of cell viability.

1.3.3. Vitamin D treatment: Functional analysis

After establishing culture conditions and ensure that Vitamin D vehicle (EtOH) did not result in toxicity to cells, HULP cells were treated with/without Vitamin D to assess its action on signaling pathways by different functional analysis, summarized in Table II.

HULP cells (n=22) were incubated at 37° C and 5% CO_2 in cell culture medium and, once they achieved 70% of confluence, were serum-starved (incubated with cell culture medium without FBS) for 20 hours to induce cell cycle synchronization.

Subsequently, HULP cells from each sample were divided in two experimental groups, 1) Control (only cell culture medium) and 2) Vitamin D ($1,25(OH)_2D_3$ 100 nM), and cultured for the analysis of cellular DNA content for 144 hours (treatment replaced every 48 hours) and for PCNA analysis by western blotting, gene and protein expression for Wnt/β-Catenin and apoptosis pathways, gene validation, and apoptosis analysis by TUNEL, cells were cultured for 48 hours.

Table II. Summary of the functional assays performed in the in vitro study.

PATHWAY OR CELL PROCESS	ASSAY	HOURS OF VITAMIN D TREATMENT
CELL CYCLE ARREST	Propidium Iodide (PI) Flow Cytometry assay	144
PROLIFERATION	PCNA expression by Western Blot	48
WNT/β-CATENIN PATHWAY	Gene expression: RT²-Profiler PCR Arrays	48
	Protein expression: Quantibody Human Cytokine array	48
APOPTOSIS	Gene expression: RT²-Profiler PCR Arrays	48
	TUNEL assay	48

1.3.3.1. Analysis of cellular DNA content by flow cytometry

To determine the effect of Vitamin D treatment on the cell cycle, HULP cells were sorted by flow cytometry. After the 144-hour treatment, HULP cells (n=22 samples) were collected and fixed for cellular DNA content analysis. Briefly, the cell culture medium was collected and, attached cells were treated with trypsin-EDTA (0.25%) (Fisher Scientific, USA) for 5 minutes at 37° C to induce cell dissociation. Cell culture medium was added to reverse the effect of trypsin, and the total volume was centrifuged, along with the medium previously collected, for 5 minutes at 600 g. Supernatant was discarded and pellet containing the cells was fixed in ice-cold 70% EtOH and stored at -20 °C (for at least for 1 h) until DNA staining.

Subsequently, fixed cells were suspended in 100 µg/mL RNase A and 50 µg/mL propidium iodide (PI) in PBS (Sigma-Aldrich, USA) to stain DNA. Then, HULP cells were incubated in darkness at 4 °C overnight and analyzed in a Cytomics-FC500 (Beckman-Coulter, USA) flow cytometer. PI fluorescence was detected in a 620-nm fluorescence channel, where PI signal area was used as a DNA measure and PI signal height was used to exclude the aggregates. Analysis was performed using FlowJo software for flow cytometry data to identify the G_0/G_1, S and G_2/M phases from PI area signal, quantifying the percentage of cells in each cell cycle phase. Cell growth arrest was represented as the difference in the percentage of cells in S-G_2/M between Vitamin D-treated and control HULP cells (100 - [%S-$G_2/M_{Vitamin\ D}$ x 100 / %S-$G_2/M_{control}$]).

1.3.3.2. Analysis of PCNA expression in HULP cells

To assess the effect of Vitamin D treatment on HULP cell proliferation, the expression of PCNA was evaluated by western blot in Vitamin D treated and control cells. A subset of representative samples (n=15) from all samples included in the study, with the same age, BMI, size and number of leiomyomas as the entire sample (n=22), was selected for that assay (Table I).

After 48 hours of treatment, HULP cells were collected as described in section 1.3.2.1 and the pellet containing the cells was stored at -80° C until protein extraction procedure following the protocol described in section 1.2.1. Subsequently, 10 µg of each cell lysate sample were analyzed by western blot, as detailed in section 1.2.2, to determine the expression of PCNA.

1.3.3.3. Gene expression analysis: Wnt/β-catenin pathway and apoptosis

To evaluate the effect of Vitamin D on Wnt/β-catenin pathway and apoptosis at the gene expression level in HULP cells, a subset of 11 representative samples from all samples included in the study, with the same age, BMI, size and number of leiomyomas as the entire sample (n=22) was selected (Table I).

After 48-hour treatment, HULP cells were collected as described in section 1.3.2.1. The expression of 84 Wnt-mediated pathway genes and 84 genes involved in apoptosis were measured using RT^2-Profiler PCR Arrays from Qiagen (Germany) according to the manufacturer's instructions. The protocol is summarized in Figure 11.

1. **RNA extraction**. Total RNA of Vitamin D-treated and control HULP cells was isolated using RNeasy kit (Qiagen, Germany), including a DNase digestion step performed with RNase-Free DNase Set (Qiagen, Germany). RNA concentration was determined by Qubit Fluorometric Quantification using Qubit RNA HS assay kit (ThermoFisher, USA). In addition, an aliquot of each RNA sample (1 µL) was run on the Agilent 2100 Bioanalyzer using an RNA 6000 Nano LabChip (Agilent Technologies, USA) to check RNA integrity. Samples with an RNA integrity number (RIN) > 7 were included in the assay.
2. **cDNA synthesis**. 500 ng of RNA were used to synthesize cDNA using First Strand Kit (Qiagen, Germany), according to manufacturer's specifications. From the 111 µL

obtained, 1 µL was used to determine the concentration of cDNA by Qubit Fluorometric Quantification using Qubit dsDNA HS assay kit (ThermoFisher, USA).

3. **Gene expression analysis.** RT^2-Profiler PCR Arrays from Qiagen (Germany) consist of a 96-well plate containing SYBR® Green-optimized primers for pathway-focused genes. In our case, we performed RT^2 Profiler PCR Array Human WNT Signaling Pathway Plus (PAHS-043Y) and RT^2 Profiler PCR Array Human Apoptosis (PAHS-012Z). Each PCR array allows the evaluation of the expression of 84 genes of the pathway of interest and 5 housekeeping (HK) genes in one sample. In addition, it contains 1 genomic DNA control well (GDC), 3 reverse-transcription Control (RTC) wells and 3 positive PCR control (PPC) wells. The list of genes evaluated in Wnt signaling and apoptosis arrays is detailed in Annexes II and III, respectively.

Briefly, 102 µL of cDNA were mixed with RT^2 SYBR Green qPCR Mastermix (Qiagen, Germany), following the manufacturer's protocol. Subsequently, the mix was aliquoted in the 96 wells of the RT^2 Profiler PCR Array, 25 µL/well. qRT-PCR was performed in StepOnePlus™ Real-Time PCR System (Applied Biosystems, USA) with the cycling conditions recommended by Qiagen: 1 cycle at 95 °C for 10 minutes, 40 cycles of 15 seconds at 95 °C and 1 minute at 60 °C.

The threshold cycle (C_T) was calculated using the StepOnePlus Software. Baseline was defined by choosing the automated baseline option, and the threshold was manually set as directed by the protocol. The same threshold was set for all the arrays included in the study, 11 control and 11 Vitamin D-treated samples. The C_T values were analyzed through Qiagen's GeneGlobe Data Analysis Center using a software-based tool. Data were normalized with the housekeeping gene with minor variability and the fold regulation of each gene in the Vitamin D-treated group compared to control group was calculated.

In the case of the Human WNT Signaling Pathway Plus (PAHS-043Y) array, Qiagen's analysis software allows the calculation of the ***pathway activity score***. This score is calculated with the expression of 16 Pathway Activity Signature Genes included in the array (*BOD1, CALM1, CCND1, CCND2, CHSY1, CXADR, CYP4V2, HSPA12A, LEF1, MT1A, MTFP1, MTSS1, MYC, NAV2, PRMT6,* and *SKP2*), along with a classification algorithm developed by Qiagen. Positive score (>0.3) indicates stimulation of pathway activity, while negative score (<-0.3) indicates repression of the pathway in the treated group compared to control.

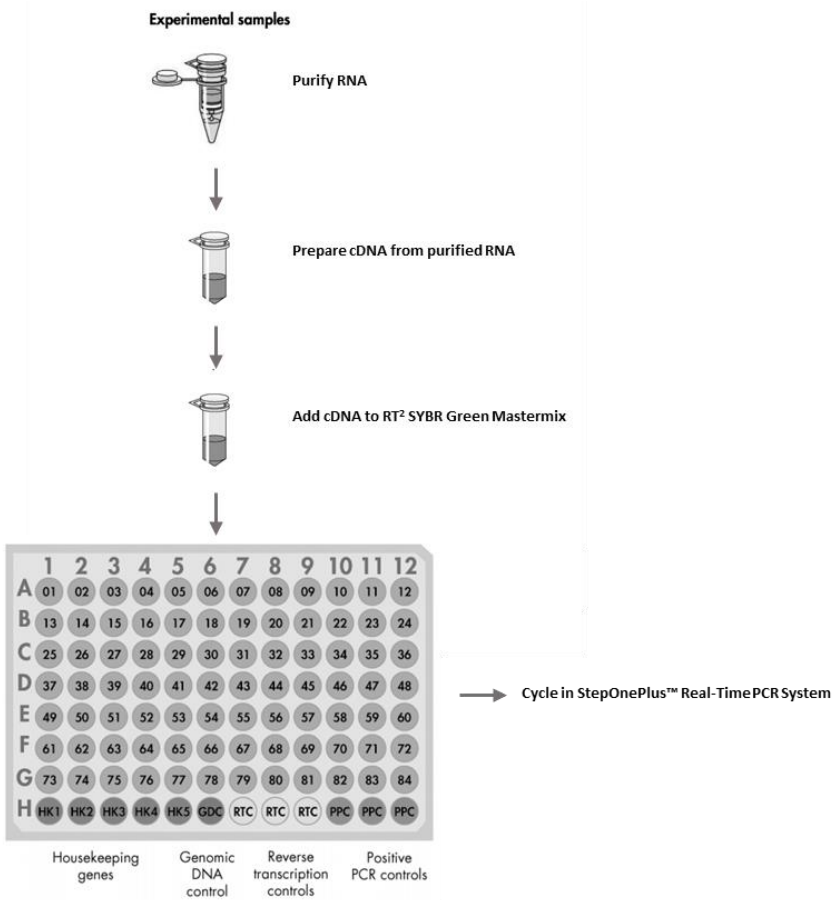

Figure 11. RT²-Profiler PCR Arrays Procedure. *Qiagen (Germany) kits were used at all steps according to the manufacturer's instructions**.** Total RNA from treated and control cells was purified and, subsequently, cDNA was synthesized from purified RNA. cDNA was mixed with RT² SYBR Green Mastermix and aliquoted in the 96 wells of an RT²-Profiler PCR Array, which contains primers for 84 pathway-focused genes as well as 5 housekeeping genes (HK). In addition, the array contains 1 genomic DNA control (GDC) well, 3 reverse-transcription control (RTC) wells and 3 positive PCR control (PPC) wells. Finally, qRT-PCR was performed in StepOnePlus Real-Time PCR System (Applied Biosystems, USA). Image adapted from Qiagen protocol.*

In addition, Kyoto Encyclopedia of Genes and Genomes (KEGG) Mapper-Color Pathway tool was used to represent a Wnt/β-Catenin pathway overview (hsa04310) after Vitamin D treatment in HULP cells compared to control HULP cells. Fold regulation data obtained for the analysis were used; upregulated genes were colored in red and downregulated genes in blue.

To validate the results, we analyzed gene expression of *WNT5A, DKK1* (for Wnt/β-Catenin pathway validation) and gene expression of *BCL2,* and *TNFRSF11B* (for apoptosis pathway validation) in the same HULP cells used in the expression analysis (n=11) and new HULP cells

(n=6) treated with/without Vitamin D for 48 hours by qRT-PCR. Relative expression levels were normalized to expression of the housekeeping *β-ACTIN*. The sequence of primers used can be found in Annex I.

1.3.3.4. Protein expression analysis: Wnt/β-catenin pathway

To assess the effect of Vitamin D treatment on the Wnt/β-catenin pathway at the protein level in the selected subset of HUPL cells samples (n=11), proteins from Vitamin D-treated and control HULP cells were extracted using lysis buffer (RayBiotech, USA). Total protein concentration was determined by Pierce™ BCA Protein Assay Kit (ThermoFisher, USA), according to manufacturer's instructions and using SpectraMax 190 Microplate Reader (Molecular Devices, USA).

Subsequently, proteins related to the Wnt/β-catenin pathway were evaluated by Quantibody Human Cytokine array from RayBiotech (USA). This assay is an array-based multiplex ELISA system for simultaneous quantitative measurement of multiple proteins. To determine the effect of the treatment in our samples, a Human Custom Quantibody was used to evaluate the expression of target proteins related to Wnt/β-catenin pathway (MMP-7, uPAR and WISP-1), following manufacturer's instructions. The procedure is summarized in Figure 12.

1. **Cytokine Standard Preparation.** To quantify the expression of the proteins of interest, a standard curve, whose concentration has been predetermined, was prepared from the standard vial provided.
2. **Blocking and Incubation.** Glass slides were air-dried, and sample diluent was added to each well for 30 minutes at room temperature to block slides. Then, diluent was removed, and standards and samples were added to each well and incubated overnight at 4 °C. Samples and standards were removed, and the slide was washed with wash buffer as directed by the protocol.
3. **Incubation with Biotinylated Antibody Cocktail.** The detection antibody was reconstituted, added to each well and incubated for 2 hours at room temperature. It was removed with washing as directed by the protocol.

4. **Incubation with Cy3 Equivalent Dye-Streptavidin.** Cy3 equivalent dye-conjugated streptavidin was added and incubated at room temperature for 1 hour in darkness. Slides were washed as directed by the protocol.
5. **Fluorescence detection.** Slides were dried and sent to Raybiotech for scanning with an Innopsys Innoscan-710A (Carbonne, France) using a dynamic PMT setting, XDR. Signals were extracted using MAPIX and sample concentrations [pg/mL] were quantified based on a standard curve.

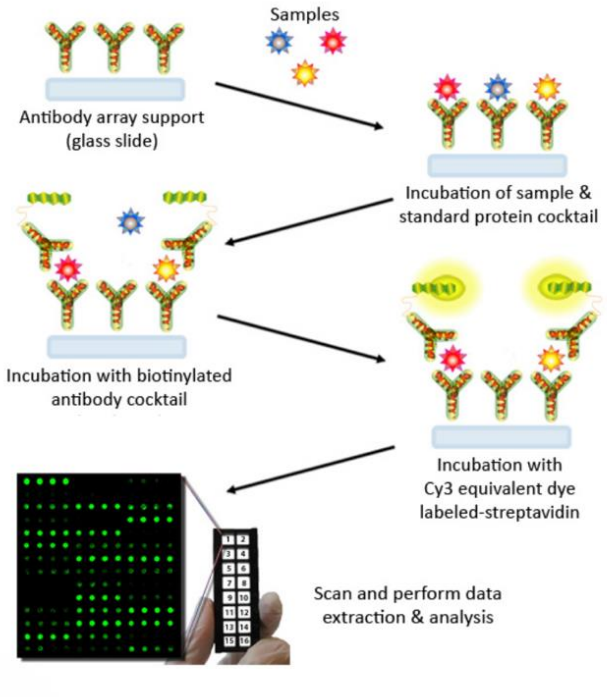

Figure 12. Quantibody Human Cytokine array procedure. *The glass slide is divided in 16 wells, each one containing capture antibodies bounded to the glass surface. After incubation with the sample, the protein of interest is trapped on the glass. The biotinylated antibody cocktail recognizes a different epitope of the target protein and, finally, the protein-antibody-biotin complex can then be visualized through the addition of the streptavidin-conjugated Cy3 equivalent dye, using a laser scanner. Image adapted from Raybiotech protocol.*

1.3.3.5. TUNEL assay

To detect and quantify apoptosis at a single-cell level in HULP cells treated with and without Vitamin D (n=11), terminal deoxynucleotidyl transferase-mediated dUTP nick end-labeling (TUNEL) staining was carried out using a TMR red IN SITU cell death detection kit (Roche, Switzerland). This technique labels DNA strand breaks generated during apoptosis, allowing the discrimination from necrosis. After the 48-hour treatment, cell culture medium was

removed and attached cells were washed with PBS. Cell **fixation** was performed by incubating attached cells for 20 min with 4% paraformaldehyde. Subsequently, HULP cells were rinsed with PBS and the **permeabilization** step was carried out by incubating cells with 0.1% Triton X-100 in 0.1% sodium citrate for 8 minutes. Cells were rinse twice with PBS.

As a positive control, two wells of each set of experiments were treated with DNase I (1000 U/mL in 50 mM Tris-HCl, pH 7.5, 1 mg/mL Bovine serum albumin [BSA]) for 10 minutes. For **labeling** process, TUNEL reaction mixture was prepared by mixing label solution with enzyme solution, following manufacturer's instruction. Cells were incubated with TUNEL reaction mixture in a humified atmosphere for 1 hour at 37 °C in darkness. Negative controls were incubated with label solution. Then, samples were rinse 3 times with PBS and cell nuclei were counterstained with DAPI (Life Technologies, USA). Stained cells were visualized and analyzed using fluorescence microscopy on a ZEISS Axio-Vert.A1 (Germany). Four fluorescent images per leiomyoma sample and condition were quantitatively assessed with Image ProPlus (Media Cybernetics, USA).

1.4. STATISTICAL ANALYSIS

GraphPad Prism 6.0 was used in this study for statistical analyses and graphics generation. Data are presented as mean ± standard deviation (SD). Wilcoxon test was performed for WB analysis of PCNA and WISP1 in leiomyoma and adjacent myometrium tissue and protein array and TUNEL analysis in Vitamin D-treated vs control HULP cells. A paired t-test was performed for WB of BAX/BCL2 ratio in leiomyoma and adjacent myometrium tissue and WB analysis of PCNA in Vitamin D-treated vs control HULP cells. Gene expression and validation analysis were carried out with Qiagen Data Analysis Software applying Student's t-test. p value<0.05 was considered statistically significant.

2. *IN VIVO* STUDY

To test Vitamin D's effect in human uterine leiomyoma *in vivo*, a xenograft mouse model was developed, in which human uterine leiomyomas fragments were implanted in immunosuppressed mice and, subsequently, they were treated with $1,25(OH)_2D_3$ at both short and long term. The experimental design is summarized in Figure 13.

Procedures took place in the animal facilities of the Central Research Unit of the Medicine Faculty at University of Valencia. Throughout this assay, mice were maintained in specified-pathogen free (SPF) facilities and fed ad libitum. In all surgery mice were anesthetized by isoflurane inhalation and were treated before surgery with pre-emptive and post-surgical analgesia (buprenorphine 0.01 mg/kg each 8 hours for 72 hours).

- SHORT-TERM TREATMENT

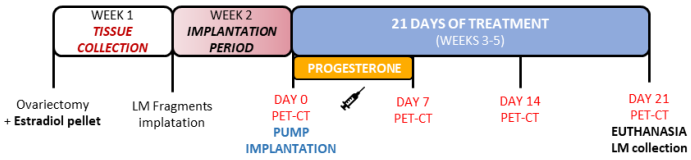

- LONG-TERM TREATMENT

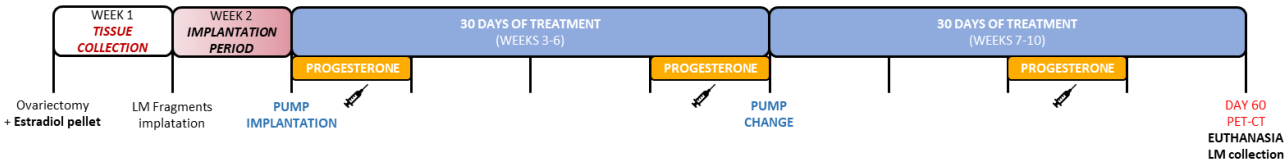

Figure 13. In vivo study experimental design. *In both short- and long-term assay models, female NOD–SCID mice were ovariectomized at 5-6 weeks of age and treated with estradiol and progesterone to mimic the menstrual cycle. One week after the ovariectomy, two leiomyoma (LM) fragments were implanted in each mouse. Treatment started one week after the LM implantation with the pump implantation. In the short-term assay, PET/CT scans were carried out once a week and animals were euthanized at day 21. In the long-term assay, at day 30 of treatment pumps were replace. At day 60, PET/CT scan was carried out and animals were euthanized.*

2.1. ESTABLISHMENT OF A HUMAN UTERINE LEIOMYOMA XENOGRAFT MOUSE MODEL

Female NOD–SCID mice (strain code 394; NOD.CB17-Prkdcscid/NCrCrl from Charles River Laboratories, France) were ovariectomized and hormonally supplemented at 5-6 weeks of age. A human uterine leiomyoma xenograft mouse model was induced by leiomyoma fragment xenotransplantation.

2.1.1. Ovariectomy and hormonal treatment

Considering that uterine leiomyoma growth depends on steroid hormones, mice were ovariectomized to avoid interindividual variation. In addition, to mimic the menstrual cycle, mice were treated with estrogen and progesterone, adapting the protocol published by Cervelló et al. (Cervelló *et al.*, 2011). Briefly, during ovariectomy surgery, both ovaries were removed by bilateral flank laparotomy, and estradiol pellets (SE121, 17β-estradiol 0.36 mg/60 days; Innovative Research of America, USA) were implanted subcutaneously at the neck. In addition, mice were injected subcutaneously with 1 mg/day of progesterone (Sigma-Aldrich, USA) for 1 week within a 2-week interval (Figure 13).

2.1.2. Xenotransplantation

Human uterine intramural leiomyoma collection: One week after ovariectomy in mice, human uterine leiomyoma tissue samples were collected from premenopausal women (n=4) undergoing either myomectomy or hysterectomy due to symptomatic uterine leiomyoma pathologies without any previous hormonal treatment (Table III). The collection of human uterine leiomyomas was approved by Clinical Ethics Committee at Hospital Univeristario y Politécnico La Fe (Spain) (2014/0691), and all participants provided informed consent.

Table III: Characteristics of patients included in the in vivo study.

Patient	Number of Intramural Leiomyomas	Average Size of Leiomyomas (cm)	AGE	BMI
1	1	9	44	28.63
2	1	10	44	19.72
3	4	4.8	54	23.59
4	4	6.2	49	25.97
Mean ± SD	**2.5 ± 1.7**	**9.5 ± 0.7**	**47.75 ± 4.8**	**24.5 ± 3.8**

BMI= body mass index; SD= standard deviation;

After human tissue collection, samples were placed in the maintenance medium described in section 1.1 and cut manually into approximately 3-4 mm^3 square-shaped pieces, measured with a digital caliper and photographed next to a reference rule. To determine **leiomyoma size,** fragment volume was calculated using the following ellipsoid formula:

$$volume = length \times width \times depth \times 0.52$$ (Halder *et al.*, 2012)

In the fragmentation process, one extra fragment from each human leiomyoma sample was fixed in 4% neutral-buffered formadehyde overnight at 4 ºC and subsequently, embedded in paraffin, as will be describe in section 2.3, for histological evaluation.

Xenotransplantation in ovariectomized and hormonally supplemented mice: During xenotransplantation 2 leiomyoma fragments were implanted intraperitoneally by suture in each flank of the mouse. To avoid interindividual variation, human leiomyoma tissue samples from the same patient were used for all animals in each of the four experimental sets. The study with animals was approved by the Ethics Committee for Animal Welfare of the University of Valencia (2017/VSC/PEA/00017).

2.2. VITAMIN D TREATMENT ON HUMAN UTERINE LEIOMYOMA XENOGRAFT MOUSE MODEL

To assess the effect of Vitamin D on human uterine leiomyoma in our xenograft mouse model, a **short-term assay** [21 days of treatment with $1,25(OH)_2D_3$] was initially carried out. With this purpose, three sets of experiments were performed with a total of 10 mice/group (set 1: 4 mice/group; set 2&3: 3 mice/group).

Subsequently, considering that uterine leiomyomas are bening tumors whose median growth rate is 9% per 6 months (Peddada *et al.*, 2008), we decided to perform an additional assay increasing the treatment time to observe the Vitamin D effect on leiomyoma growth. In this **long-term assay** (60 days of treatment with $1,25(OH)_2D_3$) 1 set of experiments with a total of 6 mice/group was conducted.

2.2.1. *In vivo* treatment

In both short- and long-term assays, one week after leiomyoma fragment implantation, ovariectomized and hormonally supplemented mice were divided in three different treatment groups:

1) Control group (EtOH, Vitamin D vehicle)
2) $1,25(OH)_2D_3$ 0.5 µg/kg/day
3) $1,25(OH)_2D_3$ 1 µg/kg/day

Although 2000 IU has been set as the Safe Tolerable Upper Intake Level of Vitamin D, absence of toxicity has been reported in clinical trials using Vitamin D dose 10 000 IU (Hathcock *et al.*, 2007). In this regard, the recommended dosage of DELTIUS 25 000 UI/2.5 mL (Italofarmaco, Spain), whose active ingredient is cholecalciferol, range from 1400 IU to 3500 IU (AEMPS, 2017).

For this reason, we wanted to assay in our *in vivo* model two Vitamin D doses between 1400 IU to 3500 IU. Considering that 1 µg of $1,25(OH)_2D_3$ is equivalent to 40 IU (Hathcock *et al.*, 2007), for mouse treatment we selected 0.5 µg/kg/day and 1 µg/kg/day, which are respectively equivalent to 1400 IU and 2800 IU for a human adult of 70 kg.

Treatments were delivered by ALZET Micro-Osmotic Pumps (USA), specifically the model 1004 was selected according to mice characteristics and treatment duration.

2.2.2. Micro-osmotic pumps preparation and implantation

To prepare the micro-osmotic pumps for Vitamin D groups, 1,25-dihydroxyvitamin D_3 (Sigma-Aldrich, USA) was diluted in ddH_2O to achieve the desired dose (0.5 µg/kg/day or 1 µg/kg/day), according to the pump delivery rate (0.11 µL/hour) and mouse average weight (20 g approximately). Control group was treated with the vehicle of Vitamin D (0.0004% EtOH) in a dose equivalent to the 1 µg/kg/day. With the aim of starting treatment immediately after implantation, pumps were filled with the different treatments and maintained in physiological saline solution at 37° C for 48 hours before pump implantation.

Pumps were implanted subcutaneously in the neck. Briefly, a small incision was made in the skin between the scapulae, and a small pocket was formed by spreading the subcutaneous connective tissue a part. The pump was inserted into the pocket, and the incision was closed by suture.

Due to the fact that pumps have a 30-day treatment release time, these pumps were replaced for a new one with the same characteristics 4 weeks after the first pump implantation in the case of the **long-term assay** (Figure 13).

2.2.3. Monitoring by micro PET/CT scan

Positron emission tomography with 2-deoxy-2-[fluorine-18] fluoro-D-glucose integrated with computed tomography (^{18}F-FDG PET/CT) is a powerful imaging tool used in human for the detection of various cancers. This technique is based on the use of the radiopharmaceutical ^{18}F-FDG, an analogue of glucose, which is metabolized similarly to glucose and provides functional information based on the increased glucose uptake and glycolysis of cancer cells (Almuhaideb *et al.*, 2011). ^{18}F-FDG enters the cell through glucose transporters and is phosphorylated to ^{18}F-FDG-6-phosphate, which cannot undergo glycolysis and becomes metabolically trapped intracellularly, in contrast to glucose-6-phosphate (Zhu *et al.*, 2011) (Figure 14). Since cancer cells have a high glycolytic rate, ^{18}F-FDG PET/CT scan allows the detection of tumors and their anatomical localization (Almuhaideb *et al.*, 2011; Zhu *et al.*, 2011). In addition, normal cells such as brain and heart cells can be imaged due their high metabolic demand, as well as bladder due to the urinary excretion of ^{18}F-FDG (Zhu *et al.*, 2011). In our case, ^{18}F-FDG PET/CT scan allows to check that uterine leiomyoma has implanted correctly and to monitor response to treatments.

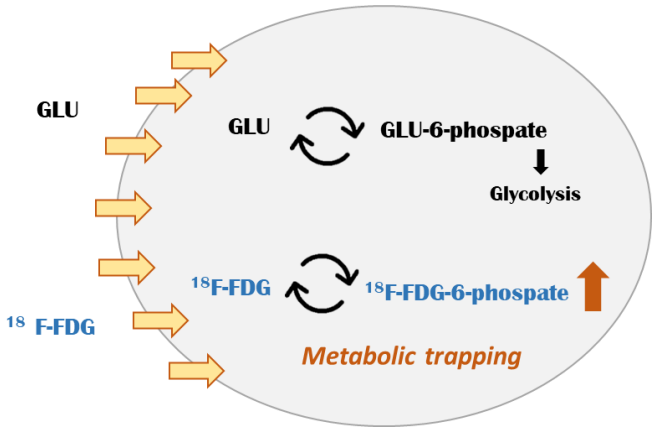

Figure 14. Metabolic trapping of ^{18}F-FDG in tumor cells. *Glucose (GLU) enters the cells through its membrane transporters and its phosphorylated to GLU-6-phosphate, which undergo glycolysis. In contrast, the analog of glucose 2-deoxy-2-[fluorine-18] fluoro-D-glucose, also known as ^{18}F-FDG, is transported across cell membranes by glucose transporters and is phosphorylated to 18F-FDG-6-phosphate, which cannot undergo glycolysis and is metabolically trapped intracellularly.*

To perform PET/CT scans, mice were anesthetized by isoflurane inhalation and injected intraperitoneally with 9250 kBq of ^{18}F-FDG (CURIUM Pharma, Spain). PET/CT scan was performed 45 minutes after the injection in a micro PET/CT ALBIRA I (Bruker Biospin PCI GmbH, Germany). During the PET/CT scan (15 minutes PET and 7 minutes CT) mice were anesthetized by isoflurane inhalation. Uterine leiomyomas were localized, and their metabolic activity was calculated by measuring the ^{18}F-FDG uptake (kBq/cm^3) in the selected region of interest (ROI) by the software A Medical Image Data Examiner (AMIDE) (Loening and Gambhir, 2003).

In the short-term assay ^{18}F-FDG PET/CT scans were carried out once a week starting on the day when pumps were implanted (DAY 0) and finishing the day of the euthanasia (DAY 21). Due to the invasiveness of this technique, a scan once a week for 60 days would not have been viable and, therefore, only one scan was performed the day of the euthanasia (DAY 60) for the long-term assay (Figure 13).

2.2.4. Euthanasia and sample collection

At the end of the experiment, day 21 in the short-term and day 60 in the long-term assay, mice were anesthetized by isoflurane inhalation, and blood was collected in a tube without anticoagulant. Mice were then euthanized by cervical dislocation and leiomyoma xenografts were collected.

2.3. Sample processing for subsequent functional analysis

Immediately after the collection, leiomyoma xenografts were measured and **leiomyoma size** was determined using digital caliper, as described in section 2.1, and photographed next to a reference rule.

Subsequently, to perform the necessary functional analysis, xenografts and blood collected from each mouse were processed as follows:

1. **Formalin-fixed paraffin-embedded tissue**. For histological, immunohistochemical and immunofluorescence analysis, one of the leiomyoma xenografts from each mouse was fixed in 4% neutral buffered formadehyde overnight at 4 ºC and then, transferred to 70%

EtOH for at least 24 hours. Consecutively, they were dehydrated in graded series of ethanol (70%, 80%, 96% and 100%) and xylol washes and embedded in paraffin wax.

For the subsequent analysis, embedded tissues were serially sectioned at 4 μm on a microtome (HM 310 microtome, Microm), mounted onto Superfrost Plus glass slides (ThermoFisher, USA) and stored at 37 °C at least for 24 hours. For the following analysis, tissue sections were deparaffined and rehydrating. For that, selected sections were placed at 60 °C for 1 hour followed by xylol washes and series of ethanol (100%, 96%, 80% and 70%) and, finally, distilled water.

2. **Protein extraction.** For western blot assays, half of one leiomyoma xenograft of each mouse was used for protein extraction following the protocol described at section 1.2.1.

3. **RNA extraction and cDNA synthesis.** For gene expression analysis by qRT-PCR, total RNA was extracted from half of one leiomyoma xenograft of each mouse with TRIzol reagent (ThermoFisher, USA), following manufacturer's instructions. Briefly, leiomyoma xenografts were mechanically dissected with scalpels to obtain fragments smaller than 1 mm^3. TRIzol reagent was added and incubated for 5 minutes at room temperature to induce lysis. Chloroform (Sigma-Aldrich, USA) was added and incubated for 2-3 minutes at room temperature. Subsequently, samples were centrifuged for 15 minutes at 4 °C at 12000 g. After centrifugation the sample separates into a lower red phenol-chloroform, and interphase, and a colorless upper aqueous phase. For RNA extraction, aqueous phase is transferred to a new tube containing isopropanol (Sigma-Aldrich, USA), mixed and incubated for 10 minutes at room temperature to induce RNA precipitation. After the incubation time, samples were centrifuged at 4 °C at 12800 g, supernatant was discarded, and pellet was washed in 75% ethanol and centrifuged for 5 minutes at 4°C at 7500 g. Finally, supernatant was discarded and pellet containing RNA was air-dried and resuspended in RNase-free water. RNA concentration was measured by Qubit Fluorometric Quantification using Qubit RNA HS assay kit (ThermoFisher, USA). Subsequently, complementary cDNA was synthesized from RNA with PrimeScript RT reagent Kit (Takara, Japan) and cDNA concentration was measured by Qubit Fluorometric Quantification using Qubit dsDNA HS assay kit (ThermoFisher, USA).

4. **Serum collection.** Collected **blood** was centrifugated at 1600 g for 10 minutes, and serum was collected and stored at –80 °C until analysis.

2.4. Treatment check, safety and toxicity studies

To corroborate that Vitamin D treatment has been correctly delivered and degraded, the expression of *CYP24A1* was measured by qRT-PCR in leiomyoma fragments, as described in section 1.3.2.1. The sequence of primers used is detailed in Annex I.

Additionally, to rule out possible hepatic damage induced by the Vitamin D treatment, liver function was evaluated by determining the serum levels of total Bilirubin (Bb) using Bb ELISA Kit (Elabscience, USA), following manufacturer's instructions.

2.5. Histological evaluation

To evaluate if uterine leiomyoma xenografts preserved their histological characteristics after implantation as well as evaluate the vascularization, tissue sections from the original tissue (before implantation) and from the different groups of treatment were subjected to hematoxylin and eosin (H&E) histological evaluation. Briefly, tissue sections were incubated in Harris hematoxylin for 5 minutes, rinsed with tap water and incubated for 5 minutes with Eosin. Then, slides were rinsed with tap water and with distilled water, air-dried and mounted with Eukitt Quick-hardening mounting medium (Sigma-Aldrich, USA).

In addition, the collagen and smooth muscle fiber content of the leiomyoma xenografts was evaluated using Trichrome Stain (Masson) Kit (Sigma-Aldrich, USA). Tissue sections were incubated in preheated Bouin's Solution (Sigma-Aldrich, USA) at 56 °C for 15 minutes. Slides were cooled and washed in running tap water. Subsequently, tissue sections were stained with Working Weigert's Iron Hematoxylin Solution (Sigma-Aldrich, USA) for 5 minutes and washed in running tap water for 5 minutes. Next, slides were rinsed in deionized water, stained in Biebrich Scarlet-Acid Fucshin for 5 minutes and rinsed in deionized water. Slides were placed consecutively in Working Phosphotungstic/Phosphomolybdic Acid Solution (5 minutes), Aniline Blue Solution (5 minutes) and acetic acid, 1% (2 minutes). Finally, the slides were rinsed, air-dried and mounted with Eukitt Quick-hardening mounting medium (Sigma-Aldrich, USA).

2.6. Functional analysis

2.6.1. Proliferation analysis

To evaluate the effect of Vitamin D treatment on proliferation in human leiomyoma xenografts, inmunihistochemistry (IHC) for the proliferation marker Ki67 and by qRT-PCR of the proliferation marker PCNA were carried out.

For proliferation evaluation in leiomyoma tissue sections by Ki67 IHC, paraffin-embedded tissues were sectioned at 4 μm, deparaffined and rehydrated as described in section 2.3. Subsequently, IHC was performed as follows:

1. **Antigen retrieval**: Slides were incubated with 10 mM citrate buffer, 0.05% Tween 20 pH 6, for 20 minutes at 95 °C.
2. **Permeabilization:** Incubation with PBS-Tween 20 0.05%, 3 times x 5 minutes.
3. **Blocking Endogenous peroxidase activity:** Incubation with H_2O_2 for 5 minutes at room temperature in darkness.
4. **Wash:** Distilled water, 3 times x 5 minutes.
5. **Blocking:** Incubation with PBS-BSA 5%- Tween 0.05% for 1 hour at room temperature.
6. **Primary antibody incubation:** Slides were incubated with Anti-Ki67 antibody (ab15580, Abcam, UK) diluted 1:300 in PBS-BSA 1%- Tween 0.05%, for 1 hour at room temperature.
7. **Wash:** Distilled water, 3 times x 5 minutes.
8. **Secondary antibody incubation:** Incubation with labeled polymer-HRP (Dako EnVision™+ Dual Link System-HRP; Agilent, USA) for 30 minutes at room temperature.
9. **Wash:** PBS-Tween 0.05%, 3 times x 5 minutes.
10. **DAB chromogen incubation:** Slides were incubated with substrate-chromogen solution (Dako EnVision™+ Dual Link System-HRP; Agilent, USA). Reaction was stopped with distilled water.
11. **Hematoxylin counterstain:** Slices were incubated for 5 minutes with Harris Hematoxylin, rinsed, dried and mounted with Eukitt Quick-hardening mounting medium (Sigma-Aldrich, USA).

To measure the % of Ki67 expression, samples were evaluated in a Nikon Eclipse 80i microscope, and four images of each sample were quantitatively assessed with Image ProPlus (Media Cybernetics, USA).

To measure the expression of *PCNA* in leioymyoma fragments from treated and control groups, qRT-PCR was performed as described in section 1.3.2.1. The sequence of primers used is detailed in Annex I.

2.6.2. Cell density

To determine cell density in leiomyoma xenografts from Vitamin D treated and control groups, hematoxylin-eosin staining was performed, as described in section 2.5 Subsequently, samples were evaluated in a Nikon Eclipse 80i microscope and four images of each sample were quantitatively assessed with Image ProPlus (Media Cybernetics, USA). Subsequently, cell density was calculated following the formula:

$$cell\ density = (nuclei\ area / total\ area) \times 100$$

2.6.3. Extracellular matrix analysis

The *in vivo* approach of Vitamin D treatment of human uterine leiomyoma allows the assessment of the effect of this treatment on extracellular matrix (ECM) formation. For that purpose, the expression of ECM-associated proteins, such as collagen I, fibronectin and plasminogen activator inhibitor-1 (PAI-1) was evaluated by western blot in proteins extracted from leiomyoma fragments, as described in section 2.3. Briefly, 20 µg of each sample were analyzed as described in section 1.2.2. The antibodies used are summarized in Table IV.

Table IV. Antibodies used in Western Blot experiments

PROTEIN	ANTIBODY	DILUTION
COLLAGEN I	70R-CR007x (Fitzgerald, USA)	1:5000
FIBRONECTIN	F3648 (Sigma-Aldrich, USA)	1:2000
PAI-1	sc-5297 (Santa Cruz Biotecnology, USA)	1:200
PRO-CASPASE 3	sc-7272 (Santa Cruz Biotecnology, USA)	1:200
CLEAVED CASPASE 3	9661 (Cell signaling Technology, USA)	1:500
β-ACTIN	sc-516102 (Santa Cruz Biotecnology, USA)	1:2000

2.6.4. Transfroming Growth Factor β signalling pathway

To assess in our xenotransplanted uterine leiomyoma the effect of Vitamin D treatment on transforming growth factor β (TGFβ) signaling, whose involvement in ECM formation has been widely described, the expression of *TGFβ3,* was measured by qRT-PCR, as described in section 1.2.3. The sequence of primers used is detailed in Annex I.

2.6.5. Apoptosis

To assess Vitamin D effect on apoptosis in leiomyoma xenografts from treated and control mice, the expression of PRO-CASPASE 3 and CLEAVED CASPASE-3 was evaluated by western blot, as described in section 1.2.2. For this purpose, 20 μg of each sample were analyzed, and the antibodies used are summarized in Table IV.

In addition, the percentage of apoptotic cells in 4-μm tissue sections from xenotransplanted leiomyomas embedded in paraffin was determined by TUNEL assay. Sections were deparaffined and rehydrated as described in section 2.3 and TUNEL assay was carried out as described in section 1.3.3.5, skipping the fixation step. Samples were evaluated in a Nikon Eclipse 80i microscope, and four images of each sample were quantitatively assessed with Image ProPlus (Media Cybernetics, USA).

2.7. Statistical analysis

GraphPad Prism 6.0 was used in this study for statistical analyses and graphics generation. Data are presented as mean ± standard deviation (SD). For PET/CT data Kruskal-Wallis test was performed. Wilcoxon test was performed for leiomyoma size analysis in the short-term assay and Student's t-test was performed in the long-term assay data analysis. For the analysis of Ki67, cell density, and western blot experiments ANOVA test and Kruskal-Wallis test were carried out to analyze data from short- and long-term assays, respectively. Gene expression and validation analysis were carried out with Qiagen Data Analysis Software applying Student's t-test. p value <0.05 was considered statistically significant.

V. RESULTS

V. RESULTS

1. *IN VITRO* STUDY

1.1. Evaluation of human uterine leiomyomas and adjacent myometrial tissues

Expression of proliferation-, Wnt/β-catenin signaling- and apoptosis-related proteins was assessed in leiomyomas and adjacent myometrium tissue (n=22) using western blotting. Higher PCNA expression was detected in 95% (20/22 samples) of leiomyomas compared to corresponding myometrium (Figure 15A), indicating greater proliferation in uterine leiomyomas. Similarly, 77% (17/22) of leiomyoma samples presented higher expression of WISP1 than in corresponding myometrium (Figure 15A), indicating altered Wnt/β-catenin signaling in uterine leiomyomas. Jointly, uterine leiomyoma samples presented quantitatively higher PCNA expression levels (fold change=8.16; p value=0.0006) (Figure 15B) and significantly increased expression of WISP1 (fold change=5.5; p value<0.0001) (Figure 15C), in both cases in comparison with myometrium.

Apoptosis was assessed in leiomyomas compared to adjacent myometrium using BAX (pro-apoptotic) and BCL2 (anti-apoptotic) protein expression (Figure 15D). No difference was detected between tumor and typical tissues in expression of BCL2 or BAX. When BAX is over-expressed it can heterodimerize with BCL2 and induce cell death. Thus, we also calculated the BAX/BCL2 ratio to determine the susceptibiliity to apoptosis in leiomyoma tissue compared to myometrium. No significant difference was identified in the BAX/BCL2 ratio between leiomyoma and myomeytium (Figure 15E).

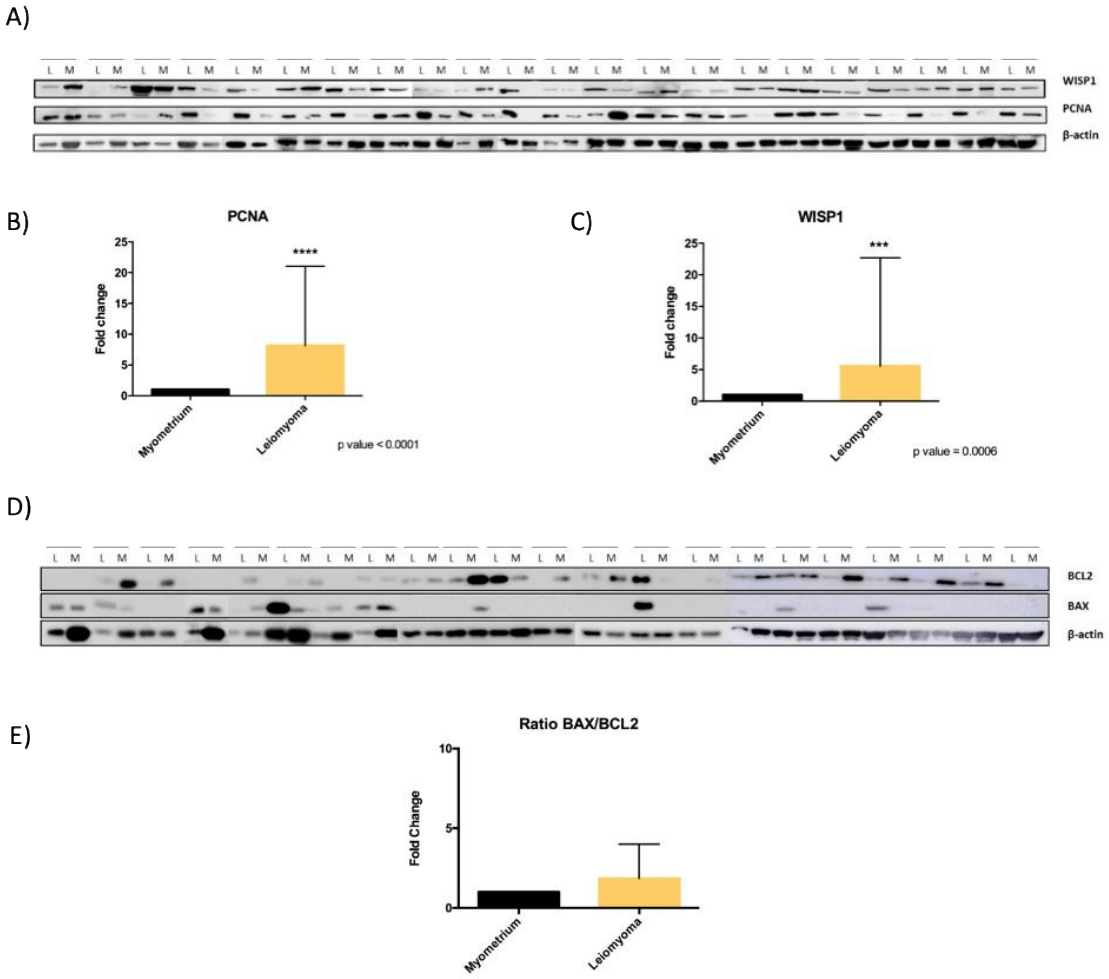

Figure 15. Proliferation rate, Wnt/β-Catenin signaling and apoptosis in human uterine leiomyoma and adjacent myometrium. *Expression levels of PCNA (36 kDa) and WISP1 (70 kDa) proteins were analyzed in uterine leiomyoma (L) and its corresponding myometrium (M) (n=22) by western blotting (A). Mean values and standard deviations of normalized data for PCNA (B) and WISP1 (C) expression, represented as fold change. BCL2 (23 kDa) and BAX (26 kDa) expression levels in L and M (n=22) were analyzed using western blotting (D). BAX/BCL2 ratio represented as a fold change (E). Note that PCNA and WISP1 expression were significantly higher in L compared to M (****p value< 0.0001 and *** p value < 0.0006)*

1.2. Establishment of Vitamin D treatment conditions

1.2.2. Vitamin D treatment: Time-dose response assay

Before starting *in vitro* experiments, time-dose assays were conducted to determine the optimal time-dose of Vitamin D based on the expression of *CYP24A1* by HULP cells (n=6). *CYP24A1* expression was measured by qRT-PCR at 24 and 48 hours after Vitamin D-treatment and compared to control HULP cells. Vitamin D treatment activated *CYP24A1* expression in HULP cells in a dose-dependent fashion (Figure 16). As expected, *CYP24A1* expression was not induced by vehicle (0.5% EtOH) treatment. However, the expression of *CYP24A1* was induced by Vitamin D in HULP cells at 10 nM, 100 nM and 1000 nM, at both 24 and 48 hours. Considering that the highest expression of *CYP24A1* was found in cells treated with 100 nM Vitamin D at 48 hours (fold change=20422.9) (Figure 16A), this was the selected Vitamin D dose for the subsequent studies.

1.2.3. Cell viability assay

After the Vitamin D dose was selected, a preliminary study was performed to check whether Vitamin D vehicle may damage HULP cells by flow cytometry (n=6). Data analysis showed that viability of HULP cells was similar in those cells treated with cell culture medium, vehicle (0.5% EtOH) and Vitamin D at both 48 and 144 hours (Figure 16B), suggesting that both Vitamin D and Vitamin D vehicle (0.5% EtOH) did not affect viability of HULP cells.

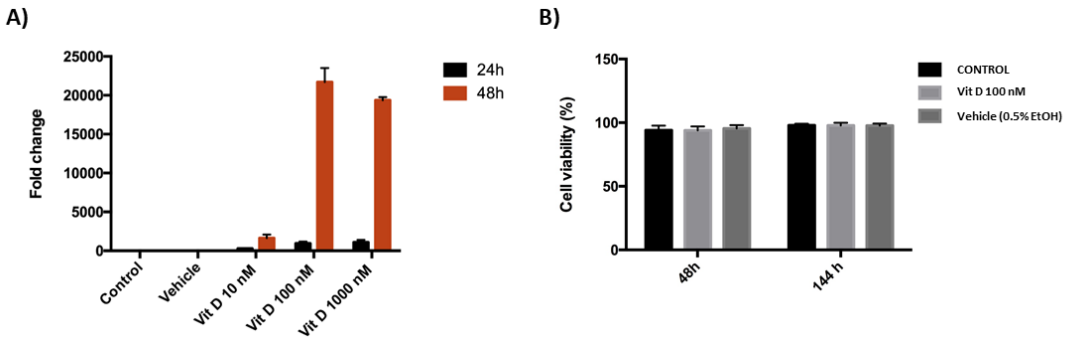

Figure 16. Vitamin D treatment: Preliminary studies. CYP24A1 *gene expression levels (represented as fold change) in HULP cells (n=6) at 24 and 48 hours after Vitamin D (Vit D) treatment at different doses (10 nM, 100 nM and 1000 nM) compared to control and vehicle (0.5% EtOH) (A). Viability of HULP cells (n=6) treated with Vit D (100 nM) and vehicle compared to control at 48 and 144 hours (B). Note that Vit D 100 nM at 48 hours showed the highest* CYP24A1 *expression*

1.3. Vitamin D effect on cell cycle in human uterine leiomyoma primary cells

To demonstrate that Vitamin D can induce cell growth arrest in HULP cells *in vitro*, cellular DNA was analyzed by PI assay in Vitamin D-treated compared to control HULP cells (n=22). Treatment with Vitamin D induced a decrease in the percentage of cells in S-G_2/M phase compared to its own control in 50% of cases (11/22) (Figure 17), causing an increase in the percentage of cells in G_0/G_1 phases. Thus, cell growth arrest was induced by Vitamin D treatment in HULP cells.

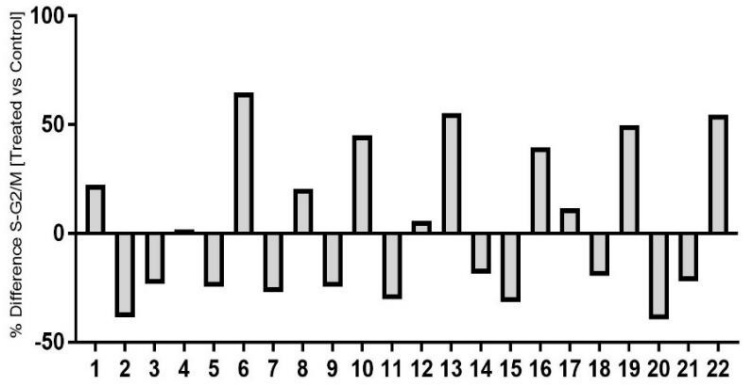

Figure 17. Vitamin D effect on cell cycle in human uterine leiomyoma primary cells in vitro. *Cell cycle distribution was determined by flow cytometry using propidium iodide (n=22). The difference in the percentage of cells in S-G_2/M between Vit D-treated and control L cells (100 - [%S-G_2/M_{vitD} x 100 / %S-$G_2/M_{control}$]) is represented in the graph.*

1.4. Vitamin D effect on proliferation in human uterine leiomyoma primary cells

The effect of Vitamin D treatment on cell proliferation was assayed using PCNA protein expression, the gold standard for proliferation, in Vitamin D-treated and control HULP cells (n=15) by western blotting (Figure 18A). Vitamin D treatment significantly decreased PCNA expression in HULP cells (fold change=0.74; p value=0.007) (Figure 18B), suggesting a decrease in proliferation in HULP cells treated with Vitamin D.

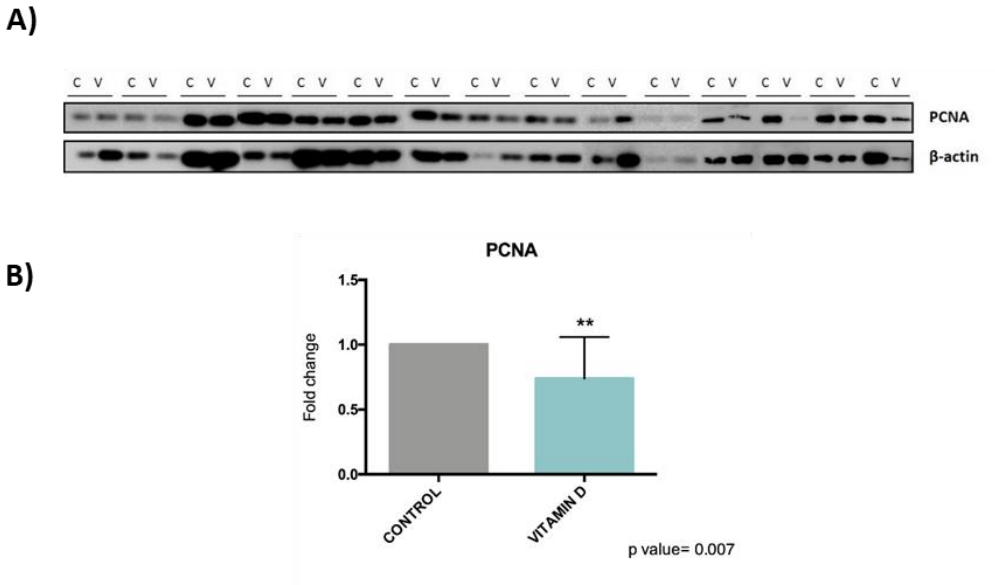

Figure 18. Vitamin D effect on proliferation in human uterine leiomyoma primary cells in vitro. *Expression levels of PCNA protein (36 kDa) were analyzed in control HULP cells (named as C) and Vitamin D-treated HULP cells (named as V) (n=15) by western blotting (A). Mean normalized values for PCNA are represented as fold change (B). Note that PCNA expression was significantly higher in Vitamin D-treated cells compared to control (p value = 0.007).*

1.5. Vitamin D effect on Wnt/β-Catenin pathway in human uterine leiomyoma primary cells

1.5.1. Gene expression analysis

To examine whether Vitamin D can affect Wnt/β-catenin pathway in HULP cells, the expression of 84 Wnt-related genes was quantified in Vitamin D-treated and control HULP cells (n=11) using RT^2-Profiler PCR Arrays (Qiagen, Germany). Although most of the genes involved in Wnt/β-catenin pathway were downregulated, none of them was significantly different from control (Table V).

Subsequently, Wnt-related genes were divided according to their role in developmental processes implicated in leiomyoma development, such as tissue polarity and cell migration, cell cycle, cell growth, and proliferation. In this regard, among genes grouped according to their involvement in **tissue polarity and cell migration**, 11 of 15 genes (73.3%) were downregulated in Vitamin D-treated HULP cells (Figure 19A) compared to control cells. Similarly, 17/22 (77.2%) of genes involved in **cell cycle, cell growth, and proliferation** were

downregulated after Vitamin D treatment in HULP cells (Figure 19B) compared to control HULP cells. Finally, we observed that 9/12 (75%) **Wnt/β-catenin target genes** were repressed in Vitamin D-treated HULP cells (Figure 19C) compared to control cells.

In addition, the pathway activity score calculated by Wnt-array determined that Vitamin D treatment significantly decreased Wnt/β-catenin pathway activity in HULP cells (activity score=−0.775; p value<0.001) (Figure 19D).

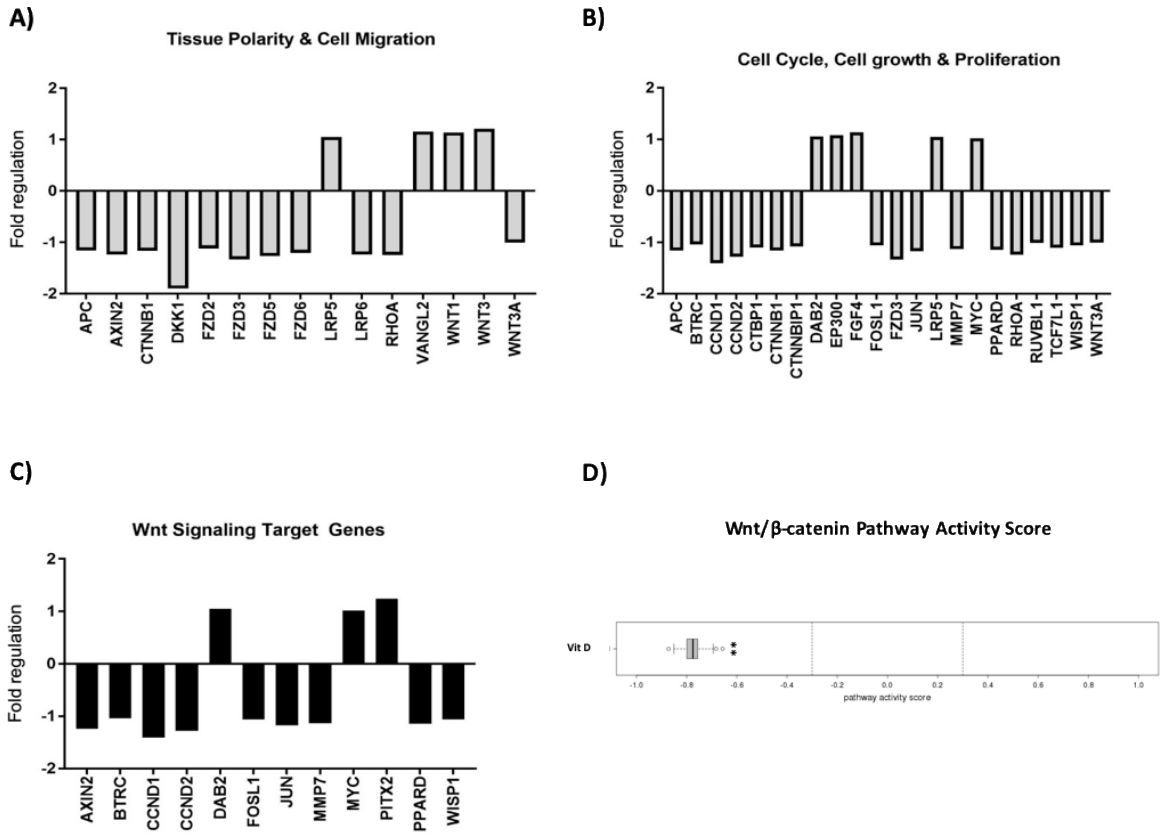

Figure 19. Vitamin D effect on Wnt/β-Catenin pathway in human uterine leiomyoma primary cells at the gene level. *Expression of Wnt-related genes involved in tissue polarity and cell migration (A), cell cycle, cell growth and proliferation (B), and Wnt/β-Catenin targets genes (C) in Vitamin D-treated compared to control HULP cells (n=11). Gene expression is represented as fold regulation. The pathway activity score in Vitamin D-treated HULP cells is represented in a box-and-whisker plot (D). ** p value < 0.001*

Table V: Fold regulation of Wnt-related genes in Vitamin D-treated human uterine leiomyoma cells compared to control.

Gene symbol	Fold Regulation	p value
APC	-1.1574	0.52955
AXIN1	-1.0102	0.710028
AXIN2	-1.2396	0.363504
BTRC	-1.0407	0.646738
CSNK1A1	-1.0846	0.581808
CTBP1	-1.101	0.565176
CTNNB1	-1.1607	0.646314
CTNNBIP1	-1.0803	0.79625
DAAM1	-1.2835	0.324044
DAB2	1.0511	0.725281
DKK1	-1.8945	0.504067
DKK3	-1.294	0.355726
DVL1	-1.1106	0.605367
DVL2	-1.119	0.562855
EP300	1.0792	0.849541
FBXW11	-1.2757	0.248725
FGF4	1.1344	0.96428
FOSL1	-1.0589	0.80053
FRAT1	1.0703	0.624061
FRZB	-1.0386	0.814856
FZD1	-1.0674	0.66584
FZD2	-1.1191	0.556217
FZD3	-1.3324	0.349138
FZD4	-1.0453	0.666818
FZD5	-1.2656	0.864154
FZD6	-1.2039	0.537245
FZD7	1.5185	0.751657
FZD8	1.1289	0.857104
FZD9	1.0161	0.947621
GSK3B	-1.1845	0.404315
JUN	-1.1714	0.750493
KREMEN1	-1.0109	0.960874
LRP5	1.0483	0.995559
LRP6	-1.2381	0.405819
MAPK8	-1.0915	0.741356
MMP7	-1.1361	0.929458
NFATC1	-1.0521	0.672323
NKD1	1.0342	0.796232
NLK	-1.05	0.895349
PITX2	1.2464	0.632669
PORCN	1.0595	0.769154
PPARD	-1.1451	0.415124
PRICKLE1	1.0368	0.833244
RHOA	-1.2423	0.193577
RUVBL1	-1.0159	0.791431
SFRP1	1.1137	0.939674
SFRP4	1.1329	0.927695
SOX17	1.0115	0.618105
TCF7	-1.0734	0.925476
TCF7L1	-1.1091	0.478641
VANGL2	1.1596	0.668138
WIF1	-1.5371	0.265442
WISP1	-1.0569	0.969949
WNT1	1.1344	0.96428
WNT10A	1.3512	0.988638
WNT11	1.0375	0.756676
WNT2	1.0804	0.980221
WNT2B	-1.2904	0.303299
WNT3	1.2083	0.869978
WNT3A	-1.0049	0.714359
WNT4	1.0039	0.764899
WNT5A	-1.8872	0.439247
WNT5B	-1.2308	0.504732
WNT6	-1.0263	0.987674
WNT7A	1.0641	0.899469
WNT7B	-1.0052	0.737202
WNT8A	-1.0116	0.624645
WNT9A	-1.4913	0.490877
BOD1	-1.1211	0.64664
CALM1	-1.3012	0.433531
CCND1	-1.4034	0.700478
CCND2	-1.2804	0.397358
CHSY1	-1.5558	0.085032
CXADR	1.3719	0.63466
CYP4V2	1.0575	0.886613
HSPA12A	-1.0927	0.51258
LEF1	-1.2966	0.362372
MT1A	-1.1182	0.811015
MTFP1	-1.1356	0.554851
MTSS1	1.1625	0.998731
MYC	1.017	0.78534
NAV2	-1.3074	0.646106
PRMT6	1.1305	0.78106
SKP2	-1.0777	0.739279

In this regard, the overview of the expression levels of genes involved in the Wnt/β-catenin pathway (KEGG identifier: hsa04310) showed that both canonical and non-canonical Wnt pathways were mostly inhibited in HULP cells treated with Vitamin D compared to control cells (Figure 20).

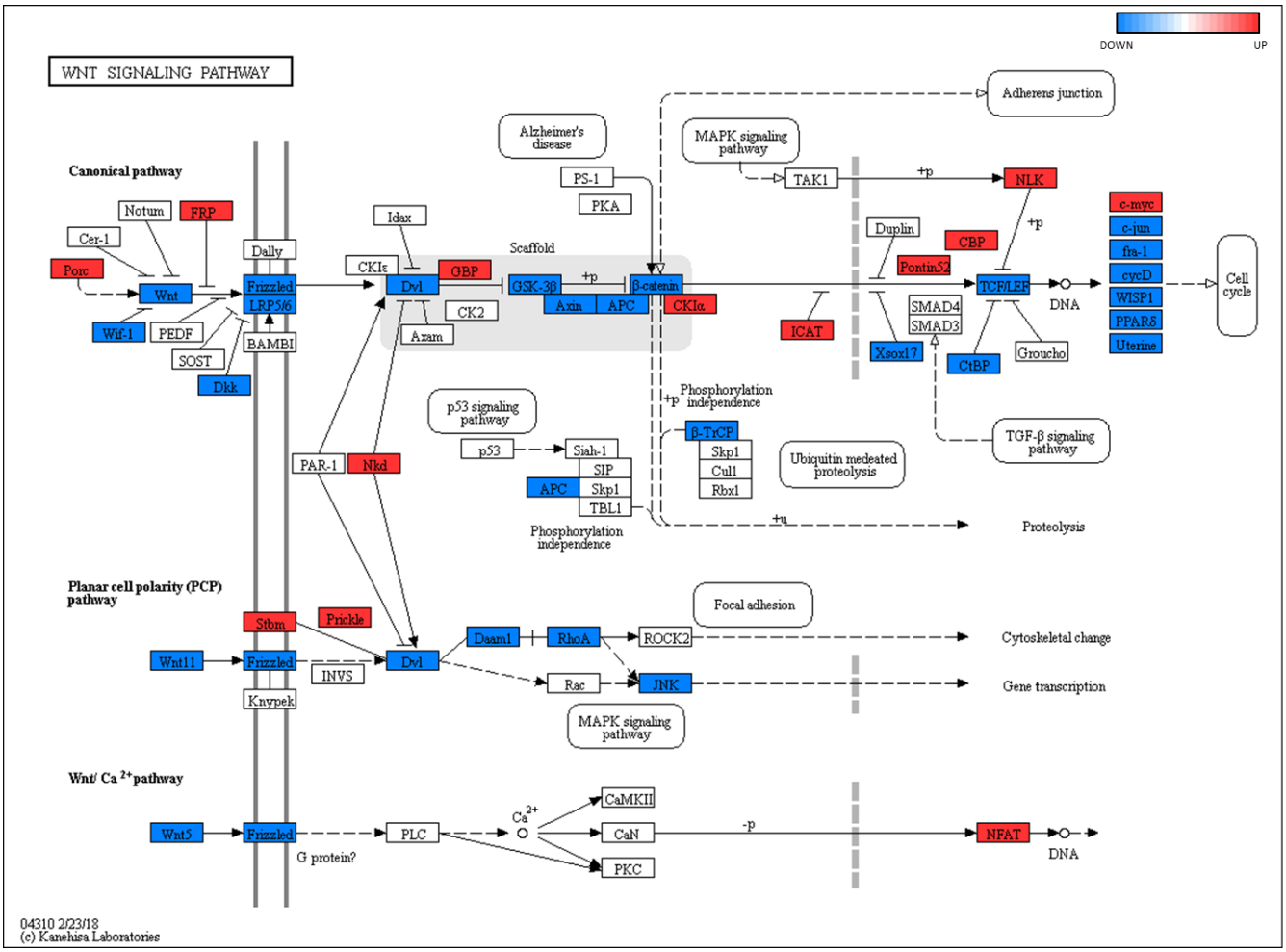

Figure 20. Wnt/β-Catenin pathway overview in human uterine leiomyoma primary cells after Vitamin D treatment. Overview of the expression levels of genes involved in *Wnt/β-Catenin pathway (KEGG identifier: hsa04310) after Vitamin D treatment in HULP cells compared to control. Upregulated genes were colored in red and downregulated genes in blue with KEGG Mapper-Color Pathway.*

To validate RT^2-Profiler PCR Array results, expression of the two genes with the highest differential expression (*DKK1* and *WNT5A*) was measured by qRT-PCR in HULP cells (n=17) treated with Vitamin D. For both genes, Vitamin D treatment decreased the relative transcript abundance compared to untreated control cells (Figure 21).

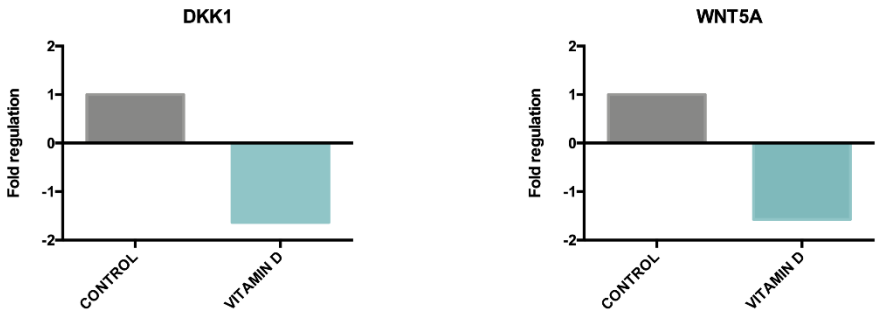

Figure 21. Gene expression analysis validation of Wnt-pathway array. *The expression of* DKK1 *and* WNT5A *was evaluated in HULP cells to validate RT^2-Profiler PCR Array results. Gene expression is represented as fold regulation.*

1.5.2. Protein expression analysis

To assess the effect of Vitamin D treatment on HULP cells at the protein level, we measured the expression of three Wnt/β-catenin target proteins (WISP1, uPAR and MMP7) in Vitamin D-treated and control HULP cells (n=11). Our results revealed a trend of Vitamin D inhibiting the expression of these protein targets in HULP cells (Figure 22).

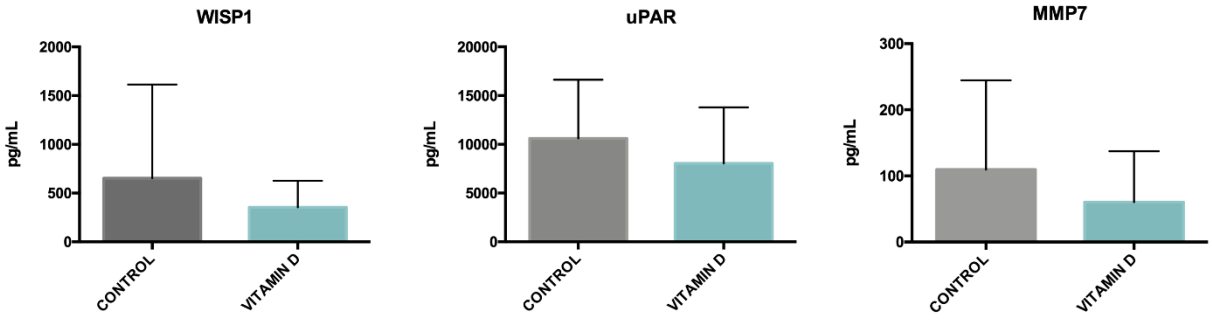

Figure 22. Vitamin D effect on the Wnt/β-Catenin pathway in human uterine leiomyoma primary cells at the protein level*. Protein expression of WISP1, uPAR and MMP7 in Vitamin D-treated compared to control HULP cells was measured using Quantibody Human arrays (n=11). The expression of each protein is expressed in pg/mL.*

1.6. Vitamin D effect on apoptosis of human uterine leiomyoma primary cells

1.6.1. Gene expression analysis

Vitamin D's effect on apoptosis in HULP cell culture was assessed via the expression of 84 genes involved in apoptosis quantified using RT^2-Profiler PCR Arrays. The fold regulation of each gene in Vitamin D-treated group compared to control is detailed in Table VI. Note that only three genes (highlighted in red in Table VI) were differentially expressed after Vitamin D treatment in HULP cells: *BCL2* and *PYCARD* were significantly upregulated, and *TNFRSF11B* was significantly downregulated.

To analyze the effect of Vitamin D treatment on the pathway, genes involved in apoptosis were divided into two groups: those that act as positive regulators (pro-apoptotic genes) or those that act as negative regulators (anti-apoptotic genes). We observed that only 15/42 (35.7%) positive regulators were upregulated in HULP cells after Vitamin D treatment (Figure 23A), while 25/32 (78.1%) negative regulators were downregulated in Vitamin D-treated HULP cells compared to control (Figure 23B). Interestingly, *TNFRSF11B* showed a significantly decreased expression (fold change=-2.02; p value=0.04). However, among these negative regulators, *BCL2* expression was significantly upregulated (fold change=2.58; p value=0.01) (Figure 23B). In sum, these data indicate that Vitamin D treatment did not induce a significant change in apoptosis in HULP cells.

Table VI: Fold regulation of apoptotic genes in Vitamin D-treated human uterine leiomyoma cells compared to control.

Gene symbol	Fold Regulation	p value
ABL1	1.0547	0.742787
AIFM1	-1.087	0.602634
AKT1	-1.004	0.908165
APAF1	-1.2279	0.464424
BAD	1.013	0.943105
BAG1	-1.0003	0.894209
BAG3	-1.0221	0.955024
BAK1	-1.0994	0.482775
BAX	-1.0462	0.833403
BCL10	-1.1762	0.332341
BCL2	2.5852	0.011412
BCL2A1	-1.38	0.555147
BCL2L1	1.0909	0.708246
BCL2L10	-1.2494	0.348537
BCL2L11	1.2548	0.322227
BCL2L2	-1.0675	0.882413
BFAR	-1.0434	0.797457
BID	-1.0216	0.957823
BIK	-1.1697	0.72798
BIRC2	-1.0735	0.730583
BIRC3	-1.5325	0.608641
BIRC5	-1.0801	0.624735
BIRC6	-1.1419	0.455174
BNIP2	-1.0685	0.702539
BNIP3	-1.2497	0.336155
BNIP3L	1.108	0.734511
BRAF	-1.0247	0.622354
CASP1	1.096	0.97466
CASP10	-1.0841	0.994772
CASP14	-1.1971	0.469901
CASP2	-1.1733	0.617096
CASP3	-1.1894	0.544941
CASP4	1.12	0.529764
CASP5	-1.3526	0.249319
CASP6	-1.0449	0.797015
CASP7	-1.0753	0.700236
CASP8	-1.0923	0.594909
CASP9	-1.0548	0.575439
CD27	1.1577	0.971028
CD40	1.1345	0.775321
CD40LG	-1.2783	0.388493
CD70	-1.3117	0.450324

Gene symbol	Fold Regulation	p value
CFLAR	-1.0112	0.759777
CIDEA	-1.4028	0.582662
CIDEB	-1.1218	0.65086
CRADD	-1.1389	0.770786
CYCS	-1.1573	0.512015
DAPK1	-1.1602	0.517227
DFFA	-1.019	0.873866
DIABLO	1.1082	0.656593
FADD	1.0025	0.82956
FAS	-1.011	0.785986
FASLG	-1.0726	0.580719
GADD45A	1.6088	0.12952
HRK	-1.1491	0.601833
IGF1R	-1.3583	0.358817
IL10	-1.6001	0.302305
LTA	-1.1211	0.728551
LTBR	1.003	0.965457
MCL1	1.0467	0.718299
NAIP	1.1525	0.82215
NFKB1	1.0077	0.901464
NOD1	1.0142	0.672034
NOL3	1.0297	0.884482
PYCARD	1.3485	0.028122
RIPK2	-1.0771	0.546991
TNF	1.1075	0.979844
TNFRSF10A	1.2055	0.879235
TNFRSF10B	-1.0874	0.611655
TNFRSF11B	-2.0138	0.044443
TNFRSF1A	1.2697	0.376084
TNFRSF1B	-1.3214	0.524153
TNFRSF21	1.2355	0.533917
TNFRSF25	1.0221	0.632808
TNFRSF9	-2.1962	0.175964
TNFSF10	-1.3184	0.796289
TNFSF8	-1.2017	0.320097
TP53	-1.0108	0.995442
TP53BP2	-1.1793	0.472651
TP73	-1.2525	0.261133
TRADD	1.1255	0.897332
TRAF2	-1.1573	0.494629
TRAF3	-1.1193	0.589066
XIAP	-1.0063	0.989487

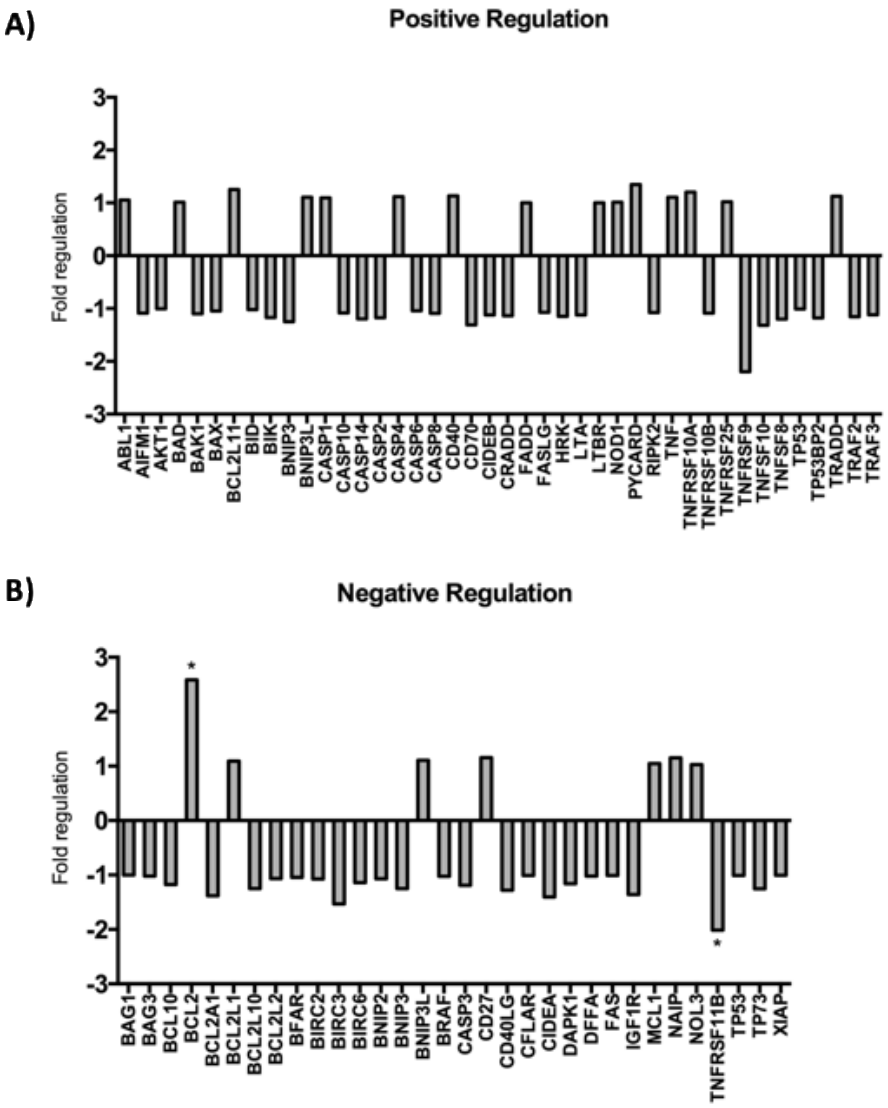

Figure 23. Vitamin D effect on apoptosis in human uterine leiomyoma primary cells at the gene level. *Expression of apoptotic positive regulators (Pro-apoptotic genes) (A) and negative regulators (anti-apoptotic genes) (B) in Vitamin D-treated compared to control HULP cells (n=11). Gene expression is represented as fold regulation.*

To validate RT^2-Profiler PCR Arrays results, we measured the expression of the two genes with the highest differential expression (*BCL2* and *TNFRSF11B*) by qRT-PCR in HULP cells (n=17) treated with Vitamin D compared to control HULP cells. In accordance with PCR Array results, Vitamin D treatment significantly increased the relative transcript abundance of *BCL2* and decreased the abundance of *TNFRSF11B* (Figure 24).

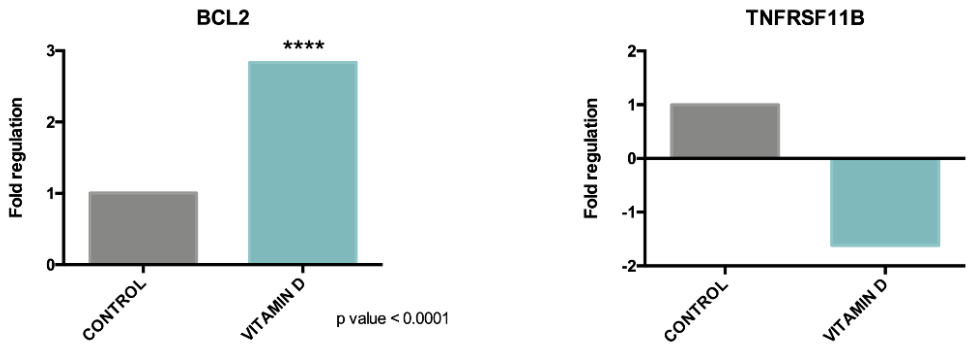

Figure 24. Gene expression analysis validation of apoptosis array. *To validate RT^2-Profiler PCR Array results, expression of BCL2 and TNFRSF11B was evaluated in HULP cells. Gene expression is represented as fold regulation. Note that BCL2 expression was significantly higher in Vitamin D-treated cells compared to control (p value< 0.001).*

1.6.2. TUNEL assay

To corroborate that Vitamin D did not induce apoptosis in HULP cells, a TUNEL assay was performed in Vitamin D-treated and control HULP cells. We observed that the % apoptotic cells was similar in both Vitamin D-treated and control cells (Figure 25A). Quantification of fluorescence images showed that Vitamin D treatment did not increase the percentage of apoptotic cells (Figure 25B), corroborating that Vitamin D treatment did not induce a significant change in apoptosis in HULP cells.

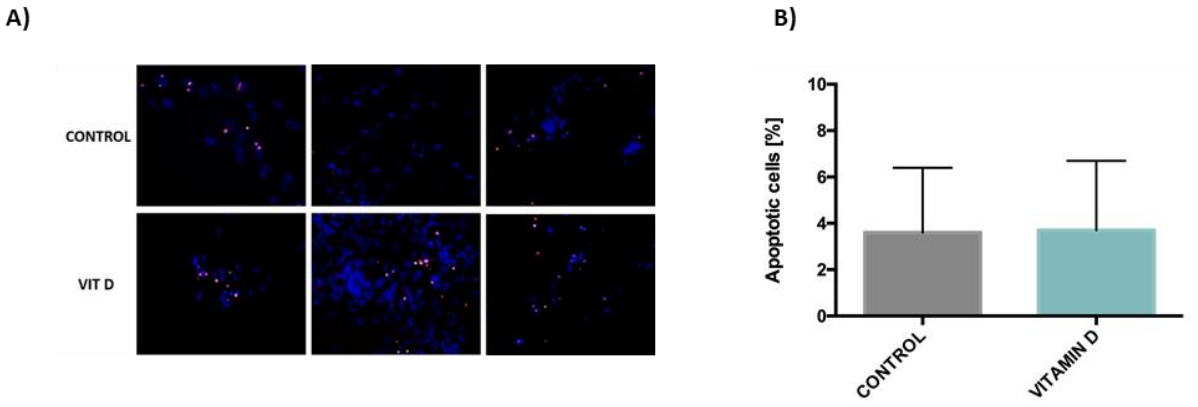

Figure 25. Apoptosis assayed by TUNEL. *The percentage of apoptotic cells was determined by TUNEL assay in HULP cells treated with Vitamin D and control (A). Average percentage of apoptotic cells in each group is represented as mean ± SD in (B).*

2. *IN VIVO* STUDY

Considering that human uterine leiomyomas are solid tumors composed of smooth muscle cells interspersed in an abundant ECM that plays an important role in tumor expansion, *in vitro* assays, even for primary cells, do not provide sufficient information for how this treatment would work in the human patient context. With that purpose, we aimed to assess the effect of Vitamin D treatment on a xenograft mouse model generated by the implantation of human uterine leiomyoma fragments, at both short and long term.

2.1. Treatment utility and toxicity assay

To ensure administered Vitamin D would be metabolized by leiomyoma cells from xenografts, the expression of *CYP24A1* in leiomyoma fragments from the different treatment groups was measured by qRT-PCR. Expression of *CYP24A1* was induced by both Vitamin D doses in a concentration-dependent manner, which was statistically significant with the higher dose at 21 days, and with both Vitamin D doses at 60 days (Figure 26A). Thus, Vitamin D degradation had begun in treated leiomyoma cells.

To rule out possible hepatic damage induced by Vitamin D in mice that received the treatment, liver function was evaluated by bilirubin serum levels analysis using ELISA assay. These levels were similar in the three study groups (Figure 26B), indicating no side effects in the liver with Vitamin D treatment.

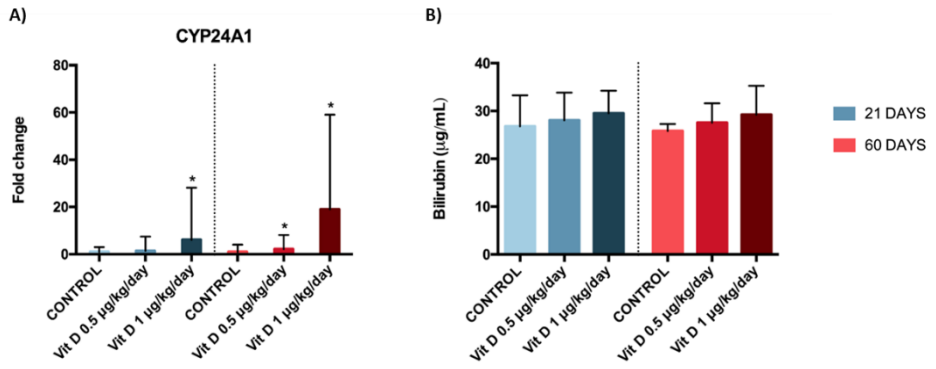

Figure 26. Treatment utility and toxicity. CYP24A1 *gene expression levels represented as fold change in leiomyoma cells from xenograft implants in the different treatment groups (A). Bilirubin serum levels represented as mean ± SD in the different treatment groups (B). Note that* CYP24A1 *gene expression was significantly induced by Vitamin D 1 µg/kg/day at 21 and 60 days, and by Vitamin D 0.5 µg/kg/day at 60 days. * p value<0.05*

2.2. In vivo monitoring

In vivo monitoring by PET/CT scans provided the leiomyoma metabolic activity, which enabled non-invasive measurement of leiomyoma xenograft size. In the short-term assay, leiomyoma xenografts were localized in each weekly PET/CT scan, corroborating that leiomyoma fragments were correctly implanted at the beginning of the treatments (Figure 27).

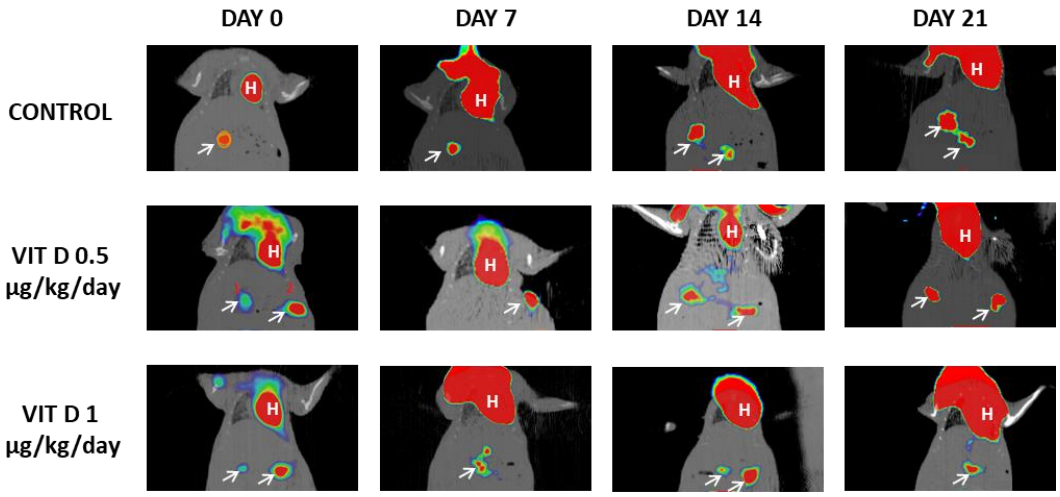

Figure 27. Non-invasive monitoring of leiomyoma xenograft by PET/CT scan. *Representative images of PET/CT scans carried out weekly during short-term assay in mice from control, Vitamin D 0.5 µg/kg/day and Vitamin D 1 µg/kg/day groups. White arrows indicate leiomyoma xenografts. "H" denotes hearts, which are observable due their high metabolic demand.*

In the short-term assay, leiomyoma xenograft metabolic activity remained constant over treatment time in control and Vitamin D 0.5 µg/kg/day groups. In contrast, mice receiving Vitamin D 1 µg/kg/day exhibited a dynamic reduction of ^{18}F-FDG uptake (kBq/cm^3) (Figure 28A). However, metabolic activity compared between groups at the end of treatment (Day 21) was not significantly different (Figure 28B).

On the other hand, PET/CT scans outcomes in the long-term assay showed that leiomyoma xenograft metabolic activity was significantly lower in both Vitamin D treatment groups compared to control group (Vit D 0.5 µg/kg/day: p value = 0.0238 and Vit D 1 µg/kg/day: p value = 0.0317) (Figure 28C).

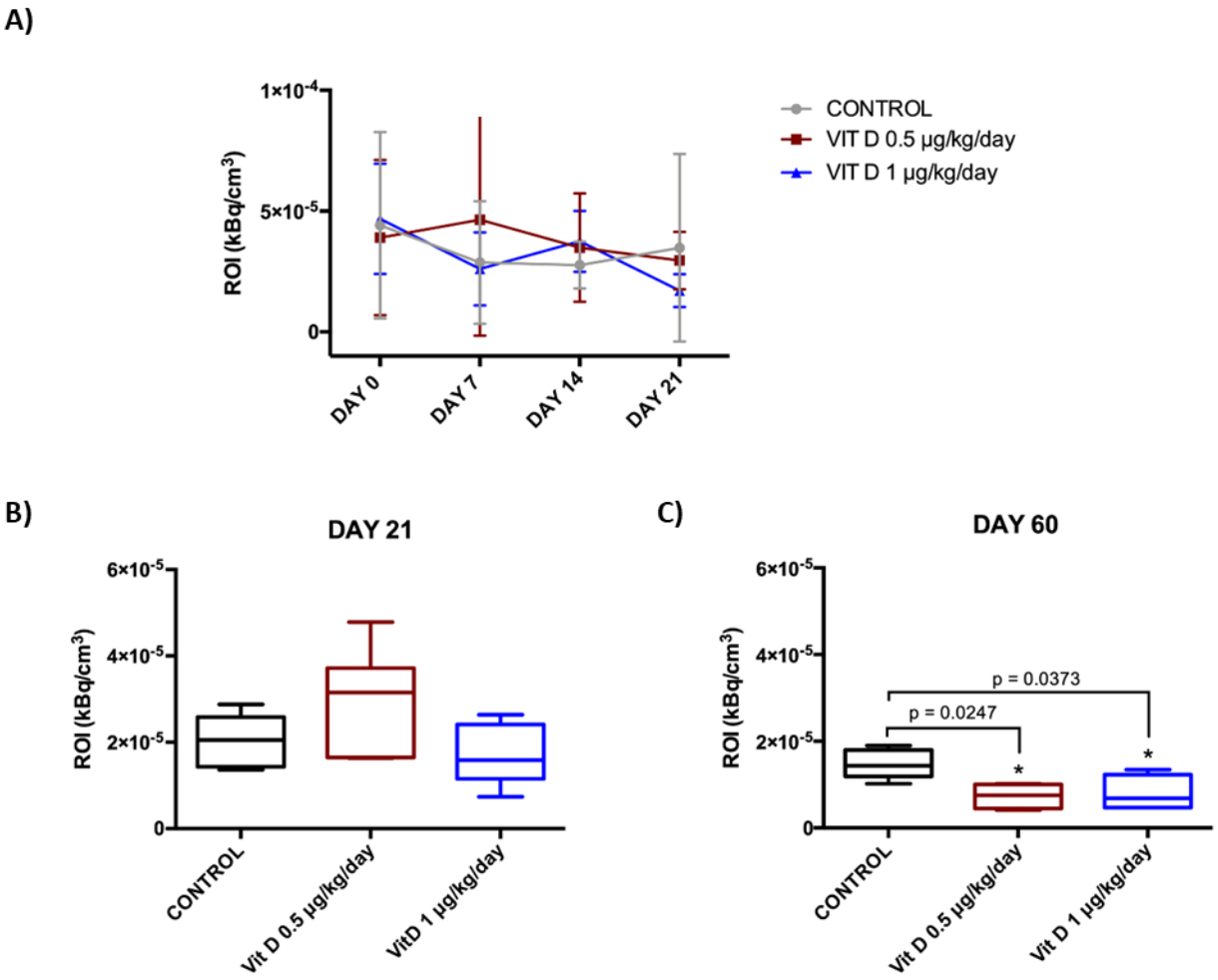

Figure 28. ^{18}F-FDG uptake of leiomyoma xenografts. *^{18}F-FDG uptake (kBq/cm^3) on region of interest (ROI) over time in the different experimental groups in short-term treatment (A). ^{18}F-FDG uptake in the three experimental groups at day 21 (B) and at day 60 (C). ^{18}F-FDG uptake was significantly decreased for both Vitamin D doses compared to control group in the long-term assay (p value<0.05).*

2.3. Uterine leiomyoma xenograft size

To macroscopically examine the leiomyoma size before and after xenotransplantation to assess Vitamin D treatment's effect on leiomyoma size, we photographed leiomyoma fragments next to a reference rule. We observed that, while macroscopic exam did not show changes in uterine leiomyoma xenograft size in any of the experimental groups after the short-term assay (Day 21) compare to control (Day 0), a noteworthy decrease was macroscopically observed in experimental groups after long-term treatment (Day 60) compare to control (Day 0) (Figure 29).

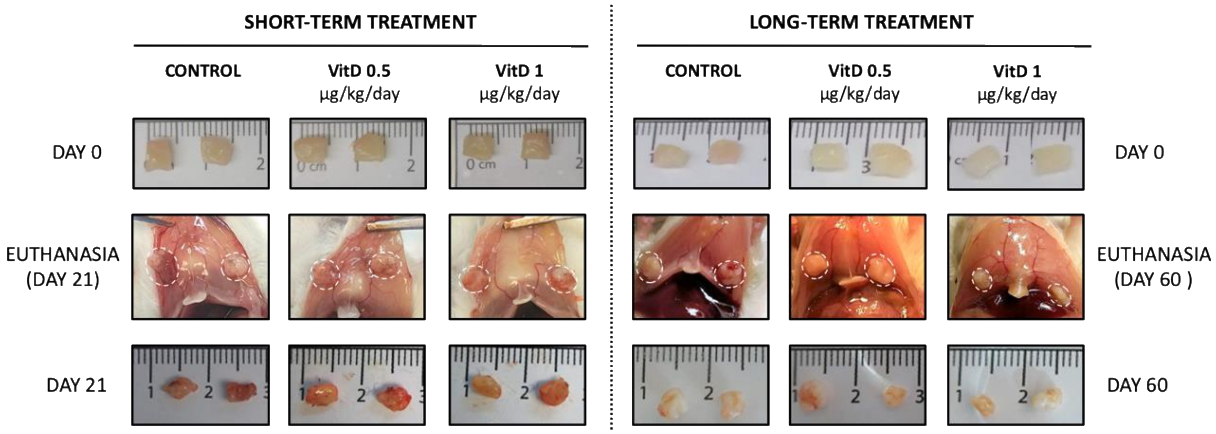

Figure 29. Human leiomyoma xenografts. *Human uterine leiomyoma fragments were measured before xenotransplantation (DAY 0) and after xenotransplantation at the end of treatment (DAY 21 in short-term or DAY 60 in long-term assay), in the three experimental groups: control, Vitamin D 0.5 µg/kg/day and Vitamin D 1 µg/kg/day.*

Subsequently, uterine leiomyoma size was measured with a digital caliper before and after xenotransplantation and volume was calculated to accurately assess the effect of Vitamin D treatment on leiomyoma size (Figure 30). While the control group showed a trend toward growth (Figure 30A), both Vitamin D 0.5 µg/kg/day (Figure 30B) and Vitamin D 1 µg/kg/day groups (Figure 30C) maintained leiomyoma xenografts size at the end of the short-term assay (Day 21) compared to Day 0 (no significant differences). After the long-term assay, no differences were found in control (Figure 30D) or Vitamin D 0.5 µg/kg/day (Figure 30E) groups, although leiomyoma size tended to increase especially in controls. In contrast, Vitamin D 1 µg/kg/day treatment significantly reduced leiomyoma xenograft size at day 60 compared to day 0 (p value = 0.0254) (Figure 30F).

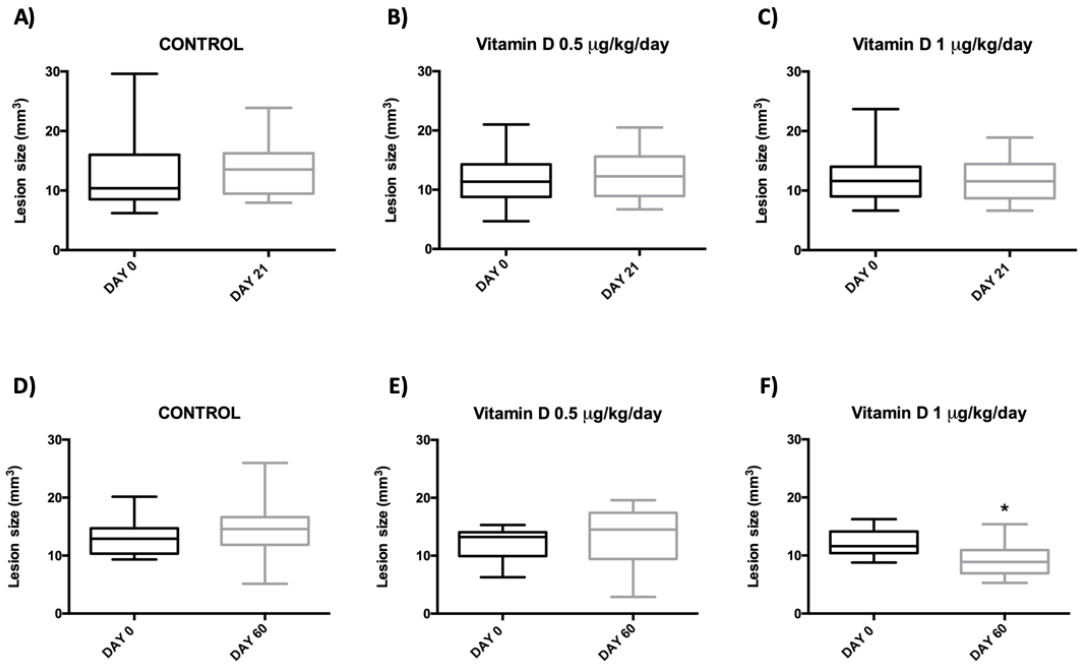

Figure 30. Human leiomyoma xenograft size. *Leiomyoma volume at day 0 and day 21 in control (A), Vitamin D 0.5 µg/kg/day (B) and Vitamin D 1 µg/kg/day (C) groups. Leiomyoma volume at day 0 and day 60 in control (D), Vitamin D 0.5 µg/kg/day (E) and Vitamin D 1 µg/kg/day (F) groups. Note that Vitamin D 1 µg/kg/day significantly decreased leiomyoma size at day 60 compared to day 0 (p value =0.0254).*

2.4. Histological evaluation

To assess if leiomyoma xenografts preserved their original histological features after xenotransplantation, H&E and Masson's Trichrome staining were applied in the original tissue (leiomyoma tissue before implantation) and leiomyoma xenografts after the treatments. H&E staining confirmed that, in both short- and long-term assays, leiomyoma xenografts maintained the original histological characteristics with smooth muscle cells interspersed in the ECM (Figure 31A-D & I-L). In addition, blood vessels with erythrocytes were found in the xenografts, indicating the presence of vascularization. Likewise, Masson's Trichrome staining corroborated that xenografts showed smooth muscle fibers (stained in red) surrounded by an abundant collagen ECM (stained in blue), indicating that implants preserved their histological characteristics (Figure 31E-H & M-P).

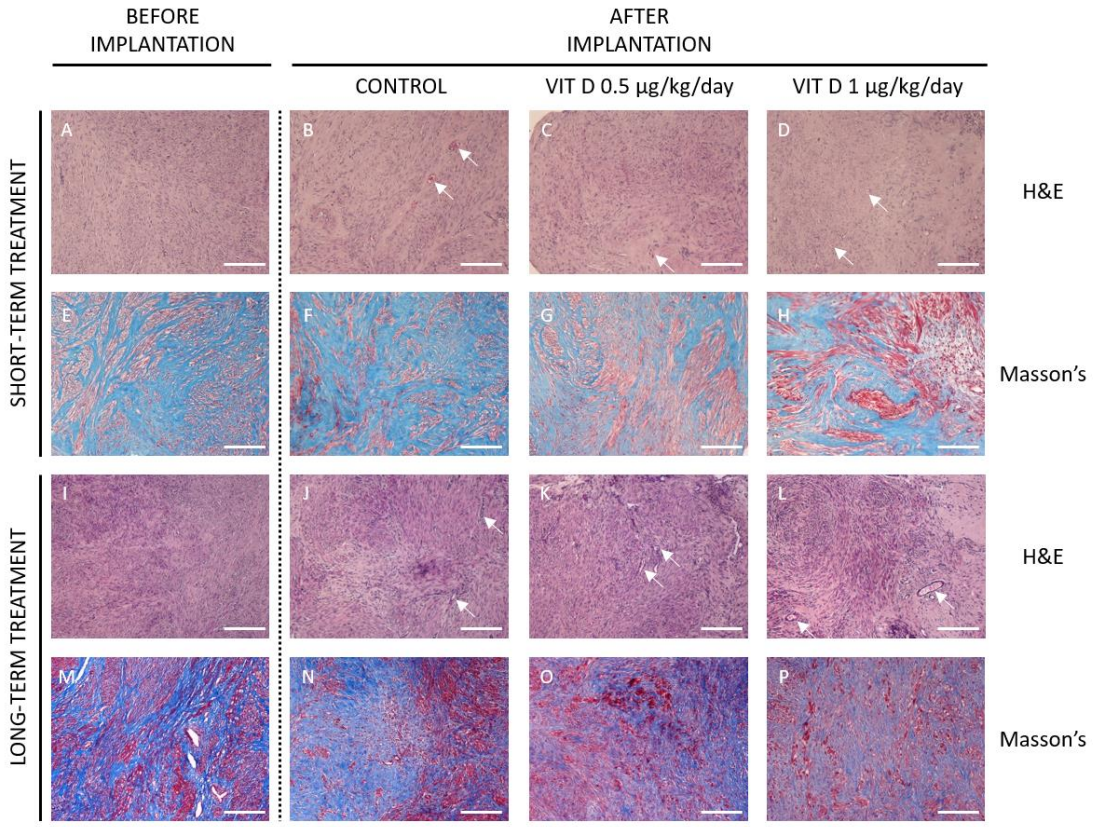

Figure 31. Histological evaluation of human uterine leiomyoma xenografts. *Leiomyoma tissues before implantation, control, Vitamin D (VIT D) 0.5 µg/kg/day and VIT D 1 µg/kg/day are shown. Representative histological sections stained with hematoxylin and eosin (H&E) in the short-term (A-D) and long-term (I-L) assays. White arrows indicate blood vessels in leiomyoma xenografts. Representative histological sections stained with Masson's Trichrome staining (Masson's) in the short-term (E-D) and long-term (M-P) assays. Scale bars: 200 µm*

2.5. Uterine leiomyoma cell proliferation

To evaluate the antiproliferative effect of Vitamin D on uterine leiomyomas *in vivo,* two proliferation markers (Ki67 and PCNA) were evaluated in leiomyoma xenografts. While Ki67 protein expression was evaluated by immunohistochemistry analysis, *PCNA* gene expression was assessed by qRT-PCR.

Immunohistochemical analysis showed that Vitamin D 0.5 µg/kg/day treatment did not reduce proliferation in the short- or long-term. However, treatment with Vitamin D 1 µg/kg/day reduced the expression of Ki67 in leiomyoma xenografts at both timepoints, and

this reduction was statistically significant for the long-term treatment (Figure 32 A-B). In addition, *PCNA* gene expression analysis corroborated that short-term Vitamin D treatment did not induce changes in leiomyoma cell proliferation. In the long-term, Vitamin D 1 µg/kg/day reduced *PCNA* expression compared to control, although no statistically significant differences were found (Figure 32C).

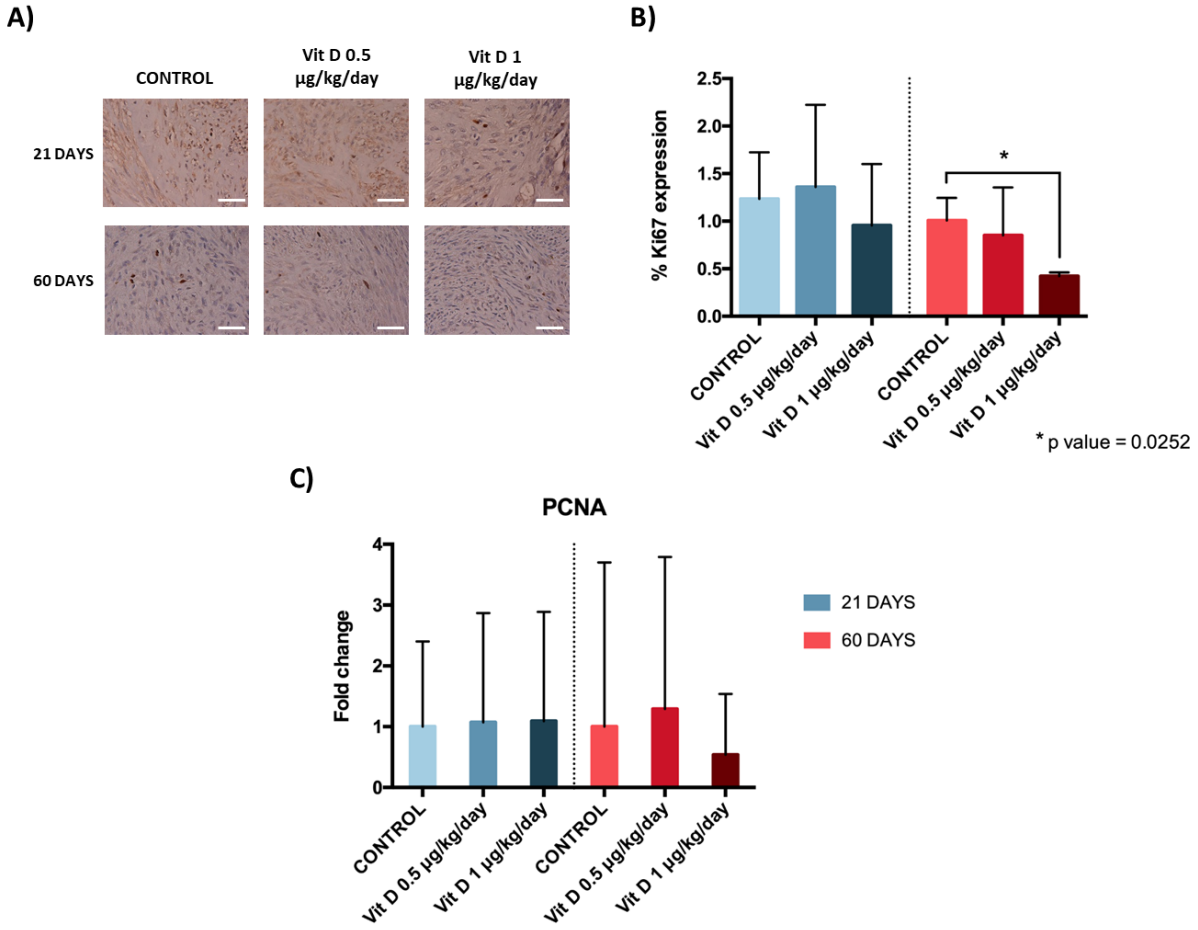

Figure 32. Cell proliferation in leiomyoma xenografts. *Representative images of Ki67 immunohistochemistry in leiomyoma xenografts (A). Ki67 expression represented as percentage (%) in the different treatment groups in short-term (21 DAYS) and long-term (60 DAYS) assays (B).* PCNA *gene expression levels represented as fold change in the different treatment groups for short-term (21 DAYS) and long-term (60 DAYS) assays (C). Note that Vitamin D 1 µg/kg/day significantly reduced Ki67 expression at day 60 (p value = 0.0252). Scale bars: 50 µm*

2.6. Cell density in leiomyoma xenografts

Cell density was evaluated in leiomyoma xenografts by analyzing the nuclei area in relation to total area per sample (Figure 33A). Although cell density was increased by both short- and long-term treatments with Vitamin D, no statistically significant differences were observed in short-term treatment groups or the Vitamin D 0.5 µg/kg/day group in the long-term assay (Figure 33B). However, the higher Vitamin D dose (1 µg/kg/day) produced a statistically significant increase in cell density in the long-term assay (p value = 0.0294) (Figure 33C).

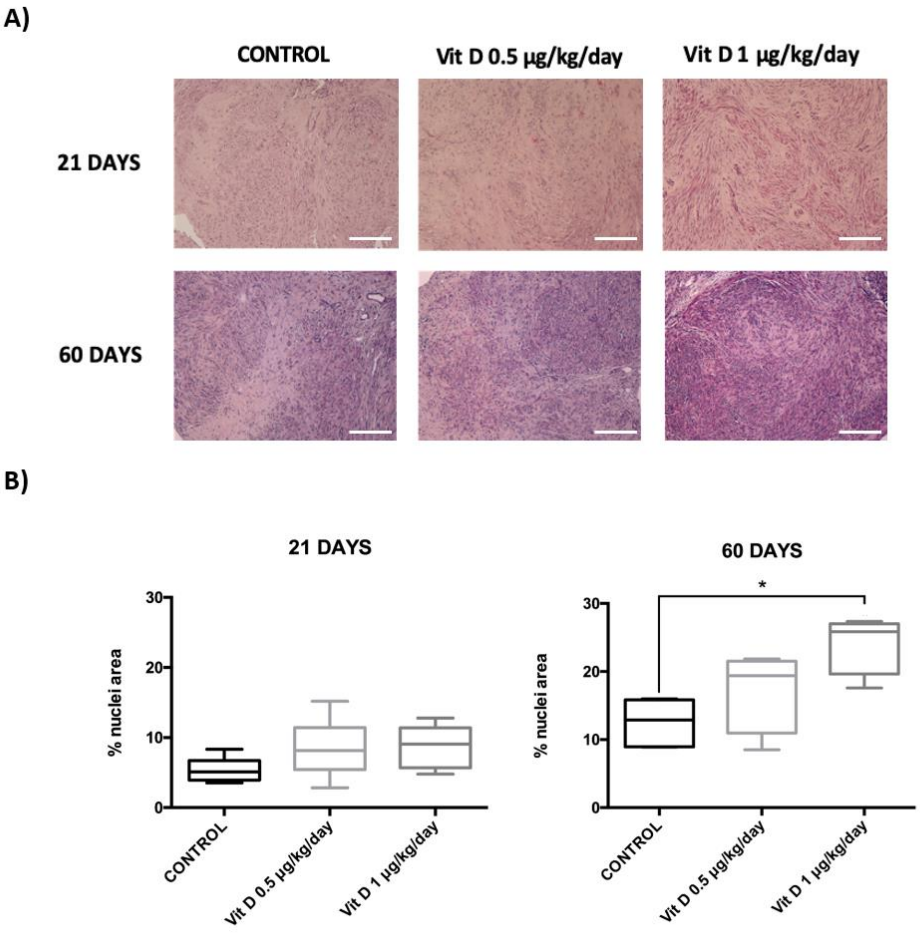

Figure 33. Cell density in leiomyoma xenografts. *Representative images of hematoxylin and eosin staining of leiomyoma xenografts (A). Cell density in the different treatment groups in both short- (B) and long-term (C) assays. Cell density is represented as the percentage (%) of nuclei area in relation to total area per sample. Note that cell density was significantly increased at Vit D 1 µg/kg/day in the long-term treatment (p value = 0.0294)*

2.7. Extracellular matrix

ECM formation was evaluated in leiomyoma xenografts after treatments by determining, COLLAGEN I, FIBRONECTIN and PAI-1 protein expression by western blotting (Figure 34 A-C). In this regard, Vitamin D treatment decreased COLLAGEN I expression in both short- and long-term treatments, but the difference was statistically significant only in the long-term with Vitamin D 1 µg/kg/day (p value = 0.0054) (Figure 34D). In addition, while no changes were found in FIBRONECTIN expression in the short-term treatment, a reduction, although not statistically significant, was observed in the Vitamin D 1 µg/kg/day group (Figure 34E). Finally, PAI-1 expression was similar in the different groups in the short-term treatment; however, Vitamin D treatment decreased PAI-1 expression in a dose-dependent manner in the long-term, which was statistically significant at the high dose (p value = 0.0154) (Figure 34F).

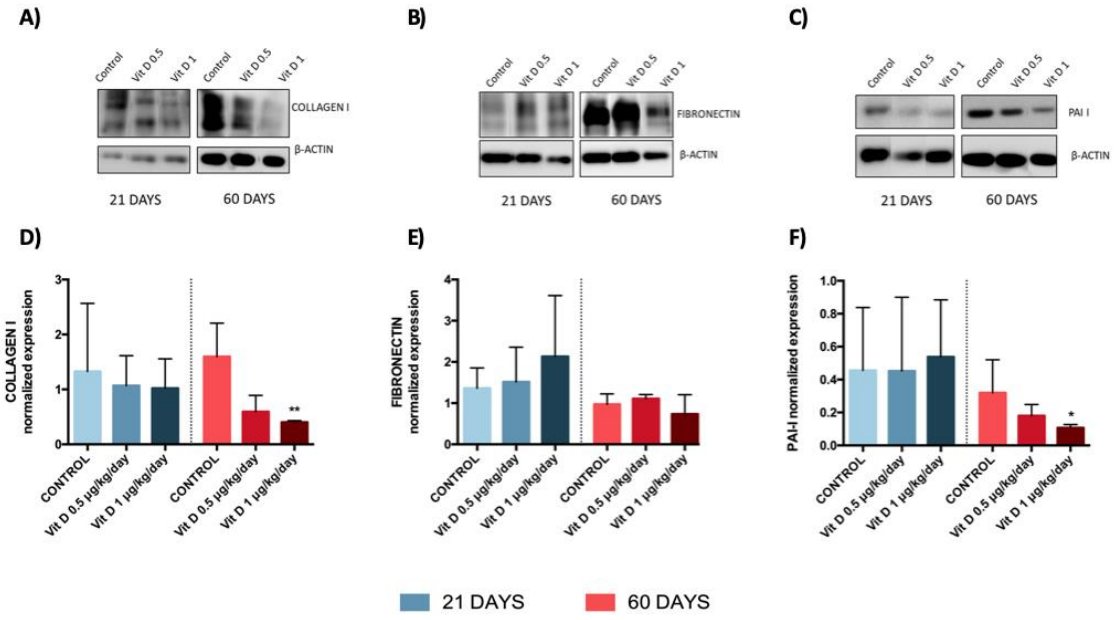

Figure 34. Extracellular matrix protein expression in leiomyoma xenografts. *Representative images of western blots for COLLAGEN I (A), FIBRONECTIN (B) and PAI-1 (C) in the different treatment groups. Quantitative protein expression of COLLAGEN I (D), FIBRONECTIN (E) and PAI-1 (F) in the different treatment groups was normalized against β-actin expression in both short- (21 DAYS) and long-term (60 DAYS) treatments. Note that COLLAGEN I and PAI-1 expression were significantly reduced by Vit D 1 µg/kg/day (p value= 0.0054 and 0.0154, respectively) compared to control.*

2.8. Transforming growth factor β signaling pathway

The TGFβ signaling pathway is involved in the expression of proteins associated with ECM formation. Gene expression of *TGFβ3* was measured in treated and untreated leiomyoma xenografts by qRT-PCR. *TGFβ3* expression was decreased in the short-term in both Vitamin D treatment groups (Figure 35), but these differences were not statistically significant. However, Vitamin D 1 µg/kg/day treatment significantly reduced *TGFβ3* expression following long-term treatment (fold change =0.1214, p value = 0.03731) (Figure 35).

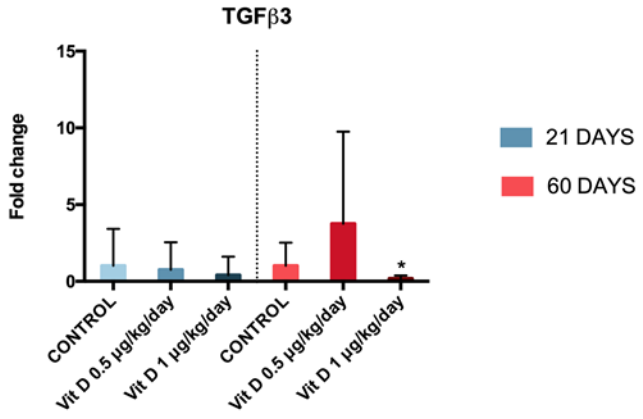

Figure 35. Transforming growth factor β signaling pathway in leiomyoma xenografts. *Gene expression levels of* TGFβ3 *in the different treatment groups for both short- (21 days) and long-term (60 days) assays, represented as fold change. Note that* TGFβ3 *gene expression were significantly reduced by Vit D 1 µg/kg/day group compared to control in the long-term assay.*

2.9. Apoptosis

To evaluate whether Vitamin D treatment increases apoptosis in leiomyoma xenografts, PRO-CASPASE 3 and CLEAVED CASPASE-3 protein expression were measured by western blotting (Figure 36 A-B). PRO-CASAPSE 3 expression was significantly decreased in both Vitamin D 0.5 µg/kg/day (p value = 0.0085) and Vitamin D 1 µg/kg/day (p value <0.0001) treatment groups after 21-day treatment (short-term assay). This decrease in PRO-CASPASE 3 expression was also observed in the Vitamin D 1 µg/kg/day group compared to control after 60-day treatment, although no statistically significant changes were found (Figure 36C). In contrast, CASPASE 3 expression was similar in the three study groups in the short-term assay, while it increased in a dose-dependent manner in the long-term assay (Figure 36D).

Further, the percentage of apoptotic cells in leiomyoma xenografts was measured by TUNEL assay (Figure 36E). This analysis showed that Vitamin D treatment increased the % of apoptotic cells in a concentration-dependent manner in the short-term, which was statistically significant in the Vitamin D 1 µg/kg/day group (p value =0.0386). Likewise, following long-term treatment, the high dose of Vitamin D showed higher % of apoptotic cells compared to control and Vitamin D 0.5 µg/kg/day group, which was statistically significant when compared to the lowest Vitamin D dose (p value= 0.0206) (Figure 36F).

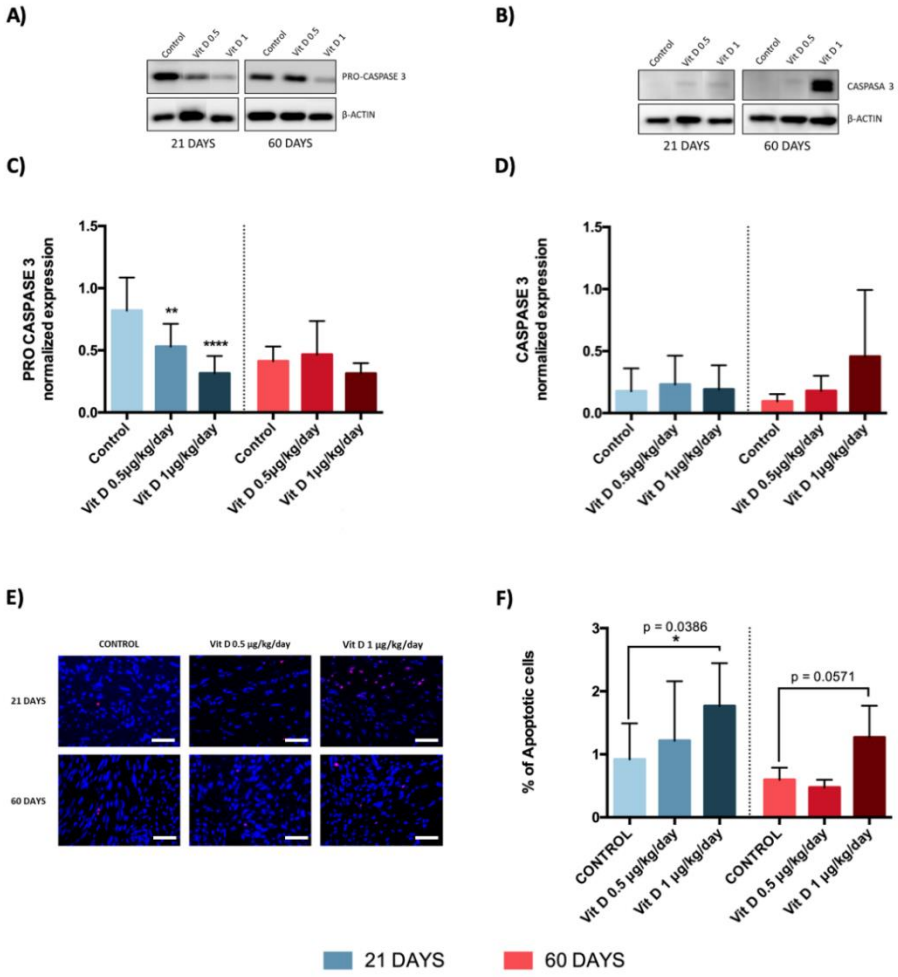

Figure 36. Apoptosis in leiomyoma xenografts. *Representative images of western blots for PRO-CASPASE 3 (A) and CASPASE 3 (B). Protein expression of PRO-CASPASE 3 (C) and CASPASE-3 (D) in the different treatment groups in both short- (21 days) and long-term (60 days) assays. Representative images of TUNEL assay in leiomyoma xenografts (E). Percentage of apoptotic cells in the different treatment groups in both short- (21 days) and long-term (60 days) assay. Scale bars: 50 µm*

VI. DISCUSSION

VI. DISCUSSION

Uterine leiomyomas affect 70 % of women of reproductive age, disturbing life quality of many of them due to its associated symptoms (Stewart *et al.*, 2017). Despite its high prevalence and the large amount of management options, there is no effective treatment for leiomyoma size reduction minimally invasive and without side effects. Although uterine leiomyoma pathogenesis is not fully understood, the relationship between Vitamin D deficiency and human uterine leiomyoma risk (Baird *et al.*, 2013; Paffoni *et al.*, 2013; Sabry *et al.*, 2013) along with its antiproliferative effects on cancer (Deeb *et al.*, 2007; Garland *et al.*, 2006; Ylikomi *et al.*, 2002), pointed to Vitamin D as a possible therapeutic option for uterine leiomyomas.

Vitamin D action have been widely studied in cancer cells, demonstrating that its anti-tumor effects imply mechanisms that are associated with G_0/G_1 cellular phase arrest, Wnt/β-Catenin pathway inhibition, and apoptosis induction (Christakos *et al.*, 2016; Deeb *et al.*, 2007). In addition, clinical trial data have indicated that Vitamin D is well tolerated in cancer patients within a proper dosing schedule (Deeb *et al.*, 2007). These data support the hypothesis that Vitamin D compounds may have an important role in therapies and prevention of both cancer and uterine leiomyoma and, thereby, merit further investigation.

In uterine leiomyomas, although Vitamin D action have been evaluated in *in vitro* studies, these focused their attention on a particular mechanism or pathway and used uterine leiomyoma cells lines (Al-Hendy *et al.*, 2016; Halder *et al.*, 2013b; Sharan *et al.*, 2011) or leiomyoma primary cells that came from a single patient and, therefore did not represent the variability found in real patients (Al-Hendy *et al.*, 2016). Similarly, Vitamin D effect on uterine leiomyomas have been studied *in vivo* using the Eker rat model or its derived cells, but not on human leiomyoma tissues. Thereby, an in-depth study of the molecular mechanisms through which Vitamin D could act on human uterine leiomyoma is still pending.

Based on these findings, the main objective of our study was to evaluate the effect of Vitamin D treatment ***in vitro*** on human uterine leiomyoma primary (HULP) cells and leiomyoma tissues ***in vivo*** on the different molecular mechanisms involved in uterine leiomyoma development, to test its potential as therapeutic option, resembling the physiological conditions of uterine leiomyomas and thereby, considering the high inter-patient variability.

For this purpose, before to study the Vitamin D role in HULP cells cultured *in vitro*, we evaluated the cell proliferation rate, Wnt/β-Catenin pathway and apoptosis status in leiomyoma tissue compared to adjacent myometrium to know the involvement of these mechanisms in leiomyoma development. Our results revealed that most human uterine leiomyoma tissues showed significant proliferation and a deregulated Wnt/β-Catenin pathway in comparison to myometrium. These results are in concordance with the published data which suggest that the upregulation of this pathway is involved in the develop of uterine leiomyomas with *MED12* mutation (Al-Hendy *et al.*, 2016). On the other hand, apoptosis status seemed to be more heterogeneous in the different leiomyomas analyzed, which could be explained why both BCL2 and BAX proteins seem to be regulated by sex steroids (Wu *et al.*, 2002; Yin *et al.*, 2007). During apoptosis, BAX protein forms a heterodimer with BCL2 and functions as an apoptotic activator (Palomba *et al.*, 2005). Considering this mechanism, BAX/BCL2 ratio is used to predetermine the susceptibility of cells to apoptosis. In our samples, the BAX/BCL2 ratio showed that apoptosis seemed not to be significantly altered in leiomyoma tissue compared to myometrium, which is supported by other studies that suggested that apoptosis does not act as a major factor in uterine leiomyoma development (Dixon *et al.*, 2002). Based on these findings, we conclude that an increased cell proliferation rate along with a deregulation of Wnt/β-Catenin pathway in leiomyoma tissue could be a key piece in the development and growth of uterine leiomyoma, while apoptosis appears not to contribute.

Subsequently, we analyzed *in vitro* the effect of Vitamin D in HULP cells from individual patients focused on its action through the three described pathways and cellular processes: cell cycle and proliferation, Wnt/β-catenin pathway and apoptosis. Our data showed that Vitamin D acts through cell cycle regulation, inducing cell growth arrest and significantly decreasing cell proliferation. These findings corroborate that, as occurs in both cancer cells (Gavrilov *et al.*, 2005; Jamshidi *et al.*, 2008) and leiomyoma cell lines (Sharan *et al.*, 2011), Vitamin D has an antiproliferative action on human leiomyoma cells. However, cell growth arrest was not observed in all HULP cells cases, which could be explain by the high variability between individual patients, leading to less homogeneity than cell lines but representing the actual variability found in women.

However, the molecular mechanisms through which Vitamin D inhibits cell proliferation in leiomyoma remains unclear. In order to determine these mechanisms, we analyzed Wnt/β-catenin pathway and apoptosis using gene expression array analysis. Wnt/β-catenin pathway is an important regulator of cell proliferation and its upregulation has been associated with the onset of several cancers (Larriba *et al.*, 2013; Pendás-Franco *et al.*, 2008) as well as with uterine leiomyoma development (Ono *et al.*, 2013). The analysis of Wnt/β-catenin pathway related genes in our HULP cells cultured with Vitamin D showed that most genes implicated in developmental processes such as tissue polarity, cell migration, cell cycle, cell growth and proliferation, were downregulated in Vitamin D-treated cells compared to control. Interestingly, among the upregulated genes was *DAB2* (tumor suppressor gene), which may inhibit the canonical Wnt/β-Catenin pathway by stabilizing the β-Catenin destruction complex (Hofsteen *et al.*, 2016; Paluszczak *et al.*, 2018). In addition, the negative pathway activity score implied that Vitamin D significantly inhibited Wnt/β-catenin pathway, demonstrating for the first time that Vitamin D has an inhibitory action on this pathway in HULP cells. The analysis of the entire Wnt/β-Catenin pathway in HULP cells complement the published data that described the reduction of β-catenin, WNT4, and WISP1 proteins by Vitamin D in a human leiomyoma cell line (Al-Hendy *et al.*, 2016). Likewise, we observed that expression of protein products of Wnt/β-Catenin pathway (WISP1, uPAR and MMP7) were also downregulated in Vitamin D-treated HULP cells. According to our findings, we suggest that Vitamin D treatment suppresses cell proliferation in HULP cells through the inhibition of Wnt/β-catenin pathway at both the gene and protein levels.

Additionally, we aimed to determine the effect of Vitamin D on apoptosis in HULP cells. Whether Vitamin D induces apoptosis, our results should show an upregulation of pro-apoptotic genes and a downregulation of anti-apoptotic genes. However, the results obtained after Vitamin D treatment did not show this trend, suggesting that Vitamin D does not act via apoptosis induction in HULP cells. Despite one of the described action mechanisms of Vitamin D as an anti-tumor agent is the induction of apoptosis, it has been reported that this is not caused in all cancer types (Fleet, 2008). In this context, our findings begin to clarify the Vitamin D effect on apoptosis regulation in leiomyoma, which could be useful to determine the effect of this vitamin on programed cell death in other cancer cell types.

Based on these findings, our *in vitro* study demonstrated for the first time that Vitamin D is able to reduce proliferation on HULP cells, through the inhibition of Wnt/β-catenin pathway, supporting the idea that Vitamin D could be a therapeutic alternative for uterine leiomyoma (Bläuer *et al.*, 2009; Halder *et al.*, 2014; Sharan *et al.*, 2011). Taking into account that the observed cell proliferation reduction *in vitro* was slight, we propose Vitamin D as an effective treatment to prevent leiomyoma growth and stabilize its size. There findings have been published in the journal *Fertility & Sterility* in February 2019 (Annex IV).

Considering that human uterine leiomyomas are solid tumors composed of smooth muscle cells interspersed in an abundant ECM, which plays an important role in tumor expansion (Bulun, 2013; Parker, 2007), it is necessary to corroborate the *in vitro* antiproliferative effects of Vitamin D in an animal model that maintains ECM structure. For this purpose, we aimed to assess the effect of Vitamin D treatment on a xenograft mouse model generated by the implantation of human uterine leiomyoma fragments, at both short and long term.

Firstly, we monitored for the first time leiomyoma xenograft in mice by ^{18}F-FDG PET/CT scans, whose efficiency detecting leiomyoma have been previously demonstrated in women (Kitajima *et al.*, 2010; Ma and Shao, 2017). ^{18}F-FDG uptake demonstrated that, while no differences were observed in metabolic activity at the end of short-term Vitamin D treatment, this activity was significantly lower with long-term Vitamin D treatment compared to control. Macroscopic examination of leiomyomas before and after xenotransplantation revealed a statistically significant decrease in leiomyoma size after long-term Vitamin D 1 µg/kg/day treatment, while short-term Vitamin D treatment maintained their size. These results support previous findings reported in other animal studies that used the Eker rat model (Halder *et al.*, 2012) or Eker rat-derived uterine leiomyoma cell line (ELT-3) (Halder *et al.*, 2014), which demonstrated reduced leiomyoma size with Vitamin D treatment compared to control. However, both studies tested Vitamin D or an analog in animal models that do not fully mimic human leiomyoma physiology. The *in vivo* study described here is the first to assess the effect of Vitamin D on a leiomyoma xenograft animal model using human uterine leiomyoma tissue fragments and suggest that Vitamin D treatment can significantly reduce human leiomyoma size.

Subsequently, we evaluated molecular mechanisms involved in leiomyoma size reduction: cell proliferation, ECM formation, and apoptosis. Our study showed that the highest dose of Vitamin D (1 µg/kg/day) reduced cell proliferation in leiomyoma xenografts with long-term treatment, suggesting that Vitamin D has an antiproliferative effect on uterine leiomyoma. These findings corroborate our previous *in vitro* results in which Vitamin D significantly decreased cell proliferation in HULP cells, reinforcing the antiproliferative action of Vitamin D in uterine leiomyoma fragments just like in cancer cells (Gavrilov *et al.*, 2005; Jamshidi *et al.*, 2008), leiomyoma cells lines (Bläuer *et al.*, 2009; Sharan *et al.*, 2011), and animal models of leiomyoma (Halder *et al.*, 2012, 2014), supporting that Vitamin D could be an effective treatment that plays an important role in uterine leiomyoma growth.

The development and expansion of human uterine leiomyomas are not only associated with cell proliferation, but also with excessive synthesis and deposition of ECM. Therefore, since ECM formation is one of the crucial molecular mechanisms involved in human uterine leiomyoma growth, we evaluated the role of Vitamin D in the regulation of ECM-associated protein expression in human leiomyoma xenograft. We observed that Vitamin D treatment significantly decreased the expression of ECM-associated proteins with the highest dose of Vitamin D (1 µg/kg/day) with long-term treatment. These findings suggested a role for Vitamin D in the regulation of key fibrotic proteins, and consequently, in uterine leiomyoma expansion similar to that observed in the Eker rat model (Halder *et al.*, 2012) and in HuLM cells (Halder *et al.*, 2013b).

In uterine leiomyomas, the production of these ECM-associated proteins is induced by TGFβ3, which is involved in ECM deposition and fibrosis process (Ciebiera *et al.*, 2017; Halder *et al.*, 2011). In this regard, a TGFβ3 overexpression leads to overproduction and oversecretion of ECM proteins, such as COLLAGEN TYPE 1, FIBRONECTIN and PAI-1, resulting in an increase in leiomyoma size. To evaluated whether Vitamin D might reverse TGFβ3-induced protein expression in leiomyoma, *TGFβ3* expression was evaluated in leiomyoma xenograft by qRT-PCR. *TGFβ3* expression was significantly decreased with long-term, high-dose Vitamin D, suggesting that this vitamin may impact fibrosis in human leiomyoma via *TGFβ3* as was suggested in HuLM cells (Halder *et al.*, 2011). Interestingly, it has been demonstrated that TGFβ produced by leiomyomas affects endometrial receptivity (Galliano *et al.*, 2015; Sinclair

et al., 2011), as well as the production of PAI-1 in endometrium, which is involved in the regulation of normal menstrual flow (Taylor, 2018). Therefore, Vitamin D treatment might not only reduce uterine leiomyoma size but also improve endometrial receptivity and bleeding in these patients.

Since Vitamin D suppresses the proliferation of malignant tumor cells and induces apoptosis in cancer cells (Deeb *et al.*, 2007; Ylikomi *et al.*, 2002), human leiomyoma cells line (Sharan *et al.*, 2011) and Eker rats (Halder *et al.*, 2012, 2014), we sought to determine whether Vitamin D could induce apoptosis in leiomyoma xenograft via changes in CASPASE 3 expression and apoptotic cells. Vitamin D treatment was found to increase both CASPASE 3 protein expression and the percentage of apoptotic cells at the highest dose when administered long term.

Based on our findings, Vitamin D given at 1µg/kg/day could prevent human uterine leiomyoma growth and stabilize its size in the short term, while long-term treatment could significantly reduce leiomyoma size without negative side effects. Considering that 1 µg of $1,25(OH)_2D_3$ is equivalent to 40 IU, 1µg/kg/day in mice is equivalent to 2800 IU/day for an human adult of 70kg, which is reported as a safe dose in clinical trials (Hathcock *et al.*, 2007).

In this regard, a Vitamin D dose lower than 2800 IU/day during long time might reduce leiomyoma size in women with Vitamin D deficiency/insufficiency. This *in vivo* approach paves the way for future clinical studies testing Vitamin D treatment effect during long term in pre- and perimenopausal patients with uterine leiomyomas and Vitamin D deficiency, improving the results obtained in a study that only included peri- and menopausal women with “small burden” leiomyomas, excluding premenopausal women with leiomyomas >50 mm (Ciavattini *et al.*, 2016). In this regard, it is worth mentioning that our group have recently started a clinical study, carried out at Hospital Universitario y Politécnico La Fe (Spain) whose objective is to determine if the restoration of normal serum levels of 25-hydroxycholecalciferol (25(OH)D) in pre- and perimenopausal patients with uterine leiomyomas >30 mm who present hypovitaminosis D is able to maintain or even reduce their size.

VII. CONCLUSIONS

VII. CONCLUSIONS

The following conclusions can be drawn from this thesis:

- An increased cell proliferation along with a deregulation of Wnt/β-Catenin pathway in leiomyoma tissue could be a key piece in the development and growth of uterine leiomyoma, while apoptosis appears not to contribute.
- Vitamin D treatment inhibits cell growth of human uterine leiomyoma primary cells *in vitro* throughout the induction of cell growth arrest in G_0/G_1 phases (decreasing cell division) and the inhibition of cell proliferation.
- Vitamin D decreases the expression of genes and proteins of Wnt/β-catenin pathway involved in molecular mechanisms, such as cell migration, growth and proliferation in human uterine leiomyoma primary cells *in vitro*, significantly inhibiting this signaling pathway. However, apoptosis is not increased by Vitamin D in human uterine leiomyoma primary cells *in vitro.*
- Although the high dose of Vitamin D (1 µg/kg/day) in the short-term decreases cell proliferation and COLAGEN I production and increases apoptosis, these effects are not statistically significant, which is reflected in the maintenance of the size and metabolic activity of leiomyoma xenografts in our *in vivo* model.
- The high dose of Vitamin D (1 µg/kg/day) in the long-term significantly decreases cell proliferation, extracellular matrix proteins production throughout TGFβ signaling pathway, as well as increases apoptosis, which is reflected in the significant reduction of the size and metabolic activity of leiomyoma xenografts in our *in vivo* model.
- Short-term Vitamin D treatment could be an effective therapy to prevent leiomyoma growth an stabilize its size, while Vitamin D treatment for an extended period could effectively reduce leiomyoma size without associated side effects.

VIII. BIBLIOGRAPHY

VII. BIBLIOGRAPHY

AEMPS. *Informe mensual sobre Medicamentos de Uso Humano y Productos Sanitarios*. 2011. Available at: http://www.aemps.gob.es.

AEMPS. *FICHA TECNICA DELTIUS 25.000 UI/2,5 ML SOLUCION ORAL*. 2017. Available at: https://cima.aemps.es/cima/dochtml/ft/78379/FichaTecnica_78379.html.

AEMPS. *ESMYA ® : VIGILAR LA FUNCIÓN HEPÁTICA Y NO INICIAR NUEVOS TRATAMIENTOS COMO MEDIDAS CAUTELARES Nota informativa*. 2018a. Available at: www.notificaRAM.es.

AEMPS. *ESMYA (ACETATO DE ULIPRISTAL): RESTRICCIONES DE USO Y NUEVAS MEDIDAS ADOPTADAS PARA MINIMIZAR EL RIESGO DE DAÑO HEPÁTICO*. 2018b. Available at: www.notificaRAM.es.

Al-Hendy A, Diamond MP, Boyer TG, Halder SK. Vitamin D3 Inhibits Wnt/β-Catenin and mTOR Signaling Pathways in Human Uterine Fibroid Cells. *J Clin Endocrinol Metab* 2016;**101**:1542–51.

Almuhaideb A, Papathanasiou N, Bomanji J. 18F-FDG PET/CT imaging in oncology. *Ann Saudi Med* 2011;**31**:3–13.

Arenas Valencia C, Lopez Kleine L, Pinzon Velasco AM, Cardona Barreto AY, Arteaga Diaz CE. Gene expression analysis in peripheral blood cells of patients with hereditary leiomyomatosis and renal cell cancer syndrome (HLRCC): identification of NRF2 pathway activation. *Fam Cancer* 2018;**17**:587–599.

Baird DD, Dunson DB, Hill MC, Cousins D, Schectman JM. High cumulative incidence of uterine leiomyoma in black and white women: ultrasound evidence. *Am J Obstet Gynecol* 2003;**188**:100–7.

Baird DD, Hill MC, Schectman JM, Hollis BW. Vitamin d and the risk of uterine fibroids. *Epidemiology* 2013;**24**:447–53.

Barker N, Clevers H. Mining the Wnt pathway for cancer therapeutics. *Nat Rev Drug Discov* 2006;**5**:997–1014.

Barnum KJ, O'Connell MJ. Cell cycle regulation by checkpoints. *Methods Mol Biol* 2014;**1170**:29–40.

Basu B. *Biomaterials for Musculoskeletal Regeneration: Concepts*. Springer, 2016.

Bertsch E, Qiang W, Zhang Q, Espona-Fiedler M, Druschitz S, Liu Y, Mittal K, Kong B, Kurita T, Wei J-J. MED12 and HMGA2 mutations: two independent genetic events in uterine leiomyoma and leiomyosarcoma. *Mod Pathol* 2014;**27**:1144–53..

Bläuer M, Rovio PH, Ylikomi T, Heinonen PK. Vitamin D inhibits myometrial and leiomyoma cell proliferation in vitro. *Fertil Steril* 2009;**91**:1919–25.

Brito LG, Candido-dos-Reis FJ, Magario FA, Sabino-de-Freitas MM. Effect of the aromatase

inhibitor anastrozole on uterine and leiomyoma Doppler blood flow in patients scheduled for hysterectomy: a pilot study. *Ultrasound Obstet Gynecol* 2012;**40**:119–120.

Bulun SE. Uterine fibroids. Longo DL (ed). *N Engl J Med* 2013;**369**:1344–55.

Bulun SE, Moravek MB, Yin P, Ono M, Coon JS, Dyson MT, Navarro A, Marsh EE, Zhao H, Maruyama T, *et al.* Uterine Leiomyoma Stem Cells: Linking Progesterone to Growth. *Semin Reprod Med* 2015;**33**:357–65.

Cervelló I, Mas A, Gil-Sanchis C, Peris L, Faus A, Saunders PTK, Critchley HOD, Simón C. Reconstruction of endometrium from human endometrial side population cell lines. *PLoS One* 2011;**6**:e21221.

Chiaffarino F, Parazzini F, La Vecchia C, Chatenoud L, Di Cintio E, Marsico S. Diet and uterine myomas. *Obstet Gynecol* 1999;**94**:395–8.

Christakos S, Dhawan P, Verstuyf A, Verlinden L, Carmeliet G. Vitamin D: Metabolism, Molecular Mechanism of Action, and Pleiotropic Effects. *Physiol Rev* 2016;**96**:365–408.

Chwalisz K, Taylor H. Current and Emerging Medical Treatments for Uterine Fibroids. *Semin Reprod Med* 2017;**35**:510–522..

Ciavattini A, Delli Carpini G, Serri M, Vignini A, Sabbatinelli J, Tozzi A, Aggiusti A, Clemente N. Hypovitaminosis D and "small burden" uterine fibroids. *Medicine (Baltimore)* 2016;**95**:e5698.

Ciebiera M, Włodarczyk M, Ciebiera M, Zaręba K, Łukaszuk K, Jakiel G. Vitamin D and Uterine Fibroids—Review of the Literature and Novel Concepts. *Int J Mol Sci* 2018;**19**:2051.

Ciebiera M, Włodarczyk M, Wrzosek M, Męczekalski B, Nowicka G, Łukaszuk K, Ciebiera M, Słabuszewska-Jóźwiak A, Jakiel G. Role of Transforming Growth Factor β in Uterine Fibroid Biology. *Int J Mol Sci* 2017;**18**.

Coad J, Dunstall M. *Anatomy and physiology for midwives*. Churchill Livingstone/Elsevier, 2011.

Colston KW, Chander SK, Mackay AG, Coombes RC. Effects of synthetic vitamin D analogues on breast cancer cell proliferation in vivo and in vitro. *Biochem Pharmacol* 1992;**44**:693–702.

Curry TE, Osteen KG. The Matrix Metalloproteinase System: Changes, Regulation, and Impact throughout the Ovarian and Uterine Reproductive Cycle. *Endocr Rev* 2003;**24**:428–465.

Day Baird D, Dunson DB. Why is Parity Protective for Uterine Fibroids? *Epidemiology* 2003;**14**:247–250.

Deeb KK, Trump DL, Johnson CS. Vitamin D signalling pathways in cancer: potential for anticancer therapeutics. *Nat Rev Cancer* 2007;**7**:684–700.

Deng L, Wu T, Chen XY, Xie L, Yang J. Selective estrogen receptor modulators (SERMs) for uterine leiomyomas. *Cochrane Database Syst Rev* 2012.

Dixon D, Flake GP, Moore AB, He H, Haseman JK, Risinger JI, Lancaster JM, Berchuck A, Barrett JC, Robboy SJ. Cell proliferation and apoptosis in human uterine leiomyomas and myometria. *Virchows Arch* 2002;**441**:53–62.

Donnez J, Courtoy GE, Donnez O, Dolmans M-M. Ulipristal acetate for the management of large uterine fibroids associated with heavy bleeding: a review. *Reprod Biomed Online* 2018;**37**:216–223.

Donnez J, Dolmans M-M. Uterine fibroid management: from the present to the future. *Hum Reprod Update* 2016;**22**:665–686.

Donnez J, Hudecek R, Donnez O, Matule D, Arhendt H-J, Zatik J, Kasilovskiene Z, Dumitrascu MC, Fernandez H, Barlow DH, *et al.* Efficacy and safety of repeated use of ulipristal acetate in uterine fibroids. *Fertil Steril* 2015;**103**:519–527.e3.

Donnez J, Tatarchuk TF, Bouchard P, Puscasiu L, Zakharenko NF, Ivanova T, Ugocsai G, Mara M, Jilla MP, Bestel E, *et al.* Ulipristal Acetate versus Placebo for Fibroid Treatment before Surgery. *N Engl J Med* 2012;**366**:409–420.

Donnez J, Tomaszewski J, Vázquez F, Bouchard P, Lemieszczuk B, Baró F, Nouri K, Selvaggi L, Sodowski K, Bestel E, *et al.* Ulipristal acetate versus leuprolide acetate for uterine fibroids. *N Engl J Med* 2012;**366**:421–32.

Donnez J, Vázquez F, Tomaszewski J, Nouri K, Bouchard P, Fauser BCJM, Barlow DH, Palacios S, Donnez O, Bestel E, *et al.* Long-term treatment of uterine fibroids with ulipristal acetate☆. *Fertil Steril* 2014;**101**:1565–1573.e18. A

Duhan N, Madaan S, Sen J. Role of the aromatase inhibitor letrozole in the management of uterine leiomyomas in premenopausal women. *Eur J Obstet Gynecol Reprod Biol* 2013;**171**:329–32.

Eder S, Baker J, Gersten J, Mabey RG, Adomako TL. Efficacy and safety of oral tranexamic acid in women with heavy menstrual bleeding and fibroids. *Womens Health (Lond Engl)* 2013;**9**:397–403.

Everitt JI, Wolf DC, Howe SR, Goldsworthy TL, Walker C. Rodent model of reproductive tract leiomyomata. Clinical and pathological features. *Am J Pathol* 1995;**146**:1556–67.

Fleet JC. Molecular actions of vitamin D contributing to cancer prevention. *Mol Aspects Med* 2008;**29**:388–396.

Galindo LJ, Hernández-Beeftink T, Salas A, Jung Y, Reyes R, de Oca FM, Hernández M, Almeida TA. HMGA2 and MED12 alterations frequently co-occur in uterine leiomyomas. *Gynecol Oncol* 2018;**150**:562–568.

Galliano D, Bellver J, Díaz-García C, Simón C, Pellicer A. ART and uterine pathology: how relevant is the maternal side for implantation? *Hum Reprod Update* 2015;**21**:13–38.

Garland CF, Garland FC, Gorham ED, Lipkin M, Newmark H, Mohr SB, Holick MF. The role of vitamin D in cancer prevention. *Am J Public Health* 2006;**96**:252–61.

Gavrilov V, Steiner M, Shany S. The combined treatment of 1,25-dihydroxyvitamin D3 and a non-steroid anti-inflammatory drug is highly effective in suppressing prostate cancer cell line (LNCaP) growth. *Anticancer Res* 2005;**25**:3425–3429.

Gupta JK, Sinha A, Lumsden MA, Hickey M. Uterine artery embolization for symptomatic uterine fibroids. *Cochrane Database Syst Rev* 2014.

Halder SK, Goodwin JS, Al-Hendy A. 1,25-Dihydroxyvitamin D $_3$ Reduces TGF-β3-Induced Fibrosis-Related Gene Expression in Human Uterine Leiomyoma Cells. *J Clin Endocrinol Metab* 2011;**96**:E754–E762.

Halder SK, Osteen KG, Al-Hendy A. Vitamin D3 inhibits expression and activities of matrix metalloproteinase-2 and -9 in human uterine fibroid cells. *Hum Reprod* 2013a;**28**:2407–2416.

Halder SK, Osteen KG, Al-Hendy A. 1,25-Dihydroxyvitamin D3 Reduces Extracellular Matrix-Associated Protein Expression in Human Uterine Fibroid Cells1. *Biol Reprod* 2013b;**89**:1–13.

Halder SK, Sharan C, Al-Hendy A. 1,25-Dihydroxyvitamin D3 Treatment Shrinks Uterine Leiomyoma Tumors in the Eker Rat Model1. *Biol Reprod* 2012;**86**:116.

Halder SK, Sharan C, Al-Hendy O, Al-Hendy A. Paricalcitol, a vitamin d receptor activator, inhibits tumor formation in a murine model of uterine fibroids. *Reprod Sci* 2014;**21**:1108–19.

Hall JE (John E, Guyton AC. *Guyton and Hall textbook of medical physiology*. Saunders Elsevier, 2011.

Hathcock JN, Shao A, Vieth R, Heaney R. Risk assessment for vitamin D. *Am J Clin Nutr* 2007;**85**:6–18.

Hawkins SM, Matzuk MM. The menstrual cycle: basic biology. *Ann N Y Acad Sci* 2008;**1135**:10–8.

Hofsteen P, Robitaille AM, Chapman DP, Moon RT, Murry CE. Quantitative proteomics identify DAB2 as a cardiac developmental regulator that inhibits WNT/β-catenin signaling. *Proc Natl Acad Sci U S A* 2016;**113**:1002–7.

Huang S, Hölzel M, Knijnenburg T, Schlicker A, Roepman P, McDermott U, Garnett M, Grernrum W, Sun C, Prahallad A, *et al.* MED12 controls the response to multiple cancer drugs through regulation of TGF-β receptor signaling. *Cell* 2012;**151**:937–50.

Huyck KL, Panhuysen CIM, Cuenco KT, Zhang J, Goldhammer H, Jones ES, Somasundaram P, Lynch AM, Harlow BL, Lee H, *et al.* The impact of race as a risk factor for symptom severity and age at diagnosis of uterine leiomyomata among affected sisters. *Am J Obstet Gynecol* 2008;**198**:168.e1-9.

Iruzubieta P, Terán Álvaro, Crespo J, Fábrega E. Vitamin D deficiency in chronic liver disease. *World J Hepatol* 2014;**6**:901.

Islam MS, Ciavattini A, Petraglia F, Castellucci M, Ciarmela P. Extracellular matrix in uterine leiomyoma pathogenesis: a potential target for future therapeutics. *Hum Reprod Update* 2018;**24**:59–85.

Jamshidi F, Zhang J, Harrison JS, Wang X, Studzinski GP. Induction of differentiation of human leukemia cells by combinations of COX inhibitors and 1,25-dihydroxyvitamin D3 involves Raf1 but not Erk 1/2 signaling. *Cell Cycle* 2008;**7**:917–24.

Karlsen K, Hrobjartsson A, Korsholm M, Mogensen O, Humaidan P, Ravn P. Fertility after uterine artery embolization of fibroids: a systematic review. *Arch Gynecol Obstet* 2018;**297**:13–25.

Kim S, Xu X, Hecht A, Boyer TG. Mediator Is a Transducer of Wnt/β-Catenin Signaling. *J Biol Chem* 2006;**281**:14066–14075.

Kitajima K, Murakami K, Kaji Y, Sugimura K. Spectrum of FDG PET/CT Findings of Uterine Tumors. *Am J Roentgenol* 2010;**195**:737–743.

Larriba MJ, González-Sancho JM, Barbáchano A, Niell N, Ferrer-Mayorga G, Muñoz A. Vitamin D Is a Multilevel Repressor of Wnt/b-Catenin Signaling in Cancer Cells. *Cancers (Basel)* 2013;**5**:1242–60.

Leppert PC, Jayes FL, Segars JH. The Extracellular Matrix Contributes to Mechanotransduction in Uterine Fibroids. 2014.

Lethaby A, Duckitt K, Farquhar C. Non-steroidal anti-inflammatory drugs for heavy menstrual bleeding. *Cochrane Database Syst Rev* 2013:CD000400.

Loening AM, Gambhir SS. AMIDE: a free software tool for multimodality medical image analysis. *Mol Imaging* 2003;**2**:131–7.

Lorenzen M, Boisen IM, Mortensen LJ, Lanske B, Juul A, Blomberg Jensen M. Reproductive endocrinology of vitamin D. *Mol Cell Endocrinol* 2017;**453**:103–112.

Ma C, Chegini N. Regulation of matrix metalloproteinases (MMPs) and their tissue inhibitors in human myometrial smooth muscle cells by TGF-beta1. *Mol Hum Reprod* 1999;**5**:950–954.

Ma Y, Shao X. Uterine fibroids with positive 18F-FDG PET/CT image and significantly increased CA19-9: A case report. *Medicine (Baltimore)* 2017;**96**:e9421.

Markowski DN, Bartnitzke S, Löning T, Drieschner N, Helmke BM, Bullerdiek J. MED12 mutations in uterine fibroids-their relationship to cytogenetic subgroups. *Int J Cancer* 2012;**131**:1528–1536.

Marshall LM, Spiegelman D, Barbieri RL, Goldman MB, Manson JE, Colditz GA, Willett WC, Hunter DJ. Variation in the incidence of uterine leiomyoma among premenopausal women by age and race. *Obstet Gynecol* 1997;**90**:967–73.

Marshall LM, Spiegelman D, Goldman MB, Manson JE, Colditz GA, Barbieri RL, Stampfer MJ, Hunter DJ. A prospective study of reproductive factors and oral contraceptive use in

relation to the risk of uterine leiomyomata. *Fertil Steril* 1998;**70**:432–9.

Maruyama T, Miyazaki K, Masuda H, Ono M, Uchida H, Yoshimura Y. Review: Human uterine stem/progenitor cells: Implications for uterine physiology and pathology. *Placenta* 2013;**34**:S68–S72.

Mas A, Cervelló I, Gil-Sanchis C, Faus A, Ferro J, Pellicer A, Simón C. Identification and characterization of the human leiomyoma side population as putative tumor-initiating cells. *Fertil Steril* 2012;**98**:741–751.e6.

Mas A, Cervello I, Gil-Sanchis C, Simón C. Current understanding of somatic stem cells in leiomyoma formation. *Fertil Steril* 2014;**102**:613–620.

Mas A, Tarazona M, Dasí Carrasco J, Estaca G, Cristóbal I, Monleón J. Updated approaches for management of uterine fibroids. *Int J Womens Health* 2017;**Volume 9**:607–617.

Matsuzaki S, Canis M, Darcha C, Pouly J-L, Mage G. HOXA-10 expression in the mid-secretory endometrium of infertile patients with either endometriosis, uterine fibromas or unexplained infertility. *Hum Reprod* 2009;**24**:3180–3187.

Mehine M, Kaasinen E, Heinonen H-R, Mäkinen N, Kämpjärvi K, Sarvilinna N, Aavikko M, Vähärautio A, Pasanen A, Bützow R, *et al.* Integrated data analysis reveals uterine leiomyoma subtypes with distinct driver pathways and biomarkers. *Proc Natl Acad Sci U S A* 2016;**113**:1315–20.

Mehine M, Kaasinen E, Mäkinen N, Katainen R, Kämpjärvi K, Pitkänen E, Heinonen H-R, Bützow R, Kilpivaara O, Kuosmanen A, *et al.* Characterization of Uterine Leiomyomas by Whole-Genome Sequencing. *N Engl J Med* 2013;**369**:43–53.

Mehine M, Mäkinen N, Heinonen H-R, Aaltonen LA, Vahteristo P. Genomics of uterine leiomyomas: insights from high-throughput sequencing. *Fertil Steril* 2014;**102**:621–629.

Munro MG, Critchley HOD, Broder MS, Fraser IS, FIGO Working Group on Menstrual Disorders. FIGO classification system (PALM-COEIN) for causes of abnormal uterine bleeding in nongravid women of reproductive age. *Int J Gynecol Obstet* 2011;**113**:3–13..

Nakagawa K, Kawaura A, Kato S, Takeda E, Okano T. 1 ,25-Dihydroxyvitamin D3 is a preventive factor in the metastasis of lung cancer. *Carcinogenesis* 2004;**26**:429–440.

Nesby-O'Dell S, Scanlon KS, Cogswell ME, Gillespie C, Hollis BW, Looker AC, Allen C, Doughertly C, Gunter EW, Bowman BA. Hypovitaminosis D prevalence and determinants among African American and white women of reproductive age: third National Health and Nutrition Examination Survey, 1988–1994. *Am J Clin Nutr* 2002;**76**:187–192.

Ono M, Maruyama T, Masuda H, Kajitani T, Nagashima T, Arase T, Ito M, Ohta K, Uchida H, Asada H, *et al.* Side population in human uterine myometrium displays phenotypic and functional characteristics of myometrial stem cells. *Proc Natl Acad Sci* 2007;**104**:18700–18705.

Ono M, Qiang W, Serna VA, Yin P, Coon JS, Navarro A, Monsivais D, Kakinuma T, Dyson M, Druschitz S, *et al.* Role of stem cells in human uterine leiomyoma growth. Papadia A (ed).

PLoS One 2012;**7**:e36935.

Ono M, Yin P, Navarro A, Moravek MB, Coon JS, Druschitz SA, Serna VA, Qiang W, Brooks DC, Malpani SS, *et al.* Paracrine activation of WNT/ -catenin pathway in uterine leiomyoma stem cells promotes tumor growth. *Proc Natl Acad Sci* 2013;**110**:17053–17058.

Ordóñez-Morán P, Larriba MJ, Pálmer HG, Valero RA, Barbáchano A, Duñach M, de Herreros AG, Villalobos C, Berciano MT, Lafarga M, *et al.* RhoA-ROCK and p38MAPK-MSK1 mediate vitamin D effects on gene expression, phenotype, and Wnt pathway in colon cancer cells. *J Cell Biol* 2008;**183**:697–710.

Paffoni A, Somigliana E, Vigano' P, Benaglia L, Cardellicchio L, Pagliardini L, Papaleo E, Candiani M, Fedele L. Vitamin D status in women with uterine leiomyomas. *J Clin Endocrinol Metab* 2013;**98**:E1374-8.

Palomba S, Orio F, Russo T, Falbo A, Tolino A, Lombardi G, Cimini V, Zullo F. Antiproliferative and proapoptotic effects of raloxifene on uterine leiomyomas in postmenopausal women. *Fertil Steril* 2005;**84**:154–61.

Paluszczak J, Kiwerska K, Mielcarek-Kuchta D. Frequent methylation of DAB2, a Wnt pathway antagonist, in oral and oropharyngeal squamous cell carcinomas. *Pathol Res Pract* 2018;**214**:314–317.

Parazzini F, Negri E, La Vecchia C, Chatenoud L, Ricci E, Guarnerio P. Reproductive factors and risk of uterine fibroids. *Epidemiology* 1996;**7**:440–2.

Parazzini F, Negri E, La Vecchia C, Fedele L, Rabaiotti M, Luchini L. Oral contraceptive use and risk of uterine fibroids. *Obstet Gynecol* 1992;**79**:430–3.

Parker WH. Etiology, symptomatology, and diagnosis of uterine myomas. *Fertil Steril* 2007;**87**:725–736.

Parsanezhad ME, Azmoon M, Alborzi S, Rajaeefard A, Zarei A, Kazerooni T, Frank V, Schmidt EH. A randomized, controlled clinical trial comparing the effects of aromatase inhibitor (letrozole) and gonadotropin-releasing hormone agonist (triptorelin) on uterine leiomyoma volume and hormonal status. *Fertil Steril* 2010;**93**:192–8.

Peddada SD, Laughlin SK, Miner K, Guyon J-P, Haneke K, Vahdat HL, Semelka RC, Kowalik A, Armao D, Davis B, *et al.* Growth of uterine leiomyomata among premenopausal black and white women. *Proc Natl Acad Sci U S A* 2008;**105**:19887–92.

Pendás-Franco N, Aguilera O, Pereira F, González-Sancho JM, Muñoz A. Vitamin D and Wnt/beta-catenin pathway in colon cancer: role and regulation of DICKKOPF genes. *Anticancer Res* 2008;**28**:2613–23..

Purohit P, Vigneswaran K. Fibroids and Infertility. *Curr Obstet Gynecol Rep* 2016;**5**:81–88.

Qin J, Yang T, Kong F, Zhou Q. Oral contraceptive use and uterine leiomyoma risk: a meta-analysis based on cohort and case–control studies. *Arch Gynecol Obstet* 2013;**288**:139–148.

Rackow BW, Taylor HS. Submucosal uterine leiomyomas have a global effect on molecular determinants of endometrial receptivity. *Fertil Steril* 2010;**93**:2027–2034.

Ramírez-González JA, Vaamonde-Lemos R, Cunha-Filho JS, Varghese AC, Swanson RJ. Overview of the Female Reproductive System. In: *Exercise and Human Reproduction*. New York, NY: Springer New York, 2016, 19–46.

Rogers K. *The reproductive system*. Britannica Educational Pub., in association with Rosen Educational Services, 2011.

Ross RK, Pike MC, Vessey MP, Bull D, Yeates D, Casagrande JT. Risk factors for uterine fibroids: reduced risk associated with oral contraceptives. *Br Med J (Clin Res Ed)* 1986;**293**:359–62.

Sabry M, Halder SK, Allah ASA, Roshdy E, Rajaratnam V, Al-Hendy A. Serum vitamin D3 level inversely correlates with uterine fibroid volume in different ethnic groups: a cross-sectional observational study. *Int J Womens Health* 2013;**5**:93–100.

Sadan O, Ginath S, Sofer D, Rotmensch S, Debby A, Glezerman M, Zakut H. The role of tamoxifen in the treatment of symptomatic uterine leiomyomata -- a pilot study. *Eur J Obstet Gynecol Reprod Biol* 2001;**96**:183–6.

Sharan C, Halder SK, Thota C, Jaleel T, Nair S, Al-Hendy A. Vitamin D inhibits proliferation of human uterine leiomyoma cells via catechol-O-methyltransferase. *Fertil Steril* 2011;**95**:247–53.

Sinai Talaulikar V. Medical therapy for fibroids: An overview. *Best Pract Res Clin Obstet Gynaecol* 2018;**46**:48–56.

Sinclair DC, Mastroyannis A, Taylor HS. Leiomyoma simultaneously impair endometrial BMP-2-mediated decidualization and anticoagulant expression through secretion of TGF-β3. *J Clin Endocrinol Metab* 2011;**96**:412–21..

Singh R, Letai A, Sarosiek K. Regulation of apoptosis in health and disease: the balancing act of BCL-2 family proteins. *Nat Rev Mol Cell Biol* 2019;**20**:175–193.

Sohn GS, Cho S, Kim YM, Cho C-H, Kim M-R, Lee SR, Working Group of Society of Uterine Leiomyoma. Current medical treatment of uterine fibroids. *Obstet Gynecol Sci* 2018;**61**:192.

Song H, Lu D, Navaratnam K, Shi G. Aromatase inhibitors for uterine fibroids. *Cochrane Database Syst Rev* 2013.

Stewart E, Cookson C, Gandolfo R, Schulze-Rath R. Epidemiology of uterine fibroids: a systematic review. *BJOG An Int J Obstet Gynaecol* 2017;**124**:1501–1512.

Stewart EA. Uterine fibroids. *Lancet (London, England)* 2001;**357**:293–8. Available at: https://linkinghub.elsevier.com/retrieve/pii/S0140673600036229. Accessed July 17, 2018.

Stewart EA. *Uterine fibroids : the complete guide*. Johns Hopkins University Press, 2007.

Available at: https://jhupbooks.press.jhu.edu/title/uterine-fibroids. Accessed January 30, 2019.

Stewart EA, Laughlin-Tommaso SK, Catherino WH, Lalitkumar S, Gupta D, Vollenhoven B. Uterine fibroids. *Nat Rev Dis Prim* 2016;**2**:16043.

Stewart L, Glenn GM, Stratton P, Goldstein AM, Merino MJ, Tucker MA, Linehan WM, Toro JR. Association of germline mutations in the fumarate hydratase gene and uterine fibroids in women with hereditary leiomyomatosis and renal cell cancer. *Arch Dermatol* 2008;**144**:1584–92.

Tanwar PS, Lee H-J, Zhang L, Zukerberg LR, Taketo MM, Rueda BR, Teixeira JM. Constitutive activation of Beta-catenin in uterine stroma and smooth muscle leads to the development of mesenchymal tumors in mice. *Biol Reprod* 2009;**81**:545–52.

Taylor HS. Fibroids: when should they be removed to improve in vitro fertilization success? *Fertil Steril* 2018;**109**:784–785.

Tristan M, Orozco LJ, Steed A, Ramírez-Morera A, Stone P. Mifepristone for uterine fibroids. *Cochrane Database Syst Rev* 2012:CD007687..

Vinatier D. *Integrins and reproduction*. 1995. Available at: https://www.ejog.org/article/0028-2243(94)01987-I/pdf. Accessed May 6, 2019.

Walker CL, Hunter D, Everitt JI. Uterine leiomyoma in the Eker rat: A unique model for important diseases of women. *Genes, Chromosom Cancer* 2003;**38**:349–356.

Whitaker LHR, Murray AA, Matthews R, Shaw G, Williams ARW, Saunders PTK, Critchley HOD. Selective progesterone receptor modulator (SPRM) ulipristal acetate (UPA) and its effects on the human endometrium. *Hum Reprod* 2017;**32**:531–543.

Willman EA, Collins WP, Clayton SG. Studies in the involvement of prostaglandins in uterine symptomatology and pathology. *Br J Obstet Gynaecol* 1976;**83**:337–41.

Wise LA, Palmer JR, Harlow BL, Spiegelman D, Stewart EA, Adams-Campbell LL, Rosenberg L. Risk of uterine leiomyomata in relation to tobacco, alcohol and caffeine consumption in the Black Women's Health Study. *Hum Reprod* 2004;**19**:1746–54.

Wrona W, Stepniak A, Czuczwar P. The role of levonorgestrel intrauterine systems in the treatment of symptomatic fibroids. *Prz Menopauzalny* 2017.

Wu X, Blanck A, Olovsson M, Henriksen R, Lindblom B. Expression of Bcl-2, Bcl-x, Mcl-1, Bax and Bak in human uterine leiomyomas and myometrium during the menstrual cycle and after menopause. *J Steroid Biochem Mol Biol* 2002;**80**:77–83.

Yin P, Lin Z, Cheng Y-H, Marsh EE, Utsunomiya H, Ishikawa H, Xue Q, Reierstad S, Innes J, Thung S, *et al.* Progesterone receptor regulates Bcl-2 gene expression through direct binding to its promoter region in uterine leiomyoma cells. *J Clin Endocrinol Metab* 2007;**92**:4459–66.

Ylikomi T, Laaksi I, Lou Y-R, Martikainen P, Miettinen S, Pennanen P, Purmonen S, Syvälä H,

Vienonen A, Tuohimaam P. Antiproliferative Action of Vitamin D. *Vitam Horm* 2002;**64**:357–406.

Zangemeister-Wittke U, Simon H-U. Apoptosis - Regulation and clinical implications. *Cell Death Differ* 2001;**8**:537–544.

Zhang X, Jiang F, Li P, Li C, Ma Q, Nicosia S V, Bai W. Growth suppression of ovarian cancer xenografts in nude mice by vitamin D analogue EB1089. *Clin Cancer Res* 2005;**11**:323–8.

Zhu A, Lee D, Shim H. Metabolic positron emission tomography imaging in cancer detection and therapy response. *Semin Oncol* 2011;**38**:55–69. Available at: http://www.ncbi.nlm.nih.gov/pubmed/21362516. Accessed May 15, 2019.

Zimmermann A, Bernuit D, Gerlinger C, Schaefers M, Geppert K. Prevalence, symptoms and management of uterine fibroids: an international internet-based survey of 21,746 women. *BMC Womens Health* 2012;**12**:6.

IX. ANNEXES

VII. ANNEXES

ANNEX I: Sequences of primers used in Q-RT-PCR assays.

GENE	Forward sequence	Reverse sequence
β-actin	CACACTGTGCCCATCTACGA	TAGCTCTTCTCCAGGGAGGA
CYP24A1	CGCATCTTCCATTTGGCGTT	GCCTGGATGTCGTATTTGCG
WNT5A	GAAGCCAATTCTTGGTGGT	GAGAAAGTCCTGCCAGTTG
DKK1	GATCATAGCACCTTGGATGGG	GGCACAGTCTGATGACCGG
BCL2	TGGATGACTGAGTACCTGAA	GACAGCCAGGAGAAATCAAA
TNFRSF11B	GTGGAATAGATGTTACCCTGTG	CAAGACACTAAGCCAGTTAGG
PCNA	GTGACACTCAGTATGTCTGC	CTTCTTCATCCTCGATCTTG
TGFβ3	CATGAACCTAAGGGCTACTATG	CTTCAGGGTTCAGAGTGTTG

ANNEX II- RT² Profiler PCR Array Human WNT Signaling Pathway Plus

POSITION	SYMBOL	DESCRIPTION
A01	APC	Adenomatous polyposis coli
A02	AXIN1	Axin 1
A03	AXIN2	Axin 2
A04	BTRC	Beta-transducin repeat containing
A05	CSNK1A1	Casein kinase 1, alpha 1
A06	CTBP1	C-terminal binding protein 1
A07	CTNNB1	Catenin (cadherin-associated protein), beta 1, 88kDa
A08	CTNNBIP1	Catenin, beta interacting protein 1
A09	DAAM1	Dishevelled associated activator of morphogenesis 1
A10	DAB2	Disabled homolog 2, mitogen-responsive phosphoprotein (Drosophila
A11	DKK1	Dickkopf homolog 1 (Xenopus laevis)
A12	DKK3	Dickkopf homolog 3 (Xenopus laevis)
B01	DVL1	Dishevelled, dsh homolog 1 (Drosophila)
B02	DVL2	Dishevelled, dsh homolog 2 (Drosophila)
B03	EP300	E1A binding protein p300
B04	FBXW11	F-box and WD repeat domain containing 11
B05	FGF4	Fibroblast growth factor 4
B06	FOSL1	FOS-like antigen 1
B07	FRAT1	Frequently rearranged in advanced T-cell lymphomas
B08	FRZB	Frizzled-related protein
B09	FZD1	Frizzled family receptor 1
B10	FZD2	Frizzled family receptor 2
B11	FZD3	Frizzled family receptor 3
B12	FZD4	Frizzled family receptor 4
C01	FZD5	Frizzled family receptor 5
C02	FZD6	Frizzled family receptor 6
C03	FZD7	Frizzled family receptor 7
C04	FZD8	Frizzled family receptor 8
C05	FZD9	Frizzled family receptor 9
C06	GSK3B	Glycogen synthase kinase 3 beta
C07	JUN	Jun proto-oncogene
C08	KREMEN1	Kringle containing transmembrane protein 1
C09	LRP5	Low density lipoprotein receptor-related protein 5
C10	LRP6	Low density lipoprotein receptor-related protein 6
C11	MAPK8	Mitogen-activated protein kinase 8
C12	MMP7	Matrix metallopeptidase 7 (matrilysin, uterine)
D01	NFATC1	Nuclear factor of activated T-cells, cytoplasmic, calcineurin-dependent 1
D02	NKD1	Naked cuticle homolog 1 (Drosophila)
D03	NLK	Nemo-like kinase
D04	PITX2	Paired-like homeodomain 2
D05	PORCN	Porcupine homolog (Drosophila)
D06	PPARD	Peroxisome proliferator-activated receptor delta
D07	PRICKLE1	Prickle homolog 1 (Drosophila)
D08	RHOA	Ras homolog gene family, member A
D09	RUVBL1	RuvB-like 1 (E. coli)
D10	SFRP1	Secreted frizzled-related protein 1
D11	SFRP4	Secreted frizzled-related protein 4
D12	SOX17	SRY (sex determining region Y)-box 17

POSITION	SYMBOL	DESCRIPTION
E01	TCF7	Transcription factor 7 (T-cell specific, HMG-box)
E02	TCF7L1	Transcription factor 7-like 1 (T-cell specific, HMG-box)
E03	VANGL2	Vang-like 2 (van gogh, Drosophila)
E04	WIF1	WNT inhibitory factor 1
E05	WISP1	WNT1 inducible signaling pathway protein 1
E06	WNT1	Wingless-type MMTV integration site family, member 1
E07	WNT10A	Wingless-type MMTV integration site family, member 10a
E08	WNT11	Wingless-type MMTV integration site family, member 11
E09	WNT2	Wingless-type MMTV integration site family, member 1
E10	WNT2B	Wingless-type MMTV integration site family, member 2B
E11	WNT3	Wingless-type MMTV integration site family, member 3
E12	WNT3A	Wingless-type MMTV integration site family, member 3A
F01	WNT4	Wingless-type MMTV integration site family, member 4
F02	WNT5A	Wingless-type MMTV integration site family, member 5A
F03	WNT5B	Wingless-type MMTV integration site family, member 5B
F04	WNT6	Wingless-type MMTV integration site family, member 6
F05	WNT7A	Wingless-type MMTV integration site family, member 7A
F06	WNT7B	Wingless-type MMTV integration site family, member 7B
F07	WNT8A	Wingless-type MMTV integration site family, member 8A
F08	WNT9A	Wingless-type MMTV integration site family, member 9A
F09	BOD1	Biorientation of chromosomes in cell division 1
F10	CALM1	Calmodulin 1 (phosphorylase kinase, delta)
F11	CCND1	Cyclin D1
F12	CCND2	Cyclin D2
G01	CHSY1	Chondroitin sulfate synthase 1
G02	CXADR	Coxsackie virus and adenovirus receptor
G03	CYPAV2	Cytochrome P450, family 4, subfamily v, polypeptide 2
G04	HSPA12A	Heat shock 70kDa protein 12A
G05	LEF1	Lymphoid enhancer-binding factor 1
G06	MT1A	Metallothionein 1A
G07	MTFP1	Mitochondrial fission process 1
G08	MTSS1	Metastasis suppressor 1
G09	MYC	V-myc myelocytomatosis viral oncogene homolog (avi
G10	NAV2	Neuron navigator 2
G11	PRMT6	Protein arginine methyltransferase 6
G12	SKP2	S-phase kinase-associated protein 2 (p45)
H01	ACTB	Actin, beta
H02	B2M	Beta-2-microglobulin
H03	GAPDH	Glyceraldehyde-3-phosphate dehydrogenase
H04	HPRT1	Hypoxanthine phosphoribosyltransferase 1
H05	RPL10	Ribosomal protein, large, P0
H06	HGDC	Human Genomic DNA Contamination
H07	RTC	Reverse Transcription Control
H08	RTC	Reverse Transcription Control
H09	RTC	Reverse Transcription Control
H10	PPC	Positive PCR Control
H11	PPC	Positive PCR Control
H12	PPC	Positive PCR Control

ANNEX III- RT² Profiler PCR Array Human Apoptosis

POSITION	SYMBOL	DESCRIPTION
A01	ABL1	C-abl oncogene 1, non-receptor tyrosine kinase
A02	AIFM1	Apoptosis-inducing factor, mitochondrion-associated, 1
A03	AKT1	V-akt murine thymoma viral oncogene homolog 1
A04	APAF1	Apoptotic peptidase activating factor 1
A05	BAD	BCL2-associated agonist of cell death
A06	BAG1	BCL2-associated athanogene
A07	BAG3	BCL2-associated athanogene 3
A08	BAK1	BCL2-antagonist/killer 1
A09	BAX	BCL2-associated X protein
A10	BCL10	B-cell CLL/lymphoma 10
A11	BCL2	B-cell CLL/lymphoma 2
A12	BCL2A1	BCL2-related protein A1
B01	BCL2L1	BCL2-like 1
B02	BCL2L10	BCL2-like 10 (apoptosis facilitator)
B03	BCL2L11	BCL2-like 11 (apoptosis facilitator)
B04	BCL2L2	BCL2-like 2
B05	BFAR	Bifunctional apoptosis regulator
B06	BID	BH3 interacting domain death agonist
B07	BIK	BCL2-interacting killer (apoptosis-inducing)
B08	BIRC2	Baculoviral IAP repeat containing 2
B09	BIRC3	Baculoviral IAP repeat containing 3
B10	BIRC5	Baculoviral IAP repeat containing 5
B11	BIRC6	Baculoviral IAP repeat containing 6
B12	BNIP2	BCL2/adenovirus E1B 19kDa interacting protein 2
C01	BNIP3	BCL2/adenovirus E1B 19kDa interacting protein 3
C02	BNIP3L	BCL2/adenovirus E1B 19kDa interacting protein 3-like
C03	BRAF	V-raf murine sarcoma viral oncogene homolog B1
C04	CASP1	Caspase 1, apoptosis-related cysteine peptidase (interleukin 1, beta, convertase)
C05	CASP10	Caspase 10, apoptosis-related cysteine peptidase
C06	CASP14	Caspase 14, apoptosis-related cysteine peptidase
C07	CASP2	Caspase 2, apoptosis-related cysteine peptidase
C08	CASP3	Caspase 3, apoptosis-related cysteine peptidase
C09	CASP4	Caspase 4, apoptosis-related cysteine peptidase
C10	CASP5	Caspase 5, apoptosis-related cysteine peptidase
C11	CASP6	Caspase 6, apoptosis-related cysteine peptidase
C12	CASP7	Caspase 7, apoptosis-related cysteine peptidase
D01	CASP8	Caspase 8, apoptosis-related cysteine peptidase
D02	CASP9	Caspase 9, apoptosis-related cysteine peptidase
D03	CD27	CD27 molecule
D04	CD40	CD40 molecule, TNF receptor superfamily member 5
D05	CD40LG	CD40 ligand
D06	CD70	CD70 molecule
D07	CFLAR	CASP8 and FADD-like apoptosis regulator
D08	CIDEA	Cell death-inducing DFFA-like effector a
D09	CIDEB	Cell death-inducing DFFA-like effector b
D10	CRADD	CASP2 and RIPK1 domain containing adaptor with death domain
D11	CYCS	Cytochrome c, somatic
D12	DAPK1	Death-associated protein kinase 1

POSITION	SYMBOL	DESCRIPTION
E01	DFFA	DNA fragmentation factor, 45kDa, alpha polypeptide
E02	DIABLO	Diablo, IAP-binding mitochondrial protein
E03	FADD	Fas (TNFRSF6)-associated via death domain
E04	FAS	Fas (TNF receptor superfamily, member 6)
E05	FASLG	Fas ligand (TNF superfamily, member 6)
E06	GADD45A	Growth arrest and DNA-damage-inducible, alpha
E07	HRK	Harakiri, BCL2 interacting protein (contains only BH3 domain)
E08	IGF1R	Insulin-like growth factor 1 receptor
E09	IL10	Interleukin 10
E10	LTA	Lymphotoxin alpha (TNF superfamily, member 1)
E11	LTBR	Lymphotoxin beta receptor (TNFR superfamily, member 3)
E12	MCL1	Myeloid cell leukemia sequence 1 (BCL2-related)
F01	NAIP	NLR family, apoptosis inhibitory protein
F02	NFKB1	Nuclear factor of kappa light polypeptide gene enhancer in B-cells 1
F03	NOD1	Nucleotide-binding oligomerization domain containing 1
F04	NOL3	Nucleolar protein 3 (apoptosis repressor with CARD domain)
F05	PYCARD	PYD and CARD domain containing
F06	RIPK2	Receptor-interacting serine-threonine kinase 2
F07	TNF	Tumor necrosis factor
F08	TNFRSF10A	Tumor necrosis factor receptor superfamily, member 10a
F09	TNFRSF10B	Tumor necrosis factor receptor superfamily, member 10b
F10	TNFRSF11B	Tumor necrosis factor receptor superfamily, member 11b
F11	TNFRSF1A	Tumor necrosis factor receptor superfamily, member 1A
F12	TNFRSF1B	Tumor necrosis factor receptor superfamily, member 1B
G01	TNFRSF21	Tumor necrosis factor receptor superfamily, member 21
G02	TNFRSF25	Tumor necrosis factor receptor superfamily, member 25
G03	TNFRSF9	Tumor necrosis factor receptor superfamily, member 9
G04	TNFSF10	Tumor necrosis factor (ligand) superfamily, member 10
G05	TNFSF8	Tumor necrosis factor (ligand) superfamily, member 8
G06	TP53	Tumor protein p53
G07	TP53BP2	Tumor protein p53 binding protein, 2
G08	TP73	Tumor protein p73
G09	TRADD	TNFRSF1A-associated via death domain
G10	TRAF2	TNF receptor-associated factor 2
G11	TRAF3	TNF receptor-associated factor 3
G12	XIAP	X-linked inhibitor of apoptosis
H01	ACTB	Actin, beta
H02	B2M	Beta-2-microglobulin
H03	GAPDH	Glyceraldehyde-3-phosphate dehydrogenase
H04	HPRT1	Hypoxanthine phosphoribosyltransferase 1
H05	RPLP0	Ribosomal protein, large, P0
H06	HGDC	Human Genomic DNA Contamination
H07	RTC	Reverse Transcription Control
H08	RTC	Reverse Transcription Control
H09	RTC	Reverse Transcription Control
H10	PPC	Positive PCR Control
H11	PPC	Positive PCR Control
H12	PPC	Positive PCR Control

ANNEX IV: Scientific production PhD student.

1. International scientific publications

Corachán A, Ferrero H, Aguilar A, García N, Monleón J, Faus A, Cervelló I, Pellicer A. "Inhibition of tumor cell proliferation in human uterine leiomyoma by vitamin D via Wnt/β-catenin pathway." *Fertility and Sterility* Vol. 111, No. 2, February 2019. https://doi.org/10.1016/j.fertnstert.2018.10.008

2. Works submitted to international conferences

Corachán A, Ferrero H, Escrig J, Monleón J, Faus A, Cervelló I, Pellicer A. "Effects of Vitamin D in human uterine leiomyoma growth in a xenograft animal model." Conference: Annual Meeting of the SRI – Paris, 12-16 March 2019. Presentation: Poster

Corachán A, Ferrero H, Aguilar A, García N, Monleón J, Faus A, Cervelló I, Pellicer A. "Anti-proliferative Action of Vitamin D in Uterine Leiomyoma Leaded by Cell Growth Arrest, Wnt/β-catenin Pathway Inhibition and Apoptosis Induction." Conference: Annual Meeting of the SRI – San Diego, 6-10 March 2018. Presentation: Poster

Corachán A, Ferrero H, Aguilar A, García N, Monleón J, Faus A, Cervelló I, Pellicer A. "Vitamin D can inhibit proliferation of uterine fibroid cells in vitro through the Wnt/ß-Catenin signaling pathway." Conference: Annual Meeting of ESHRE- Geneva, 3-5 July 2017. Presentation: Poster

Aguilar A**,** García N, **Corachán A,** Monleón J, Ferrero H, Galliano D, Navarro A, Cervelló I, Pellicer A. "In vitro Proliferation of Uterine Fibroids is Related with Vitamin D Receptor and Patient's age." Conference: Annual Meeting of ESHRE- Geneva, 3-5 July 2017. Presentation: Poster